

# **The Effect of Sorption on the Fate and Transport of Selected Pharmaceuticals in Natural Waters**

---

A Dissertation  
Presented to  
the Faculty of the School of Engineering and Applied Science  
University of Virginia

---

In Partial Fulfillment  
of the Requirements for the Degree

Doctor of Philosophy  
in  
Civil and Environmental Engineering

By

Dong Liu

December 2012

## APPROVAL SHEET

The dissertation is submitted in partial fulfillment of the  
requirements for the degree of  
Doctor of Philosophy in Civil and Environmental Engineering

---

Dong Liu  
(Author)

This dissertation has been read and approved by the examining Committee:

---

Wu-Seng Lung, Ph.D.  
(Dissertation Co-advisor)

---

Lisa M. Colosi, Ph.D.  
(Dissertation Co-advisor)

---

James A. Smith, Ph.D. (Chairperson)

---

Matthew A. Reidenbach, Ph.D.

---

Yen-Chang Chen, Ph.D.

Accepted for the School of Engineering and Applied Science:

---

Dean, School of Engineering and Applied Science

December 2012

## **Abstract**

Pharmaceuticals are one class of emerging contaminants frequently detected in drinking water supplies and even in finished drinking waters. Because these chemicals can exhibit adverse effects on aquatic ecosystems and human health, a growing number of studies have been conducted to evaluate their fate in natural water bodies. However, a quantitative tool is lacking to evaluate the relative significance of natural attenuation mechanisms and provide insight into the environmental behavior of pharmaceuticals in natural waters. The purpose of this research is to evaluate the significance of natural attenuation processes on the fate and behaviors of pharmaceuticals through modeling analyses. Special emphasis is placed on sorption processes and sorption kinetics. As part of this research, a sorption kinetics model was developed and incorporated into a water quality model for the Patuxent Estuary to evaluate the effect of sorption kinetics. Although most current models are based on the assumption of instantaneous sorption equilibrium, pharmaceutical compounds may take long times (in days) to reach sorption equilibrium, strongly suggesting that this assumption is invalid. Four hypothetical pharmaceuticals representing four possible combinations of sorption coefficients and times to reach sorption equilibrium were used as target compounds. Model results reveal that assumption of instantaneous sorption equilibrium results in significant under-prediction of water column concentrations for some pharmaceuticals: up to 150% at upstream locations. Further, sorption kinetics affects a model's ability to capture accumulation of pharmaceuticals into riverbeds and the transport of pharmaceuticals in estuaries. For the second part of this research, experiments were conducted to examine the sorption behavior, especially sorption kinetics, of two selected pharmaceuticals:

triclosan and enrofloxacin. Both chemicals exhibit slow sorption; further verifying that the assumption of instantaneous sorption equilibrium is inadequate. The slow sorption of enrofloxacin may result from reduced molecular mobility due to local sorption. Enrofloxacin shows much higher sorption capacity than triclosan due to ionic interactions. For this reason, the sorption of enrofloxacin is strongly but adversely dependent on pH and/or ionic strength. Desorption kinetics experiments reveal a 23-28% increase in sorption coefficient for both chemicals, indicating a sorption-desorption hysteresis. Enrofloxacin exhibits nonlinear sorption due to limited sorption sites. A two-compartment Langmuir model, assuming a linear sorption component of sediments, generates adequate fits to nonlinear experimental data. Experimental results were then incorporated into the fate and transport model for the Patuxent Estuary to evaluate the significance of attenuation processes. Results verify that triclosan and enrofloxacin exhibit different environmental fate and behavior than each other due to their properties. For a 20-km area immediately downstream of the upper boundary of the study area, sorption causes a 7.9% - 51.5% decrease in dissolved-phase concentrations for enrofloxacin and a 1.0%-11.2% decrease for triclosan. Photolysis results in further decrease in dissolved-phase concentrations: 7.6% - 42.4% for enrofloxacin and 6.3% - 49.9% for triclosan. The role of sorption and photolysis depends on chemical properties, total suspended solid concentrations, flow conditions and environmental parameters such as light extinction coefficient. Both chemicals exhibit significant accumulation onto riverbeds with TCS levels exceeding its no effect concentrations for algae.

## Acknowledgements

First and foremost, I would like to express my sincere gratitude to my graduate co-advisors, Dr. Wu-Seng Lung and Dr. Lisa Colosi for their support, patient, guidance and motivations. Thanks for the countless hours that they have spent reviewing and revising my proposal, publication and dissertation. Thanks to Dr. Lung, whom I have frequently consulted for his advice since the first day I have been here, for his invaluable instructions in the field of water quality modeling. Thanks to Dr. Colosi for her guidance and enlightening suggestions on my whole experimental work. I would also like to thank my other committee members, Dr. James Smith, Dr. Matthew Reidenbach and Dr. Yen-Chang Chen for their suggestions and help with my research. Their guidance and feedback have greatly helped me achieve this point. I also would like to thank Dr. Alex Nice and Dr. Sen Bai for providing me modeling framework and their model inputs. I sincere appreciation also goes to Dr. Karl Ottmar for helping me setup experiments, and providing experimental materials and other helpful information. In addition, I would express my appreciations for the help from my friends, graduate students and professors here. Especially, I would like to thank my parents for their support, patient and encouragement during my many years as a graduate student.

## Table of Contents

Abstract.....	i
Acknowledgements.....	iii
Table of Contents.....	iv
List of Abbreviations.....	v
List of Tables .....	vi
List of Figures .....	vii
Chapter 1: Introduction .....	1
1.1 Background .....	1
1.2 Hypotheses and Research Purposes .....	3
Chapter 2: Background .....	5
2.1 Natural Attenuation Mechanisms of Pharmaceuticals in Water/Sediment Systems .....	5
2.2 The Sorption of Pharmaceuticals .....	8
2.3 The Patuxent River.....	23
Chapter 3: Modeling Sorption Kinetics of Pharmaceuticals in Fate and Transport Analyses .....	27
3.1 Introduction.....	27
3.2 Materials and Methods .....	28
3.3 Improving Modeling Framework .....	33
3.4 Results and Discussion .....	43
3.5 Summary and Conclusions.....	57
Chapter 4: Measurement of Sorption Parameters for Selected Pharmaceuticals .....	59
4.1 Introduction.....	59
4.2 Materials and Methods .....	63
4.3 Results and Discussion .....	71
4.4 Conclusions and Environmental Significance.....	90
Chapter 5: Fate and Transport Modeling of Selected Pharmaceuticals in Estuaries.....	94
5.1 Introduction.....	94
5.2 Method .....	96
5.3 Results and Discussion .....	103
5.4 Conclusions.....	125
Chapter 6: Summary, Conclusions and Recommendations for Future Work....	128
6.1 Summary .....	128
6.2 Conclusions.....	130
6.3 Recommendations for Future Work.....	132
Cited References .....	134

## List of Abbreviations

AC – Activated carbon  
ACN – Acetonitrile  
AlO<sub>x</sub> – Aluminum oxyhydroxide  
CBP – Chesapeake Bay Program  
DAD – Diode array detector  
DI – De-ionized  
DRM – distributed reactivity model  
EC<sub>50</sub> – effective concentration  
ENR – enrofloxacin  
EPA – Environmental Protection Agency  
FQ – Fluoroquinolone  
FRS – Facility Registry System  
FeO<sub>x</sub> – Iron oxyhydroxide  
GAC – Granular activated carbon  
HOCs – Hydrophobic organic contaminants  
HPLC – High performance liquid chromatography  
K<sub>2</sub>HPO<sub>4</sub> – Dipotassium phosphate  
KH<sub>2</sub>PO<sub>4</sub> – Monopotassium phosphate  
LFERs – Linear free energy relationships  
LSERs – Linear solvation energy relationships  
NEC – No effect concentration  
PCBs – Polychlorinated Biphenyls  
PP-LFERs – Poly-parameter linear free energy relationships  
WWTPs – Wastewater treatment plants  
RD – Relative Difference  
RMSE – Root mean squared error  
SOM – Soil/sediment organic matter  
STPs – Sewage treatment plants  
TCS – Triclosan  
TSS – Total suspended solid  
USGS – U.S. Geological Survey

## List of Tables

Table 2-1 Sorption Equilibrium Time of Emerging Contaminants .....	16
Table 3-1 Effluent Volume of Wastewater Treatment Plants and Estimated Population Served .....	31
Table 3-2 Time to Reach Sorption Equilibrium at Different Sorbate Concentrations (Predicted by the Kinetics Model) .....	41
Table 4-1 Molecular Structures and Properties of Triclosan and Enrofloxacin .....	60
Table 4-2 The Concentration of Sorbents and pH Control for Each Experiment.....	69
Table 4-3 HPLC Method for Triclosan and Enrofloxacin .....	70
Table 4-4 Kinetics Model Results of Triclosan and Enrofloxacin .....	80
Table 4-5 Sorption Coefficient Derived from Kinetics Experiments .....	82
Table 4-6 Parameters derived from the Langmuir Isotherm for enrofloxacin.....	90
Table 5-1 Parameters for Modeling Analysis .....	97
Table 5-2 Flow Rates, Levels of Total Suspended Solid and Light Intensities for the Four Specific Days .....	103



## List of Figures

Figure 2-1 The Patuxent Watershed (adapted from Bachman and Krantz, 2000).....	25
Figure 3-1 Wastewater Treatment Plants in the Patuxent Watershed (adapted from Renee et al., 2007) .....	29
Figure 3-2 Monitoring Station Locations in the Patuxent Estuary (adapted from Nice, 2007) .....	30
Figure 3-3 Grid Setup for the Patuxent Model (adapt from Nice, 2007).....	32
Figure 3-4 Modeling Sediment Particles .....	34
Figure 3-5 Sorption Kinetics on Sediment Particles (Initial Sorbent Concentration: 11.5 µg/L, the solid line represents model results) .....	41
Figure 3-6 Sorption Isotherm on Sediment Particles at Different Reaction Time (Generated by the Kinetics Model).....	42
Figure 3-7 Spatial Distribution of Simulated and Observed Total Suspended Solid Concentrations over the Entire Length of the Studied Area .....	45
Figure 3-8 Temporal Distribution of Simulated and Observed Total Suspended Solid Concentrations (TF, RET, and LE refer to Chesapeake Bay Program Monitoring Stations). .....	46
Figure 3-9 Temporal distribution of dissolved-phase pharmaceutical concentrations for two hypothetical chemicals exhibiting high sorption coefficient ( $K_d = 10,000$ L/kg), at four selected locations within the studied region.....	47
Figure 3-10 At left: Temporal distribution of relative difference (RD) between instantaneous equilibrium and sorption kinetics modeling approaches for two hypothetical pharmaceuticals exhibiting high sorption coefficient ( $K_d = 10,000$ L/kg) at the four locations noted in Figure 3-9. ....	51
Figure 3-11 Spatial distribution of dissolved-phase concentrations for two hypothetical pharmaceuticals exhibiting high sorption coefficient ( $K_d = 10,000$ L/kg).....	53
Figure 3-12 Spatial distribution of dissolved-phase concentrations for the hypothetical pharmaceuticals exhibiting low sorption coefficient ( $K_d = 80$ L/kg).....	55
Figure 3-13 Spatial distribution of sorbed-phase concentrations for the hypothetical pharmaceuticals exhibiting low sorption coefficient ( $K_d = 80$ L/kg).....	56
Figure 4-1 The Distribution of the fraction of four enrofloxacin Species: the cation (C), the neutral (N), the Zwitterion (Z) and the anion (A) (Figure adapted from Lizondo et al., 1997) .....	64
Figure 4-2 The Distribution of the Fraction of Two Triclosan Species (Calculated using a $pK_a$ value of 7.9) .....	64
Figure 4-3 Sorption Kinetics of Triclosan at three pHs with Model Fit (Error bars represent 90% confidence interval of experimental results).....	72
Figure 4-4 Sorption Kinetics of Enrofloxacin at three pHs with Model Fit (Error bars represent 90% confidence interval of experimental results).....	73
Figure 4-5 Sorption Kinetics of Triclosan during the First Day of the Reaction (Error bars represent 90% confidence interval of experimental results).....	74
Figure 4-6 Sorption Kinetics of Enrofloxacin during the First Day of the Reaction (Error bars represent 90% confidence interval of experimental results) .....	74

Figure 4-7 Sorption Kinetics of Enrofloxacin at pH 7.2 under Different Ionic Strength (Error bars represent 90% confidence interval of experimental results; Solid line represents results of model fit).....	77
Figure 4-8 Desorption Kinetics of Triclosan at pH 6.0 and 7.2.....	82
Figure 4-9 Desorption Kinetics of Enrofloxacin at pH 7.2.....	83
Figure 4-10 Sorption Isotherm of Triclosan Fitted by the Freundlich Equation .....	87
Figure 4-11 Sorption Isotherms of Enrofloxacin Fitted by the Freundlich Equation at Three pHs.....	87
Figure 4-12 The Dependence of Sorption Coefficient ( $K_d$ ) on Sorbate-Sorbent Ratio ....	88
Figure 5-1 Longitudinal Distribution of Dissolved-Phase Concentrations of Triclosan	104
Figure 5-2 Longitudinal Distribution of Dissolved-Phase Concentrations of Enrofloxacin .....	105
Figure 5-3 Longitudinal Distribution of Total Suspended Solids.....	107
Figure 5-4 Attenuation of Dissolved-Phase Triclosan (TCS) and Enrofloxacin (ENR) within 20 km of Travel Distance .....	108
Figure 5-5 Longitudinal Distribution of Sorbed-phase Concentrations of Triclosan .....	111
Figure 5-6 Longitudinal Distribution of Sorbed-phase Concentration of Enrofloxacin.	112
Figure 5-7 Concentration of Triclosan (TCS) and Enrofloxacin (ENR) in the Active Layer of Bottom Sediment.....	113
Figure 5-8 Temporal Distribution of Sorbed-Phase Enrofloxacin from pH-Dependent Sorption Scenario and pH-Independent Sorption Scenario .....	115
Figure 5-9 Predicted Temporal Distribution of Triclosan (TCS) and Enrofloxacin (ENR) in the Active Layer of Bottom Sediments from Two Scenarios .....	116
Figure 5-10 Longitudinal Distribution of Dissolved Triclosan at Different Extinction Coefficients .....	118
Figure 5-11 Longitudinal Distribution of Dissolved Enrofloxacin at Different Extinction Coefficients .....	119
Figure 5-12 The Effect of Light Extinction Coefficients on the Attenuation of Dissolved- Phase Triclosan (TCS) and Enrofloxacin (ENR).....	120
Figure 5-13 The Effect of Extinction Coefficient on the Accumulation of Triclosan (TCS) and Enrofloxacin (ENR) in the Active Layer of Riverbeds.....	121
Figure 5-14 Spatial Profile of Triclosan Concentrations in the Active Layer of Bottom Sediments.....	123
Figure 5-15 Spatial Profile of Enrofloxacin Concentrations in the Active Layer of Bottom Sediments.....	124

## Chapter 1: Introduction

### 1.1 Background

Pharmaceuticals are emerging pollutants and include a wide range of chemicals, such as antibiotics, and veterinary and human drugs (Pan et al, 2009). These chemicals have drawn increasing research interest because they are widely detected in surface waters, ground waters, and drinking water sources (Gross et al., 2004; Kolpin et al., 2002; Focazio et al., 2008; Vieno et al, 2005). Some examples of emerging contaminants that have been frequently detected in natural waters include: caffeine, carbamazepine, triclosan, ibuprofen, naproxen, ketoprofen, gemfibrozil, diazepam, diclofenac, tetracycline and clofibric acid. The major sources of pharmaceuticals to rivers are effluents from wastewater treatment plants (WWTPs), and the urban contribution of pharmaceuticals is quite significant (Comoretto and Chiron 2005; Spongberg and Witter 2008). Pharmaceuticals have unique physiochemical properties such as sorption parameters (Lam et al., 2004; Löffler et al., 2005; Suntisukaseam et al., 2007; Yamamoto et al., 2009). Thus it is expected that they may exhibit different environmental behaviors than conventional hydrophobic organic pollutants (HOCs, e.g., PCBs), which have been well analyzed using water quality models over the past few decades. A growing number of studies have been conducted to evaluate the occurrence, fate and transport of pharmaceuticals in aquatic environments and identify fate-controlling processes (Gurr et al., 2006; Lin et al., 2006; Löffler et al., 2005; Tixier et al., 2003). Nonetheless, there is still a lack of quantitative tools to evaluate the contribution of each process (e.g., sorption) to the overall fate and transport of pharmaceuticals in water/sediment systems.

Some pharmaceuticals may exhibit more complicated sorption behavior than conventional HOCs due to their amphiphilic characteristic (Pan et al., 2009). Also, several studies illustrate that sorption to sediments and suspended materials could be a significant removal mechanism for pharmaceutical compounds in rivers (Gurr et al., 2006). Thus, there is an urgent need to better quantify the effects of sorption processes of pharmaceuticals in rivers. While most current water quality models are based on the assumption of instantaneous sorption equilibrium, many emerging contaminants (e.g. some pharmaceutical compounds) exhibit slow sorption rates. For example, the sorption of some emerging contaminants onto suspended sediments may take long times (in days) to reach equilibrium (Stein et al., 2008; Yu et al., 2004). Current water quality models, which are based on the assumption of instantaneous sorption equilibrium, do not consider sorption kinetics, thereby leading to inaccurate predictions. It is expected that the instantaneous-equilibrium based water quality models cannot accurately capture distribution between pharmaceuticals in the dissolved phase and the sorbed phase. Since chemicals in each phase (dissolved or sorbed) exhibit different environmental behaviors (e.g., settling and decomposition), incorporating sorption kinetics into water quality models could lead to significant improvement in predicted distributions of pharmaceuticals in natural water/sediment systems.

The purpose of this dissertation is to develop a modeling framework, based on previous models by Lung and Bai (2003) and Nice and Lung (2003), to understand the role of each major attenuation process in the fate and transport of pharmaceuticals in a water/sediment system when acting alone or in conjunction with other processes. In this revised

framework, special emphasis is placed on sorption processes, in particular sorption kinetics, which have not been previously incorporated into water quality models.

This research has been accomplished in three stages: 1) developing numerical models to simulate processes in natural water bodies (e.g. sediment transport and sorption kinetics), and linking them to a water quality model (summarized in Chapter 3); 2) conducting laboratory experiments to study the sorption behavior, especially sorption kinetics, of two selected pharmaceutical compounds onto suspended sediments (summarized in Chapter 4); and, 3) simulating the environmental fate and transport of pharmaceuticals in the Patuxent River using the improved water quality model (summarized in Chapter 5).

## 1.2 Hypotheses and Research Purposes

1) **Hypothesis:** Traditional water quality models under-predict pollutant levels in water columns, and cannot accurately capture the fate and mass transport of pharmaceuticals and the accumulation of pharmaceuticals into riverbeds because they do not account for sorption kinetics.

**Purpose:** Quantify the impacts of sorption kinetics on predicted concentrations of pollutants in the dissolved phase and the sorbed phase, and address how sorption kinetics, in conjunction with other processes, will affect the distribution of pharmaceuticals along the entire length of the river, including upstream and downstream locations.

2) **Hypothesis:** Some pharmaceutical compounds may exhibit slow sorption rates. They need long times (days) to reach sorption equilibrium.

**Purpose:** Conduct lab experiments to study the sorption behaviors, including sorption kinetics, of selected pharmaceutical compounds onto suspended sediments; verify that the assumption of instantaneous sorption equilibrium is invalid for some pharmaceutical compounds; and measure necessary parameters for use in modeling analyses.

**3) Hypothesis:** Different sorption properties of pharmaceuticals will cause different fates and transport of pharmaceuticals in water/sediment systems.

**Purpose:** Evaluate selected pharmaceuticals exhibiting an array of sorption parameters, and incorporate resulting parameters into the modeling framework to illustrate how differences in sorption properties, coupled with environment parameters (e.g. pH), control the fate and transport of pharmaceuticals in water/sediment systems; evaluate the relative significance of processes on the attenuation of pharmaceuticals; and conduct sensitivity analysis to examine the response of pharmaceuticals on the change of environmental parameters.

## **Chapter 2: Background**

### **2.1 Natural Attenuation Mechanisms of Pharmaceuticals in Water/Sediment Systems**

Pharmaceuticals exhibit different behaviors from each other in water/sediment systems. The natural attenuation mechanisms of pharmaceuticals include photolysis, hydrolysis, biodegradation/biotransformation, and sorption. Kümmerer (2009) illustrated that the photo degradability, biodegradability and sorption behavior of antibiotics may vary under different pH since antibiotics have multiple function groups and may exist in different species (cation, zwitterion and anion) under different pH. Volatilization is not an effective elimination process for most pharmaceuticals because most of them are large molecules, thus exhibiting low Henry's constant (Gurr et al. 2006). Generally, pharmaceuticals are resistant to hydrolysis (Nicolaou et al., 2007). Löffler et al. (2005) investigated the environmental fate of 10 selected pharmaceuticals and their metabolites in a water/sediment system and illustrated that abiotic transformation is unlikely for many selected pharmaceuticals.

The photo degradability of pharmaceuticals varies widely. Ketoprofen, tetracycline, diclofenac, naproxen and triclosan exhibit high photo degradability; carbamazepine and ibuprofen are relatively resistant to photodegradation (Buser et al., 1998; Lin et al 2006; Yamamoto et al. 2009; Tixier et al., 2003). Most pharmaceuticals show little or no solar absorption under radiation above 290 nm, thus suggesting indirect photoreaction (react with light induced hydroxyl radical) could be an important mechanism (Lam et al. 2004). As the major hydroxyl radical producer in nature water, dissolved organic matter (DOM)

plays an import role in the photolysis process. In addition to producing hydroxyl radicals, it also attenuates sunlight and scavenges free radicals, which in turn limits the rate of direct and indirect photolysis (Verma et al., 2007; Pan et al. 2009; Lam et al. 2004).

Biodegradation and biotransformation are likely the dominant removal mechanisms for ketoprofen, naproxen, gemfibrozil, ibuprofen and triclosan. Carbamazepine and diazepam are resistant to biodegradation, especially carbamazepine, which shows a half time of 5600 h ((Löffler et al. 2005; Verma et al., 2007; Lin et al 2006; Yamamoto et al. 2009; Tixier et al., 2003). Most antibiotics tested to date are resistant to biodegradation under aerobic conditions (Kümmerer 2009).

Sorption to sediment and suspended solids is significant for many pharmaceuticals (although some of them are hydrophilic). Especially, for many stable pharmaceuticals, sorption process controls their environmental behavior. Sorption by sediments and suspended matters could be effective removal mechanisms for some pharmaceutical compounds. Pharmaceuticals sorbed by suspended matters can be transported with suspended matter, and then deposit in receiving lakes. But sediments could be sources of pharmaceuticals in the absent of sediment removal (e.g. biological) mechanisms (Gurr et al., 2006). The sorption processes of some pharmaceuticals are quite complicated due to their amphiphilic characteristic (Pan et al., 2009), which are discussed in details in Section 2.2: *The Sorption of Pharmaceuticals*.



WWTPs are major sources of pharmaceuticals to rivers. For example, after being consumed by humans, antibiotics and their metabolites are excreted and then reach sewage treatment plants (STPs). Antibiotics can only be partially eliminated in STPs and eventually enter the environment, especially the water compartment (Kümmerer 2009). In order to ensure therapeutic effectiveness, pharmaceuticals are generally designed to be stable (Loffer et al., 2005). In Germany, 70% of the consumed antibiotics are excreted non-metabolized, which are still active (Kümmerer 2009).

Various contamination patterns of pharmaceuticals have been observed. Comoretto and Chiron (2005) reported that in a small Mediterranean river, concentrations of carbamazepine and bezafibrate were quite high in summer because in the dry season municipal wastewater accounted for the majority of the river water flow. However, Conely et al. (2008) reported that the maximum concentration of caffeine was observed during spring, probably due to low temperature and frequent rainfall events. Rainfall would cause increased flow in target STPs and reduce residence time in the STPs, thus increasing pharmaceutical levels in surface waters. The seasonal variation of carbamazepine was not as significant as that of caffeine, probably due to low removal efficiency of carbamazepine in the STPs. Vieno et al. (2005) also indicated that low temperature in wintertime resulted in lower biodegradation rate both in STPs and in rivers. And photo-degradation rate was also drastically reduced due to the river was covered by ice and snow. Thus maximum pharmaceutical levels were observed during March. Snow melting caused higher flow rate thus reduced residence time in the river. So

in March, pharmaceuticals can be more efficiently transported downstream and the risk of drinking water contamination was increased drastically.

## **2.2 The Sorption of Pharmaceuticals**

### ***2.2.1 Sorption Coefficient***

As an important mechanism related to the phase distribution and fate of contaminants, sorption processes of pharmaceuticals are more complex than general hydrophobic organic contaminants (HOCs), which have been extensively studied in labs during the past a few decades. For many pharmaceuticals, the sorption capacity is controlled by both the organic and the inorganic fraction of sediments due to their amphiphilic feature (Pan et al, 2009; Suntisukaseam et al., 2007; Kwon et al, 2008). For example, the moderate octanol-water partition coefficient ( $\log K_{ow}$ ) of carbamazepine, which is 2.45, indicates that the sorption of carbamazepine on organic matters is comparable to that of inorganic substances.

Because many pharmaceuticals are moderately hydrophobic, their sorption coefficients ( $K_d$ ) are positively related to organic contents of sediments. The Organic carbon normalized sorption coefficient ( $K_{OC}$ ) well represents the sorption capacity of HOCs onto soils or sediments. Generally,  $K_{OC}$  of HOCs can be derived from octanol-water partition coefficient ( $K_{ow}$ ), which is based on one-parameter linear free energy relationships (LFERs) (Eq. 1-4, Goss et al., 2001) or even from the chemical structure of HOCs by the fragment constant method (Tao et al. 1999).

$$K_{i12} = \frac{\text{Conc. of Chemical } i \text{ in Phase } 1}{\text{Conc. of Chemical } i \text{ in Phase } 2} = e^{-\Delta G_{i12} / RT} \quad (2.1)$$

In Eq. 2.1,  $K_{i12}$  is the partition coefficient between phase 1 and phase 2,  $\Delta G_{i12}$  is the free energy change of transfer from phase 2 to phase 1,  $R$  is the gas constant and  $T$  is the absolute temperature. Based on Eq. 2.1,  $K_{OC}$  and  $K_{OW}$  can be calculated by:

$$\ln K_{OC} = -\Delta G_{OC} / RT \quad (2.2)$$

$$\ln K_{OW} = -\Delta G_{OW} / RT \quad (2.3)$$

Thus, a linear relationship can be established between  $\ln K_{OC}$  and  $\ln K_{OW}$ :

$$\ln K_{OC} = (\Delta G_{OC} / \Delta G_{OW}) * \ln K_{OW} \quad (2.4)$$

However, for most pharmaceuticals, the sorption coefficients derived from  $K_{OW}$  significantly underestimate their sorption capacity. Moreover, various values of  $K_{OC}$  have been observed for each pharmaceutical on different sediments. The difference may span several orders of magnitude (Carballa et al, 2008, Yamamoto et al, 2009; Zhou et al., 2007). This indicates that factors other than hydrophobic interactions are also significant in sorption processes. Many pharmaceuticals can interact with both polar and nonpolar surfaces. Thus, specific polar interactions (H-bond) have significant impacts on the sorption process. The existence of aromatic rings, electron-donators and/or acceptors in both pharmaceuticals and sediments increases the sorption of pharmaceuticals. Therefore, the contribution of inorganic (mineral) fractions of sediments on the sorption process is important. For this reason, one-parameter LFERs well describe hydrophobic interactions, but fail to predict sorption of polar and ionic compounds. Also, normalizing observed  $K_d$

by organic content neglects the contribution of other factors, thereby showing large variations.

Sediment properties that may affect sorption process include type and amount of clay content, ion exchange capacity, hydrogen bonding, particle size, pore distribution, and surface charge density (Yamamoto et al. 2009; ter Laak et al. 2006). Chemical reaction occurs between pharmaceuticals and metal oxides in the sediment, which further complicates the reaction between pharmaceuticals and sediments (Strock et al. 2005).

According to the acidity constants ( $pK_a$ ) of pharmaceuticals, they could exist as cations, zwitterions or anions under certain pH ranges. Thus their sorption coefficients also depend on pH values since sediment particles are moderately negatively charged. For example, extremely basic pH range ( $>10.0$ ) could reduce the adsorption of bisphenol-A onto activated carbon due to the electrostatic repulsion between the bisphenolate anion and the slightly negatively charged surface of sediments (Tsai et al., 2006). Tetracycline has three  $pK_a$  values (3.3, 7.68 and 9.69), so pH is expected to significantly impact interactions of tetracycline with sediments (Gu et al, 2007). Complexation could be very significant for the sorption of some pharmaceuticals, especially zwitterionic species. In neutral or moderate acid condition, tetracycline exists in zwitterionic species. A portion of tetracycline could be bound to metals (Verma et al. 2007). Tetracycline forms strong 2:1 complexes with multivalent metal ions. Adding  $Ca^{2+}$  to humic acid would increase tetracycline sorption, indicating that the ternary complexation (humic acid-metal-tetracycline) may play an important role (Gu, 2007).

Ter Laak et al. (2006) quantified contributions of pH, organic carbon content, clay content, cation-exchange capacity, aluminum oxyhydroxide (AlOx) content, and iron oxyhydroxide (FeOx) content on sorption coefficients of three ionizable pharmaceuticals. Integrating all these properties could explain 78% of variations in sorption coefficients, which probably indicates that there are some other properties that significantly contribute to the sorption coefficients.

Non-ideal sorption of pharmaceuticals has been widely observed due to the heterogeneous nature of sediments (Pan et al., 2009). A soil/sediment particle involves three domains that participate into sorption process: exposed mineral surface (domain I), swollen amorphous organic matter (domain II) and condensed organic matter (domain III) (Weber et al 1996; Huang et al 1998). A composite model, the distributed reactivity model (DRM), has been developed to describe the different sorption mechanisms on different domains of soil/sediment particles (Weber et al. 1992; Huang et al, 1997a). It combines a linear model to simulate the linear sorption on amorphous organic matter and one or more Langmuir models, which are characterized by an asymptotic approach to some maximum sorption capacity (Q) and a factor relating to the affinity of the surface for the sorbate (b), to simulate the nonlinear sorption on condensed organic matter (Eq. 2.5).

$$q_{e,T} = K_{D,C} C_e + \sum_{i=1}^2 \left( \frac{Q_{a,i} b_i C_e}{1 + b_i C_e} \right) \quad (2.5)$$

Each Langmuir model represents the contribution of one component of a sediment particle. The sorption by amorphous organic matter is a phase distribution process and accounts for linear adsorption. The carbonaceous material with high surface area (black carbon) and hole-filling domain of the organic matters contribute to the nonlinear adsorption (Zeng et al. 2006).

However, because the sorption of pharmaceuticals is affected by many components of the sediments, the DRM model might not be adequate for simulating the sorption of pharmaceuticals on sediments. The Freundlich isotherm can result from the combination of several Langmuir isotherms occurring at different sites (site specific) and then is more applicable when the number of components contributing to sorption process increases. Tsai et al (2006) used the Freundlich and the Langmuir model to simulate the adsorption isotherm of bisphenol-A onto activated carbons. The Freundlich model yields better fit. The Langmuir model underestimates the sorbed fractions when bisphenol-A concentration is high because it only captures the adsorption on surface area (limited-site).

As discussed above, the sorption of pharmaceuticals is extremely complicated and is impacted by many factors. To better estimate the sorption capacity of pharmaceuticals, poly-parameter linear free energy relationships (PP-LFERs) have been introduced (Zukowska et al., 2006; Tülp et al 2008). PP-LFERs have been extensively used to evaluate the partition of chemicals under various systems (e.g., air/water) for their strong power of providing insights into the various intermolecular interactions that influence partition processes, especially for polar chemicals. It is possible to better estimate

sorption coefficients of pharmaceuticals between water and various types of solids by PP-LFERs because they can describe abilities of both sorbates and sorbents to engage in Van de Waals interactions or hydrogen-bond interactions (Goss et al. 2001). One wide application of PP-LFERs is linear solvation energy relationships (LSERs), which have been developed to simulate the partitioning between condensed phases by Abraham (1993) (Eq. 2.6) and recently have been applied to predict the equilibrium partition of pharmaceuticals under three systems: heptan/methanol, octanol/water and air/water (Tülp et al 2008).

$$\log K_{i,xy} = r_{xy}R_2 + s_{xy}\pi_2^H + a_{xy}\sum\alpha_2^H + b_{xy}\sum\beta_2^H + v_{xy}V + c \quad (2.6)$$

Where  $K_{i,xy}$  represents the partition property of chemical  $i$  between phase  $x$  and  $y$ ,  $R_2$  is excess molar refraction,  $\pi_2^H$  is dipolarity / polarizability,  $\sum\alpha_2^H$  is overall hydrogen-bond acidity (H-donating),  $\sum\beta_2^H$  is overall hydrogen-bond basicity (H-accepting),  $V$  is McGowan's characteristic volume of "cavity term", and  $c$  is a system constant.  $R_2$ ,  $\pi_2^H$ ,  $\sum\alpha_2^H$ ,  $\sum\beta_2^H$  and  $V$  are solute descriptors, representing the properties of the chemical. The corresponding phase descriptors ( $r_{xy}$ ,  $s_{xy}$ ,  $a_{xy}$ ,  $b_{xy}$  and  $v_{xy}$ ) describe the difference in capacity of any two phases participating into the same reactions.

Solute descriptors for some pharmaceutical compounds have been studied (Zukowska et al. 2006; Tülp et al., 2008). Tülp et al. (2008) determined solute descriptors for 76 diverse pesticides and pharmaceuticals, and derived partition coefficients of these chemicals in three systems: heptan/methanol, octanol/water and air/water using solute descriptors. Calculated values show most consistency with measured or literature values in

heptan/methanol system. However, the maximal deviations between measured and calculated values span several orders of magnitude for other two systems. Although PP-LFERs have the potential to better quantify the phase distribution of pharmaceuticals between water and sediments, their application is limited by available parameters describing the ability of pharmaceuticals and sediments to participate in Van der Waals interactions and H-bond interactions. Currently, only a few studies applied PP-LFERs to soil (sediment)/water systems. Poole and Poole (1999) reported the phase descriptors for the water/soil system and predicted  $K_{OC}$  for neutral organic compound using Eq. 2.7. The predicted  $K_{OC}$  are in reasonable agreement with literature values, which a regression coefficient ( $R^2$ ) of 0.907.

$$\log K_{OC} = 0.21(\pm 0.09) + 2.09(\pm 0.10)V_x + 0.74(\pm 0.04)R_2 - 0.31(\pm 0.09)\sum \alpha_2^H - 2.27(\pm 0.11)\sum \beta_2^0 \quad (2.7)$$

Poole and Poole's method cannot generate reasonable predictions for ionized compounds (e.g., carboxylic acids, phenols and amines) since it does not consider electrostatic interactions and ion exclusion. In contrast, pharmaceutical compounds may exhibit amphiphilicity and exist in ionized species. This limits the application of Poole and Poole's method to pharmaceuticals. Further, while most PP-LFERs are developed for high sorbate concentrations (i.e., near solubility of sorbates), they significantly underestimate  $K_{OC}$  values by up to 1 order of magnitude in a more environmentally relevant sorbate concentration range (Endo et al., 2009). Endo et al. (2009) derived PP-LFERs under a typical environmental sorbate concentration, and developed a correlation between the nonlinearity ( $1/n$  in Freundlich equation) and the sorbate dipolarity/polarizability descriptor (S) to estimate  $K_{OC}$  values at varying sorbate concentrations. One important drawback of previous PP-LFER studies is that currently they focus on the



prediction of  $K_{OC}$ . However,  $K_{OC}$  cannot reasonably represent the sorption of pharmaceuticals onto soils/sediments.

In order to adequately estimate sorption coefficients of pharmaceutical compounds onto soils and sediments, the following work should be achieved: 1) quantifying the sorbate descriptors for diverse pharmaceutical compounds; 2) developing correlations between solute (phase) descriptors of water/sediment system and  $K_d$ , instead of  $K_{OC}$ , under an environmentally relevant sorbate range; 3) addressing how properties of sediments are correlated to the values of phase descriptors.

### ***2.2.2 Sorption Kinetics***

Currently, most water quality models are based on the assumption of instantaneous sorption equilibrium. However, emerging contaminants (e.g., pharmaceuticals) exhibit large variations of sorption equilibrium time due to their properties and/or properties of sorbents. Table 2.1 lists the equilibrium times for the sorption of some emerging contaminants onto different types of sorbents. Further, the time to reach sorption equilibrium depends on sorbate concentrations. Yu et al. (2004) illustrated that estrogenic chemicals exhibited slower sorption rate when under sub-microgram per liter levels. Kinetic models are necessary to determine the phase distribution of chemicals exhibiting slow sorption behavior.

**Table 2-1 Sorption Equilibrium Time of Emerging Contaminants**

<i>Compounds</i>	<i>Sorbent</i>	<i>Sorption Equilibrium Time</i>
Beta-blockers <sup>a</sup>	Sediment	6 hr
Estradiol and testosterone <sup>b</sup>	Soils	48 – 72 hr
Atorvastatin <sup>c</sup>	Soils/sediments	72 hr
Tetracycline <sup>d</sup>	Humic acid	72 hr
Estrogens <sup>e</sup>	Soils/sediments	10 –14 d

<sup>a</sup>. Ramil et al., 2010; <sup>b</sup>. Sangsupan et al., 2006; <sup>c</sup>. Ottmar et al., 2010a; <sup>d</sup>. Gu et al., 2007; <sup>e</sup> Yu et al., 2004

It has been reported that sorption onto sediment particles initially exhibits high sorption rates, which decrease over time (Yu et al., 2004). This behavior is indicative of multiple-domain features of sediment particles. As discussed in *Section 2.2.1*, a heterogeneous sediment particle consists of three domains: an exposed inorganic mineral domain (Domain I), a highly swollen amorphous organic domain (Domain II) and a condensed organic matter domain (Domain III). Each domain exhibits different sorption behaviors (Weber et al, 1996; Huang et al., 1998). Exposed mineral surfaces show low sorption capacity for hydrophobic chemicals. Domain II engages in linear absorption processes, and sorption rates (i.e., diffusion rates) in this domain are very fast. Finally, Domain III, which is physically covered by Domain II, consists of condensed organic matter. Chemicals exhibit low diffusion rates in this domain and can only reach this domain after they penetrate Domain II. Chemicals can penetrate Domain II in several minutes, corresponding to fast sorption rates at the initial stage. Diffusion of chemicals into condensed soil/sediment organic matter (SOM) matrices likely controls the overall rate of sorption by sediments. Weber et al. (1996) reported that the linearity of sorption process was also time-dependent. The linearity drops from 0.93 at a reaction time of 1 h to 0.73

after 1 d, strongly suggesting that the linear absorption occurs in Domain II and nonlinear adsorption occurs in Domain III. Heterogeneity of sediment should be considered when simulating the sorption kinetics of pharmaceuticals.

Sorption-desorption hysteresis has been widely observed for both HOCs and pharmaceuticals and is quantified using the Hysteresis Index (Williams et. al., 2006; Gu et al., 2007, Huang et al., 2003; Ran et al. 2004, Stein et al., 2008). Desorption hysteresis could be caused by the slow desorption kinetics (Miller and Pedit; Stein et al., 2008), sediment heterogeneity (Weber et al, 1992) and/or sorbate-induced pore deformation (Sander and Pignatello, 2005). Miller and Pedit (1992) illustrated that equilibrium distribution between the aqueous (dissolved) and sorbed phase was not actually achieved after a desorption step due to sufficiently slow desorption rates. This likely suggests that the sorption-desorption hysteresis would be less apparent if the reaction time is sufficiently long. Pignatello and Xing (1996) pointed out that slow desorption rates may be caused by high activation energy of sorptive bonds, since the activation energy of desorption is generally greater than that of sorption. As adsorption could be unactivated or slightly activated thus achieving equilibrium instantaneously when chemicals reach specific sorption sites, desorption of large molecules should be activated. Thereby, desorption is rate-limited by both mass transfer (diffusion) and the release of chemicals from sorption sites, which further slows down desorption processes.

Hysteresis may also result from irreversible processes, such as entrapment of sorbed molecules in meso- and micro-pores within inorganic components of natural sorbents,

and entrapment of sorbed molecules in the SOM matrix. More pronounced desorption hysteresis was observed in sediment sample containing higher content of condensed SOM matrix (Huang et al, 1997b; Weber et al, 1998; Ran et al, 2004). The irreversible bonding between the molecule and organic matter surfaces, and hole-filling domain, are thought to be the reason for the hysteresis (Zeng et al. 2006). Gu et al. (2007) attributed the hysteretic behavior of tetracycline to a significant fraction of tetracycline being irreversibly retained in the humic acid through physical entrapment. Sander and Pignatello (2005) ascribed the sorption-desorption hysteresis of naphthalene, when being sorbed onto lignite, to structural deformation of the sorbents (i.e., swelling). Pore-deformation may occur by via dilation of existing holes, due to thermal motions of the sorbate, or via creation of new holes by incoming sorbates.

Some models have been developed to describe sorption kinetics of chemicals from aqueous phase onto solids. Among them, the Elovich model, fractal model, pseudo-first-order model, pseudo-second-order model and diffusion model have been extensively used. While most models are used to simulate adsorption processes, heterogeneity of sediment particles should be considered when applying them to pharmaceutical compounds.

### ***Elovich Model***

The Elovich Model was originally developed to describe the adsorption of gases on solids and recently was applied to simulate the aqueous phase adsorption of chemicals onto solids (Cheung et al., 2001; Li 2006). The Elovich model can be written as (Cheung et al., 2001):

$$\frac{dq_t}{dt} = a \exp(-bq_t) \quad (2.8)$$

Integrating Eq. 2.8 yields:

$$q_t = \frac{1}{b} \ln[abt + \exp(-bq_0)] \quad (2.9)$$

In Eq. 2.8 and 2.9,  $q_t$  is the sorption capacity at time  $t$ ,  $a$  and  $b$  are constants, and  $q_0$  is the sorption capacity at time  $t = 0$ .

### ***Fractal Model***

The theory of fractals has attracted much interest for it can account for the structures of irregular sorbents and the processes in porous materials. It generally has been applied to simulate the adsorption kinetics on activated carbon (AC). An irregular sorbent (e.g., AC) can be characterized by the pore fractal, the surface fractal and the mass fractal. The sorption process on AC is heterogeneous and may involve chemical interactions, electrostatic interactions, Van de Waals, H-bonding and hydrophobic interactions (Gaspard, et al., 2006). Fractal kinetic can be capable of simulating the complex sorption processes. A general equation of fractal kinetics has been developed (Brouers and Sotolongo-Costa, 2006; Gaspard, et al., 2006):

$$-\frac{dC}{dt^\alpha} = K_{\alpha,n} C^n \quad (2.10)$$

Where  $\alpha$  is a fractional time index,  $n$  is a fractional reaction order, and  $C$  is the chemical concentration.

In a similar way, the pseudo-  $(n, \alpha)$  equation for the adsorbed chemicals can be introduced as

$$\frac{dq_t}{dt} = K_{\alpha,n} (q_e - q_t)^n \quad (2.11)$$

Where  $K_{\alpha,n}$  is the rate constant,  $q_t$  is amount of chemicals adsorbed onto solids at time  $t$ ,  $q_e$  is the amount adsorbed at equilibrium and  $n$  indicates the order of reactions.

If  $n = 1$ , the integration form of Eq. 2.11 is

$$\ln(q_e - q_t) = \ln(q_e - q_0) - K_{\alpha,1} t^\alpha \quad (2.12)$$

Where  $q_0$  is the amount of sorbed chemicals at time  $t = 0$ .

If  $\alpha = 1$ , Eq. 2.12 becomes the *pseudo-first-order model* of Lanergen.

If  $n > 1$ , integrating form of Eq. 2.11 gives

$$(q_e - q_t)^{1-n} = (q_e - q_0)^{1-n} - (n-1)K_{\alpha,n} t^\alpha \quad (2.13)$$

Eq. 2.13 reduces to *pseudo-second-order model* if  $n = 2$  and  $\alpha = 1$ .

### ***Diffusion Model***

While above models have been widely used to simulate *adsorption* kinetics and can well describe heterogeneity of sorbents, they are basically semi-empirical equations and can hardly explain mechanisms of sorption processes. Various diffusion models (e.g., pore and surface diffusion model, and retarded pore diffusion model) have been developed for porous media (e.g., a sediment particle) to capture the detailed steps and mechanisms of sorption processes. According to these models, sorbate molecules in porous water move

from high-concentration areas to low-concentration areas by diffusion. Once they reach available sorption sites (e.g., pore walls), local sorption reaches equilibrium instantaneously. Thereby, the times to reach sorption equilibrium are actually controlled by mass transfer rates of sorbate molecules in porous media, which are retarded by local sorption and properties of sediment particles (e.g., porosity and tortuosity) (Rügner et. al., 1999). The diffusion of solutes in spheres can be described by Fick's second law in spherical coordinates:

$$\frac{\partial C(r)}{\partial t} = D \left[ \frac{\partial^2 C(r)}{\partial r^2} + \frac{2}{r} \frac{\partial C(r)}{\partial r} \right] \quad (2.14)$$

Where  $C$  is solute concentrations in porous water,  $r$  is the radial distance from the center of the sphere,  $D$  is the diffusion rate constant.

In porous media, which can be modeled as spheres, the change of total sorbate concentrations in the media is controlled by diffusion of dissolved-phase sorbates in pore water, so Eq 2.14 can be written as (Wu et al., 1986):

$$\frac{\partial S(r)}{\partial t} = D\epsilon \left[ \frac{\partial^2 C(r)}{\partial r^2} + \frac{2}{r} \frac{\partial C(r)}{\partial r} \right] \quad (2.15)$$

Where  $S(r)$  is the total chemical concentration in porous media and  $\epsilon$  is the porosity. The concentration gradient of dissolved-phase chemicals causes the change of total concentrations. Note that porosity indicates the area in through which molecules flow in the porous media.

When considering sorption, the following two equations are introduced:

$$S(r) = (1 - \varepsilon)\rho_s q(r) + \varepsilon C(r) \quad (2.16)$$

$$q(r) = K_d C(r) \quad (2.17)$$

Where  $S(r)$  is the total concentration of sorbate in porous media,  $q(r)$  is the sorbed-phase concentration,  $K_d$  is sorption coefficient and  $\rho_s$  is the solid density.

Combining Eq. 2.15-2.17 yields:

$$\frac{\partial S(r)}{\partial t} = D_{eff} \left[ \frac{\partial^2 S(r)}{\partial r^2} + \frac{2}{r} \frac{\partial S(r)}{\partial r} \right] \quad (2.18)$$

Where:

$$D_{eff} = \frac{D\varepsilon}{[(1 - \varepsilon)\rho_s K_d + \varepsilon]} \quad (2.19)$$

is the effective diffusion coefficient. From Eq. 2.19, high  $K_d$  retards diffusion process since less sorbate molecules are in the dissolved phase. The correlation between effective diffusion coefficient and first-order rate constant can be described as (Wu and Gschwend, 1988; Gong and Depinto, 1998):

$$k = \alpha \frac{D_{eff}}{r^2} \quad (2.20)$$

Where  $k$  is the first-order rate constant and  $\alpha$  is a correlation factor that depends on time and system factors (e.g., pore size). Thus  $k$  is not a constant. Rügner et al. (1999) incorporated the impact of the tortuosity of sorbents and the nonlinearity of sorption, and re-wrote effective diffusion coefficient as:

$$D_{eff} = \frac{D\varepsilon}{(\varepsilon + K_{Fr} 1/n C^{1/(n-1)} \rho_s) \tau_f} \quad (2.21)$$



Where  $\tau_f$  is the tortuosity factor, and  $K_{Fr}$  and  $1/n$  are Freundlich parameters.

A more sophisticated diffusion model, the pore and surface diffusion model, has been promoted to describe more detailed steps in the sorption process. It assumes that the sorption process contains several steps from the liquid phase to porous surface: 1) diffusion in liquid phase; 2) external mass transfer (diffusion in a hydrodynamic film surrounding a porous sorbent); 3) intrapartical diffusion, which includes porous diffusion (a) and surface diffusion (b); and 4) adsorption on the sites (Yong, 2007; Weber and Smith, 1987). Step 1 is much faster than Steps 2 and 3, and Step 4 occurs instantaneously. Thus the whole sorption rate is controlled by the mass transfer rate in the second and third step, which is driven by concentration gradients. This model has been successfully used to describe the adsorption of pollutants onto granular activated carbon (GAC) (Yong, 2007; Yu et al., 2009).

Although diffusion models can explain mechanisms, they need more parameters, some of which are generally difficult to acquire. Further, under most circumstances, numerical methods should be applied to solve governing equations thereby hugely increasing computational time.

### **2.3 The Patuxent River**

The Patuxent River, a tributary of the Chesapeake Bay in Maryland, has been the subject for many water quality studies and has been a test-bed for management strategies (Weller et al., 2003; Breitburg et al., 2003). A map of the Patuxent Watershed is displayed in

Figure 2-1. Middle Patuxent River, Little Patuxent River and Western Branch are the three largest tributaries of the Patuxent River. Middle Patuxent River flows into the Little Patuxent River, which then joins the Patuxent River at Route 50 near Bowie, Maryland. The river further downstream Bowie (the Lower Patuxent River) then becomes a tidal estuary. The watershed area of the Patuxent is approximately 2,290 km<sup>2</sup> (Nice, 2006), 28% of which is in the Piedmont Province and the remainder is in the Coastal Plain (Weller, 2003). The land use of the Patuxent Watershed primarily consists of residential (17.7%), agriculture (28.9%), forest and wetlands (48.5%), and other developed land (4.9%) (Bockstael, 1996). Thus, the physiochemical processes in the Patuxent River are relatively uncomplicated compared with industrialized areas, which makes the Patuxent River a good test-bed for water quality issues (e.g., eutrophication).

In this research, a 100-km branch of the Patuxent River, which is bounded upstream by the Patuxent River at Route 50 near Bowie and downstream by the river mouth meeting the Chesapeake Bay, is used as a test-bed to evaluate the contribution of natural attenuation processes on the fate and transport of pharmaceuticals in natural aquatic systems. The study area is actually a tidal estuary and the upstream boundary is the limit of tidal intrusion. Totally, there are 42 tributaries flowing into the study area, including the upper Patuxent River at Route 50 and the Western Branch.

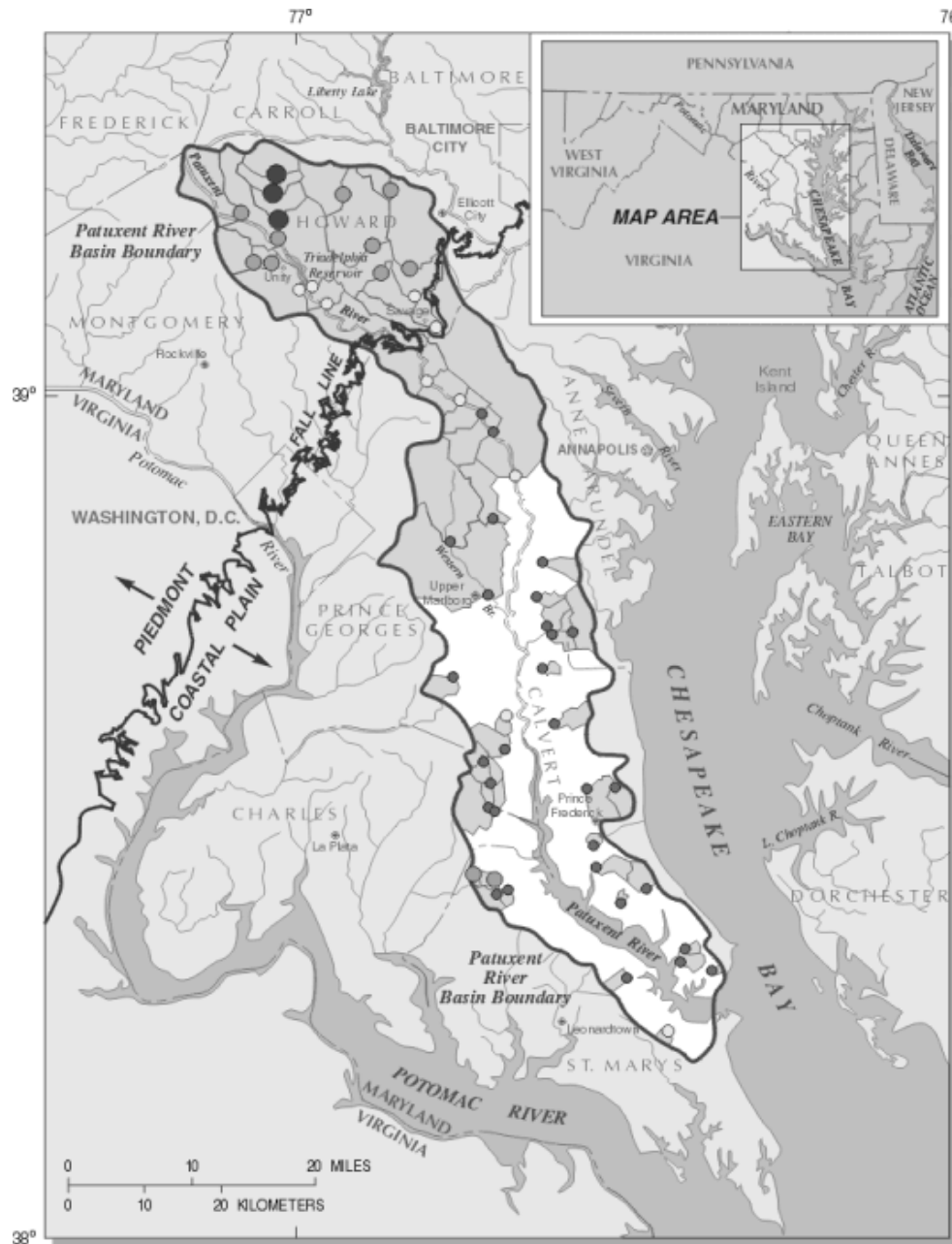


**Figure 2-1 The Patuxent Watershed (adapted from Bachman and Krantz, 2000)**

A water quality model, the Patuxent Model, was previously developed to simulate the fate and transport of conventional pollutants in the Patuxent River and address various water quality issues (Lung and Bai, 2003; Nice and Lung, 2008; Lung and Nice, 2007). It is based on the modeling framework of CE-QUAL-W2, which is a two-dimensional

(longitudinal-vertical) hydrodynamics and water quality model for surface water systems, such as rivers, estuaries and lake. CE-QUAL-W2 uses the finite difference method to predict surface elevations, and vertical and horizontal velocities by solving laterally averaged continuity equations and two laterally averaged momentum equations (Cole and Wells, 2000). The Patuxent Model performs hydrodynamic and mass transport calculations as well as reaction kinetics for pollutants (Nice, 2006). Its hydrodynamic component has been well calibrated and is capable of describing complicated mass transport in estuaries. Thus it was the starting point for this research.

## **Chapter 3: Modeling Sorption Kinetics of Pharmaceuticals in Fate and Transport Analyses**

### **3.1 Introduction**

Water quality models are widely applied to simulate the fate and transport of contaminants in natural waters. While most current water quality models are based on the assumption of instantaneous sorption equilibrium, some pharmaceutical compounds exhibit slow sorption rates and very long times (in days) to reach equilibrium (Stein et al., 2008; Yu et al., 2004), strongly suggesting that the assumption of instantaneous sorption equilibrium is invalid. Thus the predictions from traditional instantaneous-equilibrium based water quality models may not be accurate. Further, the amphiphilic nature of some pharmaceuticals compounds may render their sorption behavior more complex than that of conventional organic compounds (Pan et al., 2009). Also, several studies have illustrated that sorption to sediments/suspended materials can be a significant removal mechanism for pharmaceutical compounds in rivers (Gurr et al., 2006; Lin et al., 2006). Thus, there is an urgent need to improve quantification of pharmaceuticals' sorption behavior in rivers so that their environmental behavior can be better understood. Although the sorption kinetics of some pollutants, including a few pharmaceutical compounds, has been previously analyzed at laboratory scales, its implications for the fate and transport of pollutants in the natural environment have not been studied. The purpose of this study is to develop a modeling framework, based on previous models by Lung and Bai (2003) and Nice and Lung (2008), to quantify how sorption kinetics, when acting alone or in conjunction with other processes, affects the fate and transport of pharmaceuticals in the water/sediment systems.

A first hypothesis of this study is that traditional water quality models will under-predict pollutant concentrations in a water column, and thus exposure to wildlife, because they do not account for slow sorption kinetics and cannot accurately capture distribution between pharmaceuticals in the dissolved phase and the sorbed phase. Since sorbed-phase and aqueous-phase chemicals exhibit different environmental behaviors (e.g., accumulation into riverbeds for sorbed-phase compounds), a second, related, hypothesis for this study is that slow sorption kinetics may cause reduced removal of pharmaceuticals from water columns compared to what is normally predicted by instantaneous equilibrium models. As a result, slow-sorbing pharmaceutical compounds are actually transported downstream more efficiently than has been predicted by traditional fate and transport models. In this study, two otherwise identical fate and transport models, based on instantaneous sorption equilibrium or sorption kinetics, were used to simulate the distribution of hypothetical pharmaceuticals in natural water/sediment systems, in order to evaluate the two hypotheses noted above.

## **3.2 Materials and Methods**

### ***3.2.1 Study Area***

The simulation area is the 100-km branch of the Patuxent River, bounded upstream by the river at Route 50 near Bowie, Maryland and downstream by the river mouth. The whole simulation area is a tidal estuary. There are 42 tributaries flowing into the focused branch (including the upper Patuxent River at Route 50) and the Western Branch is the major tributary. Effluents from municipal WWTPs are the major sources of

pharmaceuticals into the simulation area. There are ten major WWTPs in the Patuxent Watershed with design flow > 0.5 MGD: eight are located along the upper Patuxent River, and two are located along the Western Branch (Figure 3-1). The effluent volume and served population of each WWTP is displayed Table 3-1. There are 10 Chesapeake Bay Program (CBP) monitoring stations (TF 1.3 - TF 1.7, RET 1.1, and LE 1.1 – LE 1.4) in the study area, which are shown in Figure 3-2.

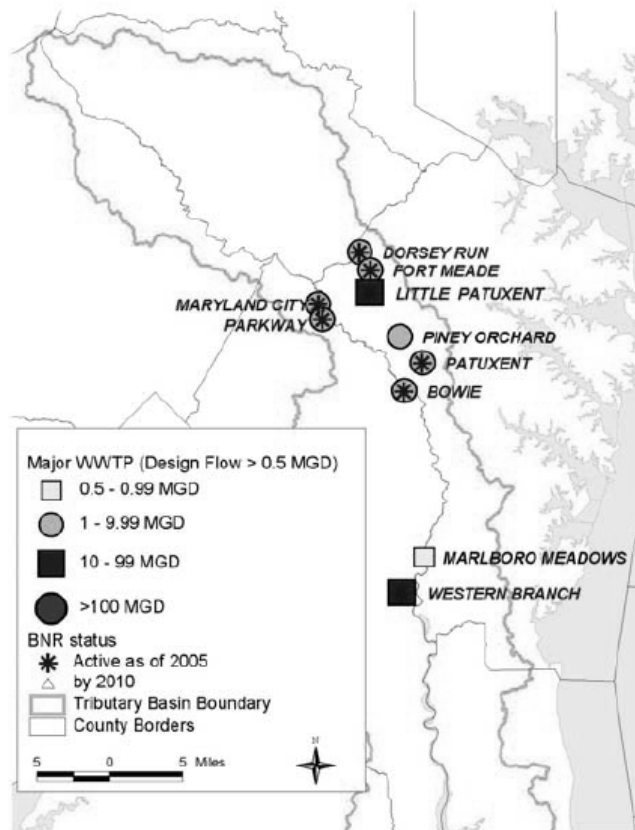


**Figure 3-1 Wastewater Treatment Plants in the Patuxent Watershed (adapted from Renee et al., 2007)**

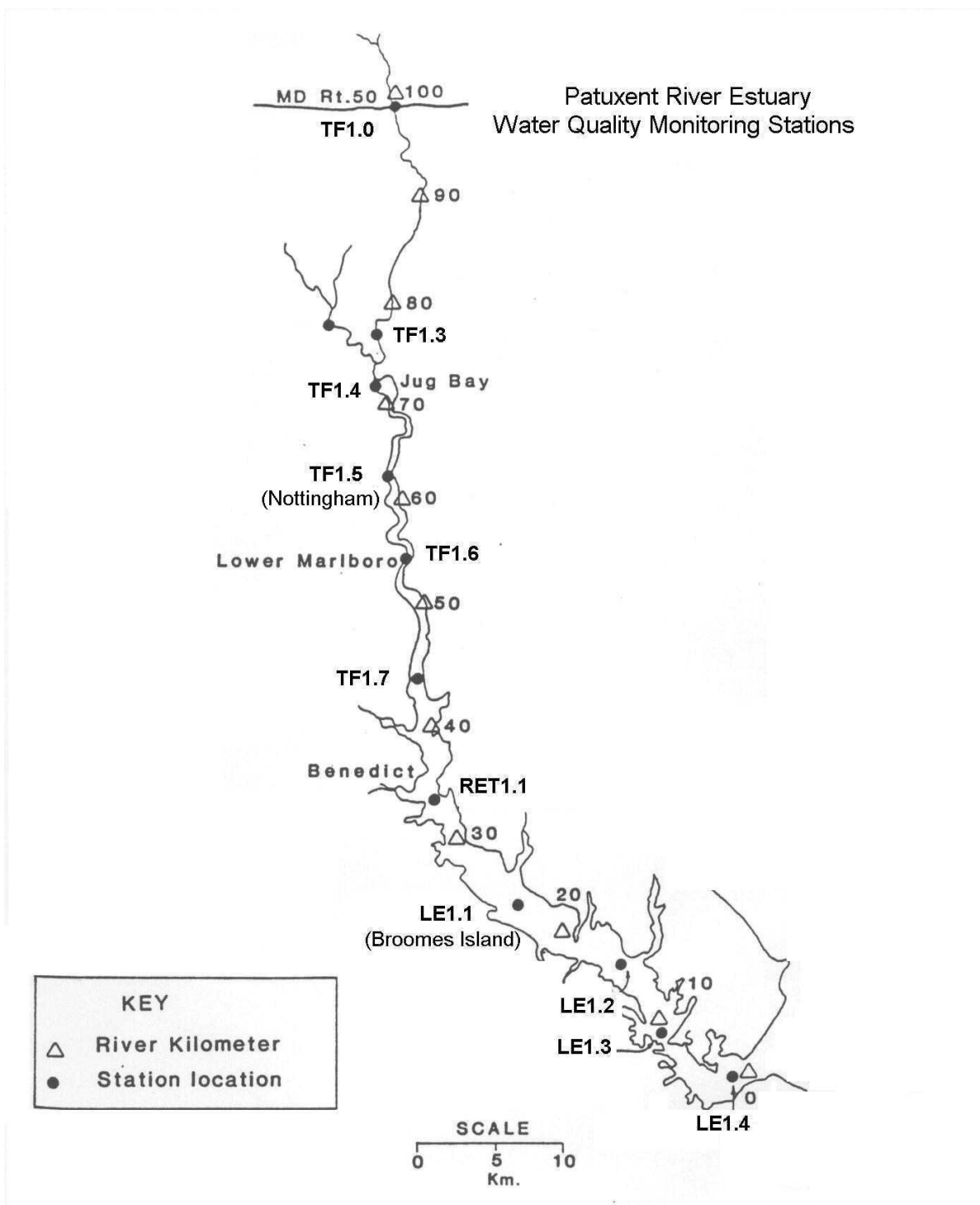


**Figure 3-2 Monitoring Station Locations in the Patuxent Estuary (adapted from Nice, 2007)**



**Table 3-1 Effluent Volume of Wastewater Treatment Plants and Estimated Population Served**

<i>Wastewater Treatment Plant</i>	<i>Annually Averaged Effluent Volume in 2005(MGD) <sup>a</sup></i>	<i>Estimated Population Served <sup>b</sup></i>	<i>Population in Surrounding Area (3-mile Radius) <sup>c</sup></i>
DORSEY RUN	1.2	5,742	38,390
FORT MEADE	1.8	N/A	36,376
LITTLE PATUXENT	18	175,000	23,992
MARYLAND CITY	1.1	9,458	N/A
PARKWAY	6	55,800	49,915
PINEY ORCHARD	0.5	N/A	28,303
PATUXENT	0.33	N/A	8,828
BOWIE	1.7	N/A	45,892
MARLBORO	5.1	N/A	42,497
MEADOWS			
WESTERN BRANCH	19	194,900	7,943

<sup>a</sup>. Rennee et al., 2007; <sup>b</sup>. Maryland Department of the Environment, website: <http://www.mde.state.md.us>; <sup>c</sup>. EPA Facility Registry System (FRS) Query, available online at [http://www.epa.gov/enviro/html/fii/fii\\_query\\_java.html](http://www.epa.gov/enviro/html/fii/fii_query_java.html)

### **3.2.2 Numerical Models**

The Patuxent Estuary Model was previously developed to simulate the fate and transport of conventional pollutants in the Patuxent River (Lung and Bai, 2003; Lung and Nice, 2007; Nice and Lung, 2008). It links hydrodynamics and mass transport to a water quality component, which calculates reaction kinetics for constituents including chlorophyll *a*, dissolved oxygen, nitrate, ammonia, phosphate, arsenic, copper and cadmium. It was chosen as a starting point for the current study because the hydrodynamic component has been previously well calibrated. The model consists of 163 longitudinal and 39 maximum vertical grids (Figure 3-3). For this study, a sorption kinetics module and a sediment transport module were developed and linked to the existing hydrodynamic model to simulate the sorption behavior of pharmaceuticals and also capture interactions between the water column and sediments.

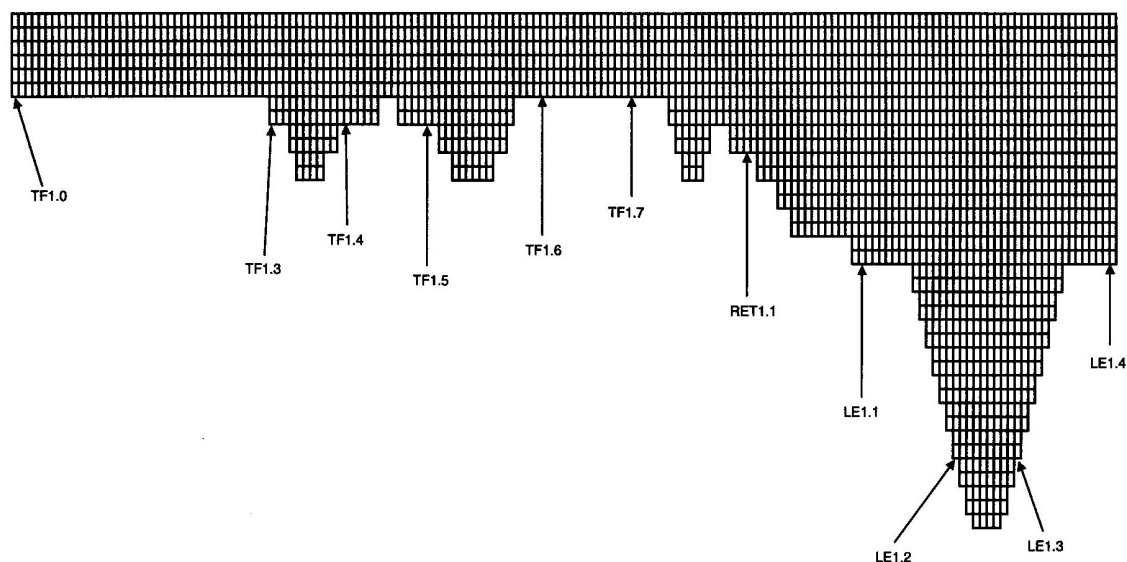


**Figure 3-3 Grid Setup for the Patuxent Model (adapt from Nice, 2007)**

### **3.2.3 Target Compounds**

Emerging contaminants (e.g., some pharmaceuticals) may exhibit a large range of sorption rates (i.e., time to reach equilibrium –  $t_e$ ) onto sediments. For example,  $t_e$  values may be  $\leq 6$  hours for some beta-blockers (Ramil et al., 2010), 2 days for diazepam (Stein et al., 2008), and 10-14 days for some estrogens (Yu et al., 2004). The sorption coefficient ( $K_d$ ) of pharmaceuticals onto soils or sediments also shows large variability, from 0.4 L/kg for sulfathiazole to 312,447 L/kg for tetracycline (Pan et al., 2009). Moreover, the  $K_d$  value of a single pharmaceutical compound may vary significantly for sorption onto different sediments (Yamamoto et al., 2009). For this study, four hypothetical pharmaceuticals were chosen to represent the possible combinations of  $K_d$  and  $t_e$ : high  $K_d$  + high  $t_e$ , high  $K_d$  + low  $t_e$ , low  $K_d$  + high  $t_e$  and low  $K_d$  + low  $t_e$ .

High and low values were selected based on literature values:  $K_{d,HIGH} = 10,000$  L/kg and  $K_{d,LOW} = 80$  L/kg for sorption coefficient, and  $t_{e,HIGH} = 10$  d and  $t_{e,LOW} = 12$  h. Each contaminant was evaluated under both a sorption kinetics scenario and an instantaneous sorption equilibrium scenario. In order to better address the effects of sorption kinetics, all hypothetical pharmaceuticals are assumed to be conservative substances (i.e., degradation was not considered).

### **3.3 Improving Modeling Framework**

#### ***3.3.1 Sorption Kinetics Model***

In order to describe mechanisms of sorption process as well as save computational efforts, sorption kinetics models were developed based on the theory of intraparticle pore diffusion (Wu et al., Rügner et al., 1999; Fan et al., 2006). In addition, the multiple domain features of sediment particles are considered by the kinetics model. According to the theory of intraparticle pore diffusion, sorption occurs instantaneously when chemicals reach sorption sites. However, in porous media (e.g., sediment particles), mass transfer is controlled by diffusion into the pore water. Sorption onto pore walls (local sorption) and particle properties (e.g., tortuosity) retard the diffusion of chemicals, thereby slowing down the sorption process (Rügner et al., 2004). It has been reported that sorption onto sediment particles initially exhibits high sorption rates, which decrease dramatically over time (Yu et al., 2004). This behavior is indicative of multiple-domain features, whereby a heterogeneous sediment particle consists of three domains: an exposed inorganic mineral domain (Domain I), a swollen amorphous organic domain (Domain II), and a condensed organic matter domain (Domain III). Each domain exhibits different sorption behavior. Domain I shows very low sorption capacity for hydrophobic chemicals. Domain II

engages in linear absorption processes with very fast sorption rates (i.e., diffusion rates). Finally, Domain III exhibits low diffusion rates, whereby diffusion into this domain likely controls the overall rate of sorption by sediments (Weber et al., 1996; Huang et al., 1998)

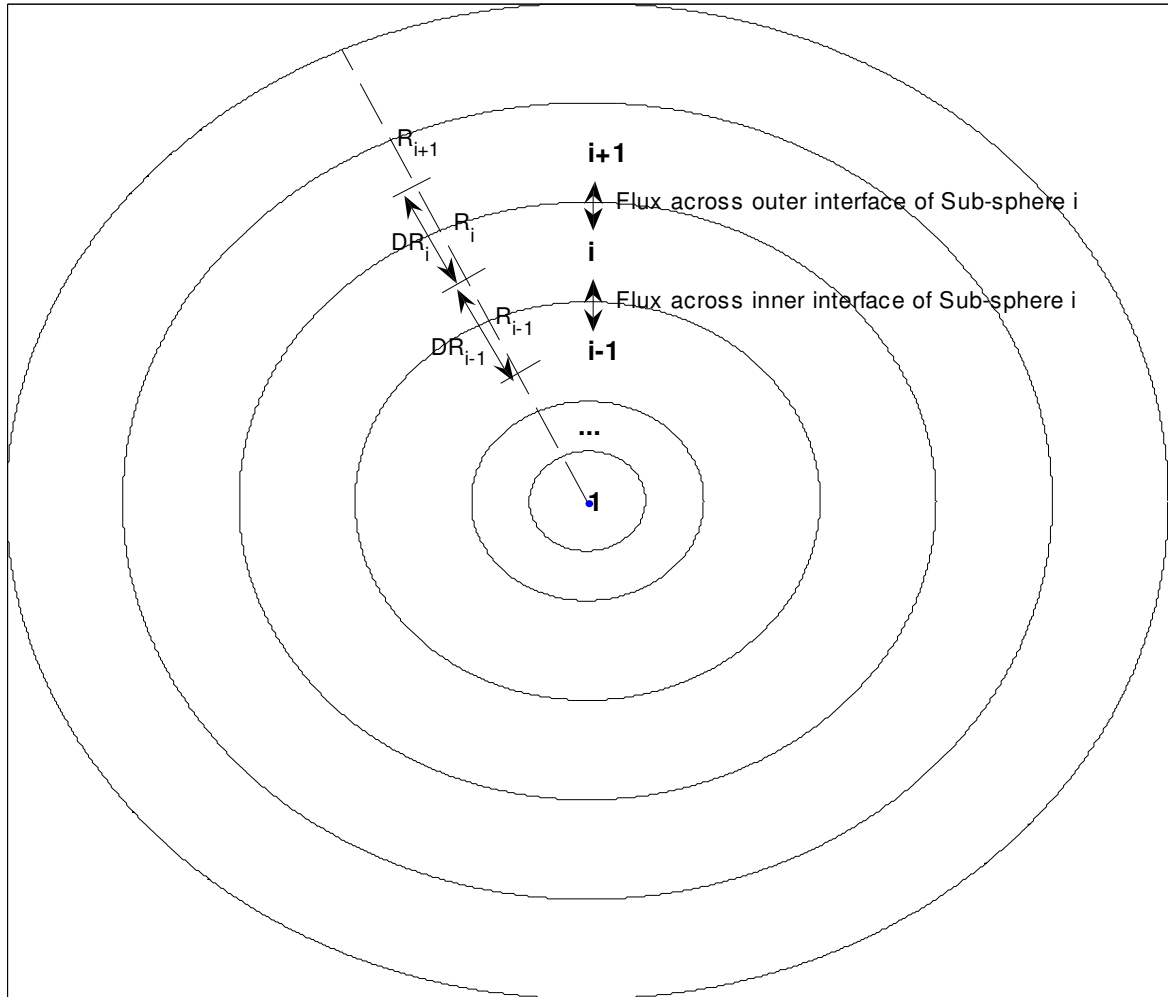


**Figure 3-4 Modeling Sediment Particles**

The finite-volume method is adopted to obtain a numerical solution for the governing equation of intraparticle pore diffusion adapted from Wu et al. 1986. A sediment particle is modeled as a sphere that has been sub-divided into several concentric spheres. Chemicals enter or leave one sub-sphere through diffusion, which is driven by concentration gradient (Figure 3-4). Different diffusion rates are assigned to concentric spheres representing different sediment domains (Domains II and III).

In 3-dimension, the flux across outer interface or inner interface of the sub-sphere  $i$  can be calculated by

$$OuterFlux = D_a A_{outer} \frac{C_{i+1} - C_i}{\Delta R_i} \quad (3.1)$$

$$InnerFlux = D_a A_{inner} \frac{C_i - C_{i-1}}{\Delta R_{i-1}} \quad (3.2)$$

Where  $D_a$  is the diffusion coefficient,  $\Delta R_i$  and  $\Delta R_{i-1}$  are the diffusion distances (Figure 3-4),  $A_{outer}$  and  $A_{inner}$  are surface area (diffusion area) of the outer interface and inner interface, respectively, and  $C$  is the dissolved-phase sorbate concentration (subscripts indicate sub-spheres).  $\Delta R_{i+1}$ ,  $\Delta R_i$ ,  $A_{outer}$  and  $A_{inner}$  can be calculated by:

$$\Delta R_i = \frac{R_{i+1} - R_i}{2} + \frac{R_i - R_{i-1}}{2} \quad (3.3)$$

$$\Delta R_{i-1} = \frac{R_i - R_{i-1}}{2} + \frac{R_{i-1} - R_{i-2}}{2} \quad (3.4)$$

$$A_{outer} = 4\pi R_i^2 \cdot \varepsilon \quad (3.5)$$

$$A_{inner} = 4\pi R_{i-1}^2 \cdot \varepsilon \quad (3.6)$$

Where  $R$  is the radius of sub-spheres (Figure 3-4) and  $\varepsilon$  is the porosity. So the mass change rate in the sub-sphere  $i$  can be written as:

$$\Delta V \frac{\partial S_i}{\partial t} = \text{Outerflux} - \text{Innerflux} \quad (3.7)$$

Where  $S_i$  is the total sorbate concentration in sub-sphere  $i$ , and  $\Delta V$  is the volume of sub-sphere  $i$  and is calculated by:

$$\Delta V = \frac{4}{3}\pi R_i^3 - \frac{4}{3}\pi R_{i-1}^3 \quad (3.8)$$

Combining Eq. 3.1 – 3.6 yields:

$$\frac{\Delta S_i}{\Delta t} = D_a \varepsilon \left[ R_i^2 \frac{C_{i+1} - C_i}{\Delta R_i} - R_{i-1}^2 \frac{C_i - C_{i-1}}{\Delta R_{i-1}} \right] \frac{3}{(R_i^3 - R_{i-1}^3)} \quad (3.9)$$

Eq 3.9 has been applied to calculate the time-dependent values of  $S_i$ . Note that for the inner most sub-sphere (Sub-sphere 1), there is no inner flux. The mass change rate of this sub-sphere is only determined by the flux crossing outer interface (i.e. the interface between Sub-sphere 2 and Sub-sphere 1). This removes the problem of zero-denominator (the term  $\frac{2}{r} \frac{\partial C(r)}{\partial r}$  in Eq. 2.15).

The relationship between  $S_i$  and  $C_i$  can be established by combining Eq. 2.16 and 2.17:

$$S_i = [(1 - \varepsilon)\rho_s K_d + \varepsilon]C_i \quad (3.10)$$

Where  $\varepsilon$  is the porosity of sediment particles,  $\rho_s$  is the solid density and  $K_d$  is the sorption coefficient. Then,  $S_i$  can be calculated directly by:

$$\frac{\Delta S_i}{\Delta t} = \frac{D_a \varepsilon}{(1 - \varepsilon)\rho_s K_d + \varepsilon} \left[ R_i^2 \frac{S_{i+1} - S_i}{\Delta R_i} - R_{i-1}^2 \frac{S_i - S_{i-1}}{\Delta R_{i-1}} \right] \frac{3}{(R_i^3 - R_{i-1}^3)} \quad (3.11)$$

**Consistency of the Scheme.** If the scheme was consistent to the original partial differential equation (Eq. 2.15), it should be reduced to the equation when  $\Delta R$  is approaching zero. Note that if the radii of Sub-spheres, the  $R_s$ , are equally spaced, following equation is satisfied:

$$\Delta R = \Delta R_i = \Delta R_{i-1} = R_{i+1} - R_i = R_i - R_{i-1} \dots \quad (3.12)$$

Thus Eq. 3.9 can be written as:

$$\frac{\partial S_i}{\partial t} = D_a \mathcal{E} \left[ R_i^2 \frac{C_{i+1} - C_i}{\Delta R} - (R_i - \Delta R)^2 \frac{C_i - C_{i-1}}{\Delta R} \right] \frac{3}{\Delta R [R_i^2 + R_i(R_i + \Delta R) + (R_i + \Delta R)^2]} \bigg|_{\Delta R \rightarrow 0} \quad (3.13)$$

By rearranging, Eq 3.13 becomes:

$$\frac{\partial S_i}{\partial t} = D_a \mathcal{E} \left[ \frac{R_i^2 (C_{i+1} - C_i)}{\Delta R} - \frac{C_i - C_{i-1}}{\Delta R} + \frac{2R_i \Delta R (C_i - C_{i-1})}{\Delta R} - \frac{\Delta R^2 (C_i - C_{i-1})}{\Delta R} \right] \frac{3}{3R_i^2 + 3R_i \Delta R + \Delta R^2} \bigg|_{\Delta R \rightarrow 0} \quad (3.14)$$

Since  $\Delta R \rightarrow 0$ ,  $3R_i^2 \gg 3R_i \Delta R + \Delta R^2$ . Then Eq. 3.14 is transformed to:

$$\frac{\partial S_i}{\partial t} = D_a \mathcal{E} \left[ \left( \frac{R_i^2}{R_i^2} \frac{C_{i+1} - C_i}{\Delta R} - \frac{C_i - C_{i-1}}{\Delta R} \right) \bigg|_{\Delta R \rightarrow 0} + \frac{2}{R_i} \frac{(C_i - C_{i-1})}{\Delta R} \bigg|_{\Delta R \rightarrow 0} - (C_i - C_{i-1}) \bigg|_{\Delta R \rightarrow 0} \right] \quad (3.15)$$

, which can be reduced to

$$\frac{\partial S(r)}{\partial t} = D_a \mathcal{E} \left[ \frac{\partial^2 C(r)}{\partial r^2} + \frac{2}{r} \frac{\partial C(r)}{\partial r} \right] \quad (3.16)$$

Thus the numerical scheme, Eq. 3.9, is consistent to the original governing equation for pore diffusion, Eq. 2.15.

**Stability of the Scheme.** Since Euler's method has been applied to derive time-dependent data, the stability of the scheme has been analyzed to calculate maximum allowed time steps. A method, *positive central coefficient*, has been applied to determine the stability of the scheme.

Following equation can be established by combining Eq. 3.9 and Eq. 3.10:

$$\frac{\Delta C_i}{\Delta t} = \frac{D_a \varepsilon}{(1 - \varepsilon) \rho_s K_d + \varepsilon} \left[ R_i^2 \frac{C_{i+1} - C_i}{\Delta R_i} - R_{i-1}^2 \frac{C_i - C_{i-1}}{\Delta R_{i-1}} \right] \frac{3}{(R_i^3 - R_{i-1}^3)} \quad (3.17)$$

Thus, when applying Euler's method, the coefficient of  $C_i$  is:

$$1 - \left\{ \left( \frac{R_i^2 C_i}{\Delta R_i} + R \frac{C_i}{\Delta R_{i-1}} \right) \frac{3 D_a \varepsilon}{(R_i^3 - R_{i-1}^3) [(1 - \varepsilon) \rho_s K_d + \varepsilon]} \right\} \Delta t \quad (3.18)$$

, which should be positive. Thus the time step ( $\Delta t$ ) should satisfy:

$$\Delta t \leq \frac{(R_i^3 - R_{i-1}^3) [(1 - \varepsilon) \rho_s K_d + \varepsilon]}{3 D_a \varepsilon \left( \frac{R_i^2}{\Delta R_i} + \frac{R_{i-1}^2}{\Delta R_{i-1}} \right)} \quad (3.19)$$

Apparently, faster diffusion of sorbates, higher sorption coefficient, smaller sediment particle size and finer grid step up (small  $\Delta R$ ) lead to more stringent limits on maximum allowable time steps.

**Incorporating the Nonlinearity of Sorption.** Sediment particles may exhibit nonlinear sorption at certain domains. Simply by replacing linear sorption isotherm (Eq. 3.10) with the Langmuir isotherm (Eq. 3.20) or the Freundlich nonlinear isotherm (Eq. 3.21), the kinetic model can describe the nonlinear sorption behavior.

$$q_i = \frac{Q_{a,i} b_i C_i}{1 + b_i C_i} \quad (3.20)$$



$$q_i = K_d C_i^{1/n} \quad (3.21)$$

Where  $q_i$  is the concentration of sorbates in the sorbed phase,  $Q_{a,i}$  is the maximum sorption capacity of sorbents,  $b_i$  is a factor relating to the affinity of the sorbent surface for sorbates and  $n$  is a parameter indicating the nonlinearity of the sorption process. Since  $Q_{a,i}$  and  $b_i$  indicate properties of sorbents, their values are independent of time. However, the values of  $K_d$  and  $n$  may change over time (Weber, et al., 1996). When Eq. 3.21 has been applied, the  $C_i$  can be expressed explicitly as a function of  $S_i$  by:

$$C_i = \frac{-(\varepsilon + \rho_s Q_{a,i} b_i - b_i S_i) + \sqrt{(\varepsilon + \rho_s Q_{a,i} b_i - b_i S_i)^2 + 4\varepsilon b_i S_i}}{2\varepsilon b_i} \quad (3.22)$$

Thus Eq. 3.10 is replaced by Eq. 3.22 for nonlinear sorption. When applying Eq. 3.21,  $C_i$  can not be expressed explicitly as a function of  $S_i$ . Therefore, the strategy becomes that the value of  $S_i$  is first updated by Eq. 3.9 (the total concentration in Sphere i is changed due to dissolved-phase concentration gradient). Then a numerical method of finding roots (e.g. bisection method) should be applied to Eq. 3.21 to update  $C_i$  and  $q_i$ , which increases the complexity of the scheme as well as computational time.

**Sorption Kinetics Model Testing.** The sorption kinetics model was fully calibrated by fitting sorption kinetics data from literature (Weber, et al., 1996). It combines a linear pore diffusion model to describe the linear absorption on domain II and a nonlinear pore diffusion model to simulate the nonlinear adsorption on domain III, which exhibits slow sorption rate (diffusion rate). Model results are presented in Figure 3-5 with observed data. Weber et al. (1996) reported the time-dependent values of sorption coefficients ( $K_d$ ) and linearity ( $n$ ) rather than actual concentration versus time data. Thereby, the time-

dependent observed concentrations (dissolved or sorbed) are derived by values of  $K_d$  and  $n$  using Eq. 3.21. The model fits the observed data well in the whole simulation period (up to 20,000 minutes) (Figure 3-5). Then initial concentration was modified to test the model. The sorption isotherms at different reaction times generated by the model are presented in Figure 3-6. The model predicts that the linearity decreases over time, which is consistent with has been reported by literatures.

***Time to Reach Sorption Equilibrium.*** It has been reported that the times to reach sorption equilibrium would increase under lower sorbate concentrations, which Yu et al. (2004) ascribes to the nonlinear sorption. Under lower concentrations, higher portion of sorbates are in sorbed-phase (i.e. higher sorption coefficients), thus retarding the diffusion rates (Eq. 2.19). The model was run under various initial sorbate concentrations to verify their effects on the time to reach sorption equilibrium ( $t_e$ ) (Table 3-2). It successfully predicts that lower sorbate concentrations result in longer times to reach sorption equilibrium and verifies that it is due to nonlinear sorption.

Generally, the model successfully captures the features of sorption process, which include the rapid linear sorption at the initial stage, the dramatic decrease of sorption rate over time due to diffusion in Domain III and the decrease of linearity. The model verifies that the partition of sorbates between aqueous phase and Domain II keeps equilibrium and SOM (Domain III) controls the time to reach sorption equilibrium. It also demonstrates that nonlinear sorption results in longer times to reach sorption equilibrium

**Table 3-2 Time to Reach Sorption Equilibrium at Different Sorbate Concentrations  
(Predicted by the Kinetics Model)**

<i>Initial Sorbate Conc. (<math>\mu\text{g/L}</math>)</i>	<i>10</i>	<i>50</i>	<i>100</i>	<i>500</i>	<i>1000</i>
<i><math>t_e</math> (min)</i>	2242	2091	1878.6	593.6	236.2

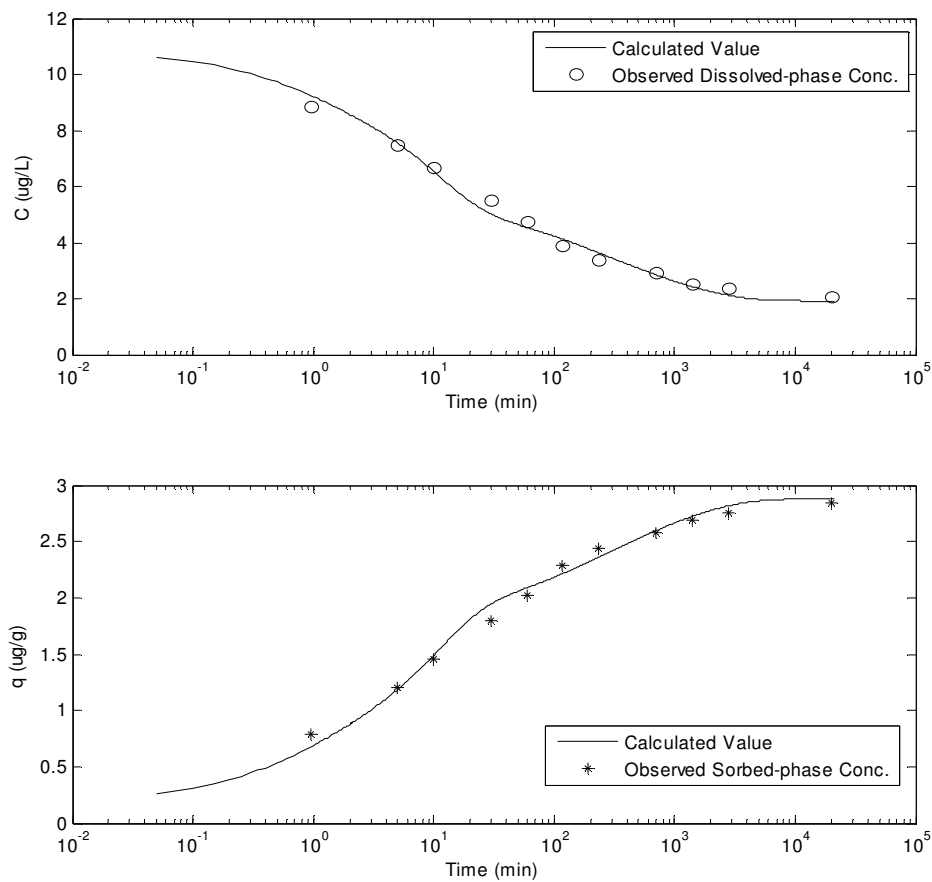


**Figure 3-5 Sorption Kinetics on Sediment Particles (Initial Sorbate Concentration: 11.5  $\mu\text{g/L}$ , the solid line represents model results)**

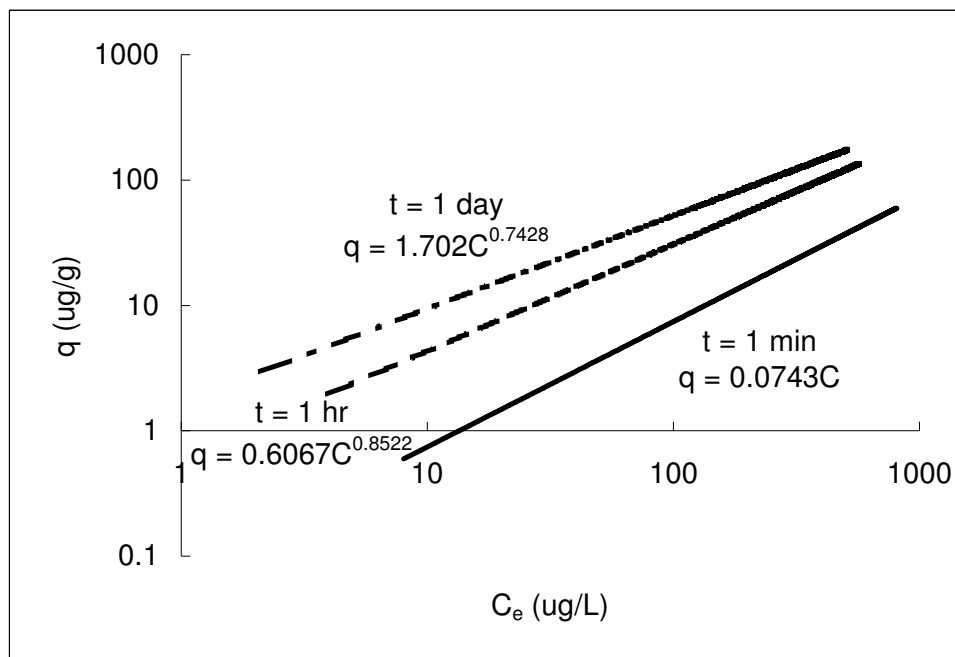


**Figure 3-6 Sorption Isotherm on Sediment Particles at Different Reaction Time  
(Generated by the Kinetics Model)**

### **3.3.2 Sediment Transport Model.**

In estuaries, sediment particles may undergo settling, transport, and resuspension (scouring), thereby playing a key role in the fate and transport of many pharmaceuticals. These processes affect the total suspended solid (TSS) concentrations within the water column. Moreover, TSS controls the fraction of pollutants that will be present in the sorbed phase. This is significant because sorbed-phase contaminants exhibit different fates than those in the dissolved phase (e.g., a lower decay rate). Sorbed pollutants can be transported with suspended solids, settle to the bottom sediments, or re-enter the water column with sediment particles via scouring. Quantifying the rates and extents of these processes thus provides insight into the accumulation of contaminants in bottom sediments and addresses interactions across the water/sediment interface. Development

of the sediment transport module was based largely on Ambrose et al. (1993) and Nice (2006). The sediment compartment is divided into two layers: a 10-cm top active layer, which directly interacts with the water column; and an inactive layer, which is below the active layer and does not interact with the water column. If the depth of the active layer is calculated to be greater than 10 cm, additional sediment is transferred to the inactive layer. If it is less than 10 cm, sediment is transferred from the inactive layer to the active layer to bring its depth back to 10 cm. The probability of deposition and resuspension depends on the stream velocity and sediment particle size. Two critical velocities are assigned to determine when sediment deposition, transportation, and resuspension occur (Nice, 2006). If the water column velocity is above the high critical velocity (0.2 m/s), the bottom sediments are resuspended into the water column. If the water column velocity falls below the low critical velocity (0.07 m/s), suspended sediments settle to the active layer of bottom sediments. Between the high and low critical velocities, suspended sediments transport with water without settling to bottom sediments.

### **3.4 Results and Discussion**

#### ***3.4.1 Sediment Module Calibration.***

TSS concentrations along the study branch were simulated by the model for the 3-year period from 2008 to 2010 based on TSS loadings from U.S. Geological Survey (USGS) gauging station 01594440. Model-predicted TSS concentrations were compared to observed data from the Chesapeake Bay Program (CBP) monitoring stations (TF 1.3 - TF 1.7, RET 1.1, and LE 1.1 – LE 1.4). Settling velocities of suspended solids and resuspension rates of bottom sediments, which vary longitudinally, were adjusted to fit

the observed data. The simulated spatial and temporal concentration profiles of TSS are presented alongside measured data in Figure 3-7 and Figure 3-8, respectively. CBP station TF 1.0 is located at the upstream boundary and is only 53 m away from the USGS station; however, its data record is missing measurements during a period in which the USGS data indicate very high TSS levels. Thus, TF 1.0 was unable to capture especially rapid TSS fluctuations at the upstream boundary. For this reason, data from USGS 01594440 were used as the upstream boundary conditions for TSS. Further, TSS data from the CBP stations downstream from TF 1.0 probably did not capture the high TSS concentrations during certain periods.

### **3.4.2 Hypotheses Testing.**

To evaluate the hypothesis that sorption kinetics strongly impacts the fate and transport of pharmaceuticals contaminants, four hypothetical compounds were selected. These correspond to the four possible combinations of high and low  $K_d$  and  $t_e$ , and all were tested for both instantaneous sorption equilibrium and sorption kinetics. The simulation period for both modeling scenarios was one year. Differences between the two scenarios were quantified using relative difference (RD), as computed using Eq. 3.23.

$$RD(\%) = \frac{C_{SorptionKinetics} - C_{InstantaneousEquilibrium}}{C_{InstantaneousEquilibrium}} \times 100\% \quad (3.23)$$

Where  $C_{SorptionKinetics}$  is predicted concentration from the sorption kinetics model and

$C_{InstantaneousEquilibrium}$  is predicted concentration from the traditional instantaneous

equilibrium model. Positive values of RD indicate that the traditional model under-predicts concentrations, and negative values indicate over-predictions by the traditional model.

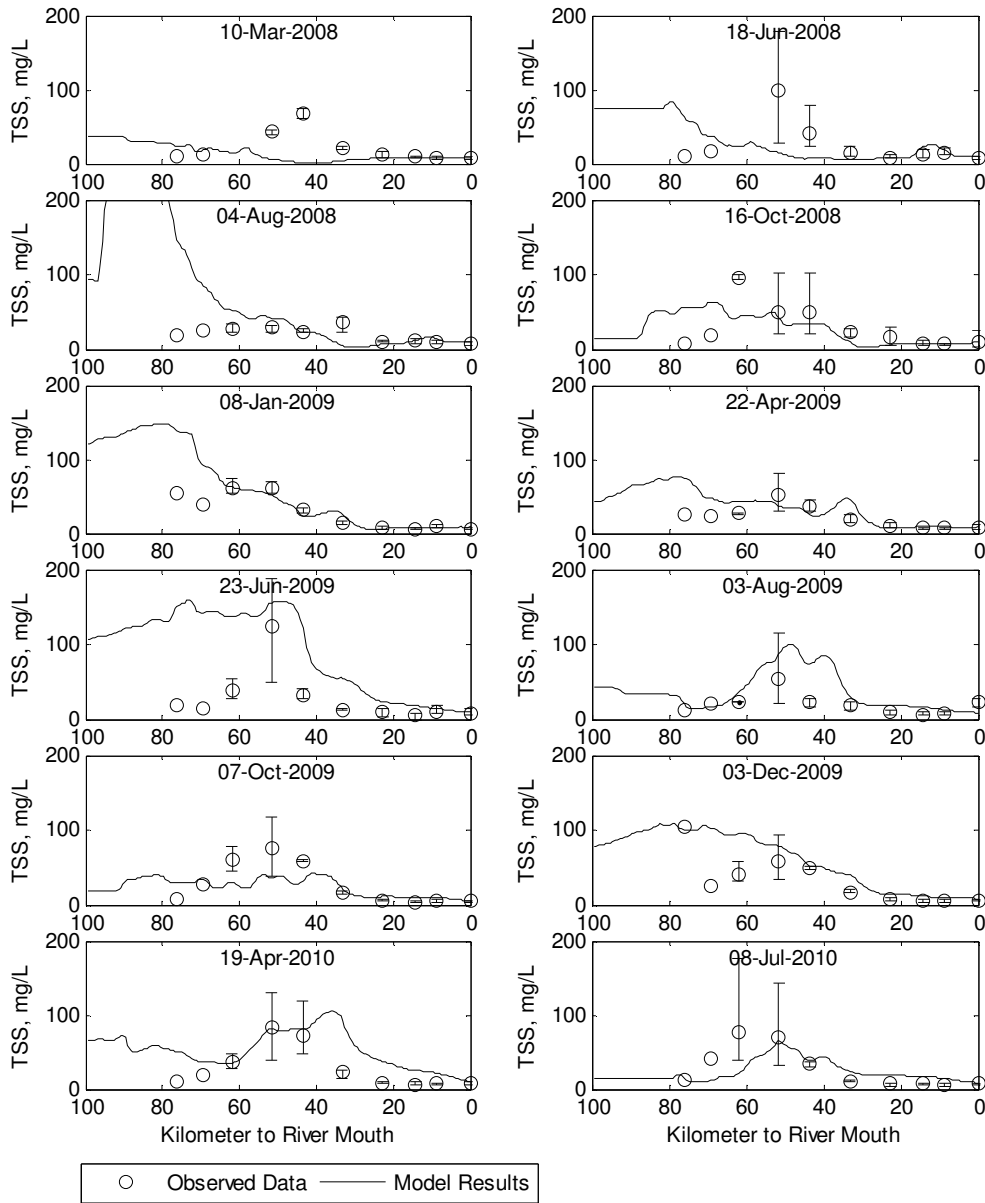


**Figure 3-7 Spatial Distribution of Simulated and Observed Total Suspended Solid Concentrations over the Entire Length of the Studied Area**

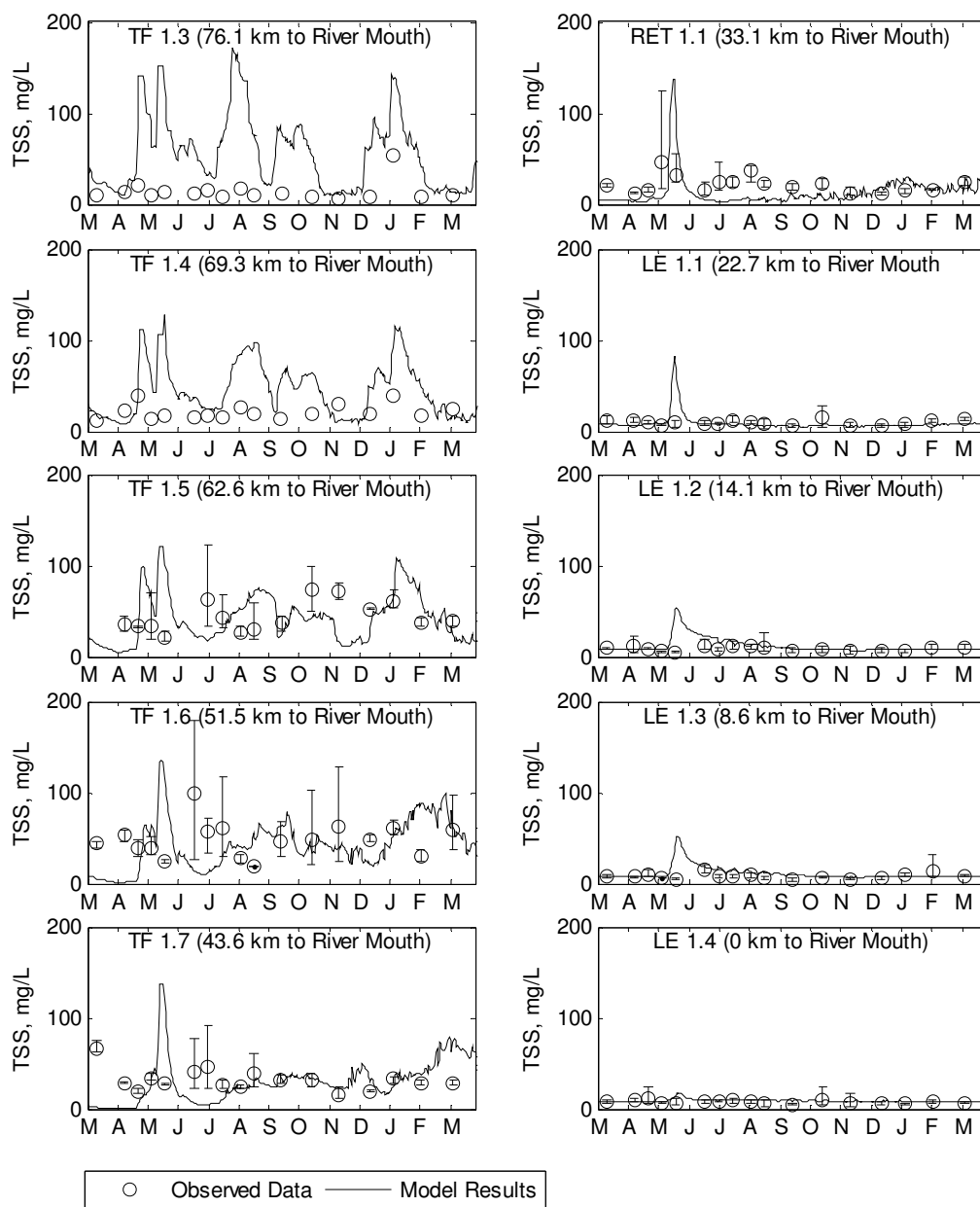


**Figure 3-8 Temporal Distribution of Simulated and Observed Total Suspended Solid Concentrations (TF, RET, and LE refer to Chesapeake Bay Program Monitoring Stations).**



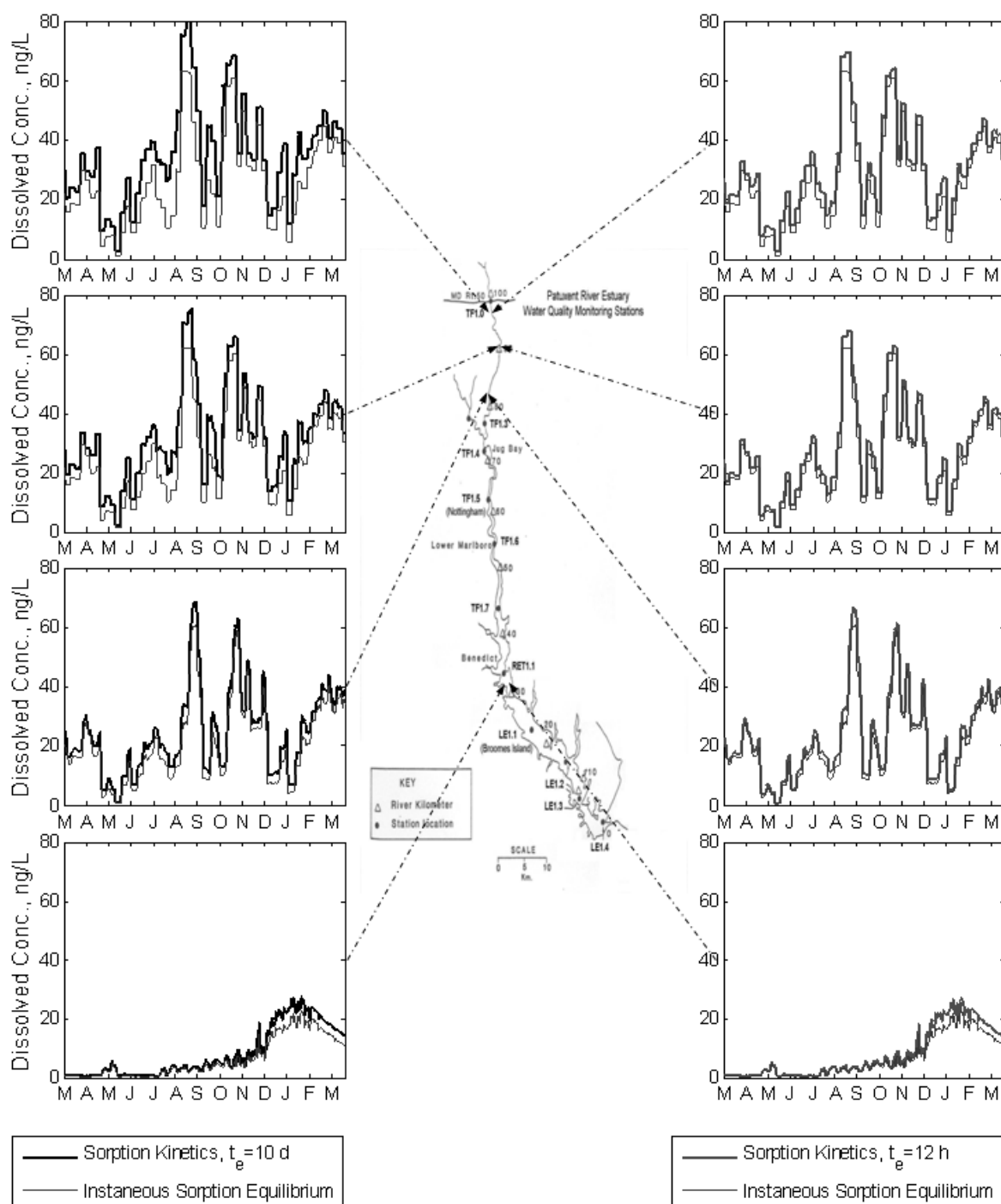


**Figure 3-9 Temporal distribution of dissolved-phase pharmaceutical concentrations for two hypothetical chemicals exhibiting high sorption coefficient ( $K_d = 10,000 \text{ L/kg}$ ), at four selected locations within the studied region.**

**High Sorption-Coefficient Compounds.** Figure 3-9 displays the temporal profiles of dissolved concentrations for two pharmaceuticals exhibiting “high” sorption coefficient ( $K_d = 10,000$  L/kg) but with different times to reach sorption equilibrium ( $t_e = 10$  d and 12 h, respectively). Results from four representative model locations are shown: one upstream, two mid-estuary, and one lower estuary. From these data, the sorption kinetics scenario predicts higher dissolved-phase concentrations than the instantaneous equilibrium scenario, especially for the hypothetical chemical with slow sorption, and for both chemicals at upstream locations. For the chemical with fast sorption (i.e.,  $t_e = 12$  h), the two modeling approaches yield appreciably different results, although the differences are not as significantly different as for the chemicals with slow kinetics. At an upstream location 2.4 km below the upper boundary, RDs reach up to 150% for the chemicals showing slow sorption ( $t_e = 10$  d) and 80% for the chemicals showing fast sorption ( $t_e = 12$  h). In the lower estuary, RDs between the two scenarios decrease because the pharmaceuticals have had longer times to interact with suspended solids and sorption processes are approaching equilibrium. Yet, slight differences still exist. At the most downstream location (66.9 km below the upper boundary), RDs are roughly 25% and 20% for the slowly and quickly sorbed pharmaceuticals, respectively. Thus, the assumption of instantaneous sorption equilibrium, although it is widely used in current water quality models, results in significant underestimation of dissolved-phase concentrations, even for chemicals that reach sorption equilibrium quickly.

The RD values for downstream locations reflect differences in each model’s ability to capture sedimentation of sorbed-phase pharmaceuticals. The selected study area contains

one location (roughly 75-80 km to the river mouth) of low-velocity flow, where suspended particles are known to settle out of the water column. As they settle, they take sorbed-phase pharmaceuticals with them. However, settling-induced attenuation of water-column concentrations is apparently overemphasized by traditional instantaneous equilibrium-based models. In actuality, sorbed-phase concentrations in upstream reaches are lower than what is predicted by instantaneous equilibrium, because the pharmaceutical compounds have had a very short time to interact with the suspended particles. This gives rise to an over-prediction of how much pharmaceutical compound is removed via deposition, which in turn causes under-prediction of total pharmaceutical concentrations (i.e., aqueous-phase concentrations + sorbed-phase concentrations) at all downstream locations. The instantaneous equilibrium model under-predicts total concentrations by roughly 20% and 15% at lower estuary locations for pharmaceuticals showing slow sorption and fast sorption, respectively.

Another reason for the apparent RDs at downstream locations is bottom sediment resuspension (i.e., scouring). From Figure 3-7, the observed TSS measurements exhibit a typical estuarine distribution; whereby highest levels are located in the “middle”, where freshwater converges with seawater. In this region, TSS concentrations are increased due to vertical velocities and the resuspension of bottom sediments (Thomann and Mueller 1987). The instantaneous equilibrium model assumes that the sorption sites afforded by the re-suspended solids are immediately occupied by pharmaceuticals. In contrast, the sorption kinetics approach tracks the sorption behavior over time, thus predicting different amount of pharmaceuticals sorbed by re-suspended solids, which will likely be

deposited in further downstream reaches. Thus, scouring of bottom sediments prevents true sorption equilibrium from occurring in the study system. This further amplifies the differences between concentration predictions from each modeling approach.

Figure 3-10 presents another view of the temporal dissolved-phase concentration data in Figure 3-11. At left, RD values are presented for comparison of dissolved-phase pharmaceutical concentrations predicted by both modeling approaches. Temporal distributions of TSS concentrations for the same locations are presented at right. These two datasets are presented together to show the similarity in RD and TSS profiles, especially at upstream locations for chemicals with slow sorption ( $t_e = 12$  d). Quantitatively, the correlation coefficient between RD and TSS at the farthest upstream location in Figure 3-9 and Figure 3-10 (approximately 97.5 km to the river mouth) is greater than 0.98 for the slow-sorption chemicals. This suggests that high TSS concentrations magnify the difference between instantaneous equilibrium and sorption kinetics predictions for locations corresponding to short travel times from the upper boundary. There is less similarity in RD and TSS profiles at points further downstream; the correlation coefficient for the slow-sorption chemicals decreases to 0.35 at the farthest downstream location (33.1 km to the river mouth). This indicates that TSS has a smaller impact on the disparity between modeling approaches for locations corresponding to longer travel times from the upper boundary.

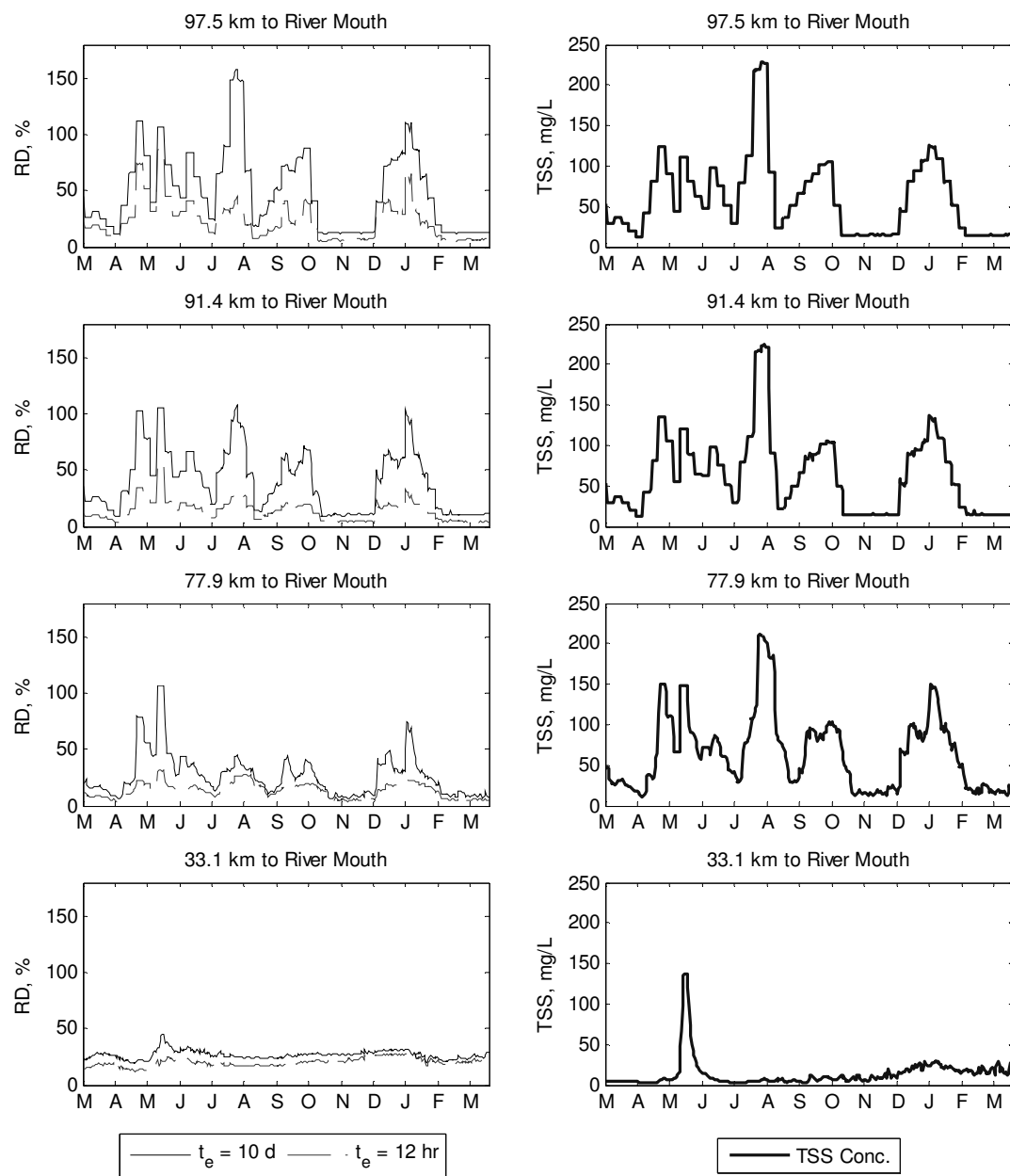


**Figure 3-10 At left: Temporal distribution of relative difference (RD) between instantaneous equilibrium and sorption kinetics modeling approaches for two hypothetical pharmaceuticals exhibiting high sorption coefficient ( $K_d = 10,000$  L/kg) at the four locations noted in Figure 3-9.**

The decreasing similarity between RD and TSS profiles at points farther downstream seems reasonable, since higher TSS at the upper boundary will drive a larger fraction of the pharmaceutical into the sorbed phase. But, because the transition from dissolved-phase to sorbed-phase does not proceed instantaneously, the inaccuracy of the instantaneous equilibrium assumption is clearest in the farthest upstream locations. At downstream locations, the pharmaceutical has had longer times to equilibrate with the TSS such that the correlation coefficient decreases.

Figure 3-11 shows the spatial distribution of dissolved-phase concentrations for both high- $K_d$  pharmaceuticals. Here it is apparent that the instantaneous equilibrium scenario generally under-predicts pollutant levels along the whole river branch. Also, there is a gradual drop in concentrations of these pharmaceuticals moving from upstream to downstream. This occurs largely because of dilution. A sudden drop in dissolved-phase concentration can be observed roughly 75-80 km from the mouth because the width of the river channel rapidly increases at this location. This causes a dramatic decrease in flow velocity, with a concomitant increase in suspended solid sedimentation. This mediates a decrease in total pharmaceutical concentration as the sorbed-phase pharmaceutical molecules exit the water column with settling solids. Thus, sedimentation is still an important attenuation mechanism for compounds exhibiting slow sorption kinetics, but traditional water quality models have over-predicted this effect. Finally, a rapid increase in dissolved concentration can be observed immediately after the sudden drop, which reflects a fresh influx of pharmaceuticals from the Western Branch WWTPs.

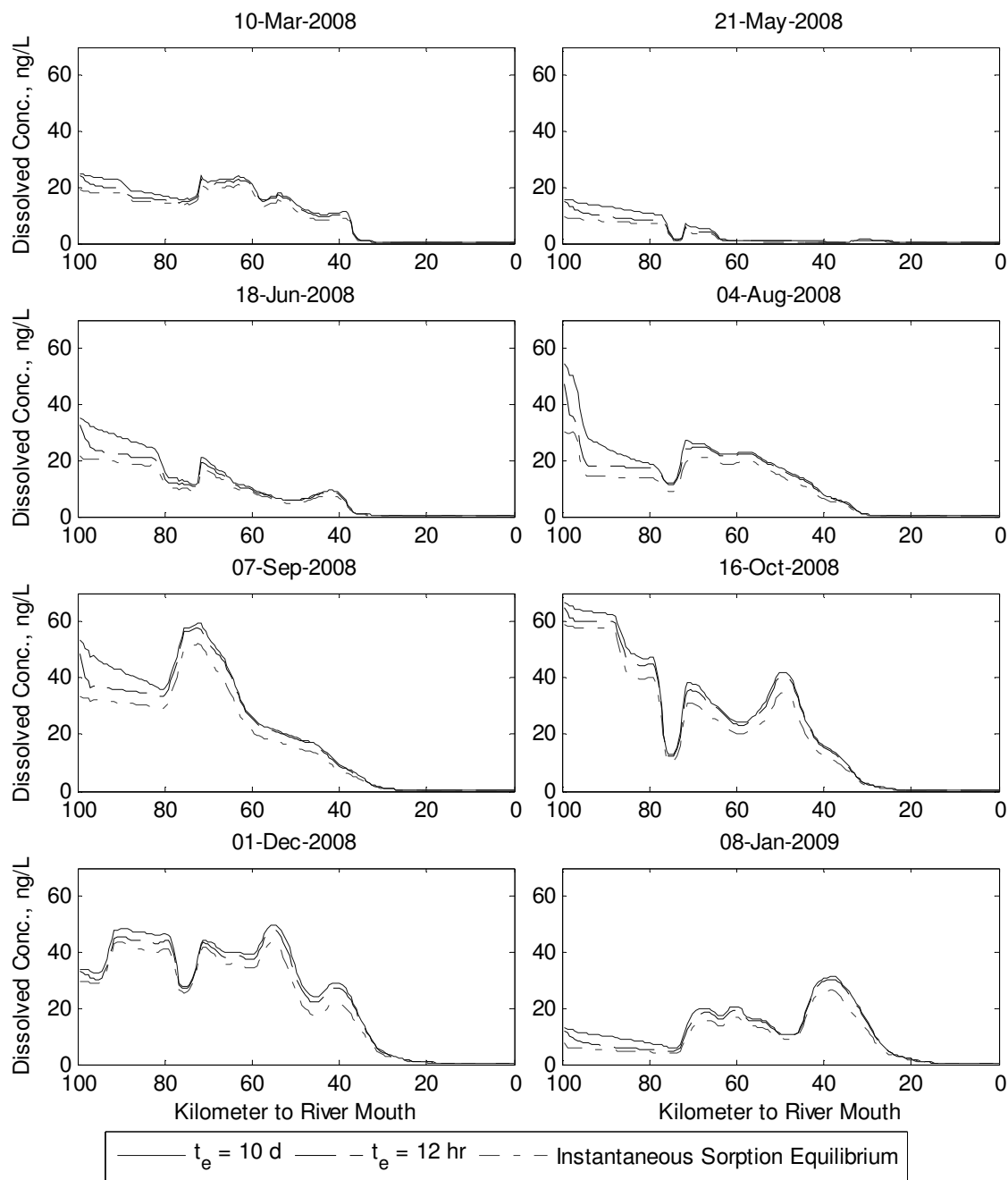


**Figure 3-11 Spatial distribution of dissolved-phase concentrations for two hypothetical pharmaceuticals exhibiting high sorption coefficient ( $K_d = 10,000$  L/kg).**

**Low Sorption-Coefficient Compounds.** Two hypothetical pharmaceutical compounds exhibiting low sorption coefficient ( $K_d = 80$  L/kg) were also evaluated using the

instantaneous equilibrium and sorption kinetics ( $t_e = 12$  h or 10 d) modeling scenarios. However, no apparent differences in *dissolved-phase* concentrations were obtained between these approaches (Figure 3-12). This is likely because sorption processes are unimportant for these compounds. For example, at  $K_d = 80$  L/kg and TSS concentration = 50 mg/L (typical), approximately 99.6% of the total compounds exists in the dissolved phase. Thus, sorption onto sediments particles, rapid or otherwise, will not appreciably change the dissolved-phase concentrations.

For *sorbed-phase* concentrations, there are some apparent differences between the results from the instantaneous equilibrium approach or the sorption kinetics approach (Figure 3-13). Sorbed-phase concentrations are quite low for both scenarios; however, the instantaneous equilibrium scenario predicts much higher sorbed-phase concentrations than the sorption kinetics scenario. Thus, the instantaneous equilibrium scenario points to higher accumulation of low- $K_d$  pharmaceuticals in the riverbed.



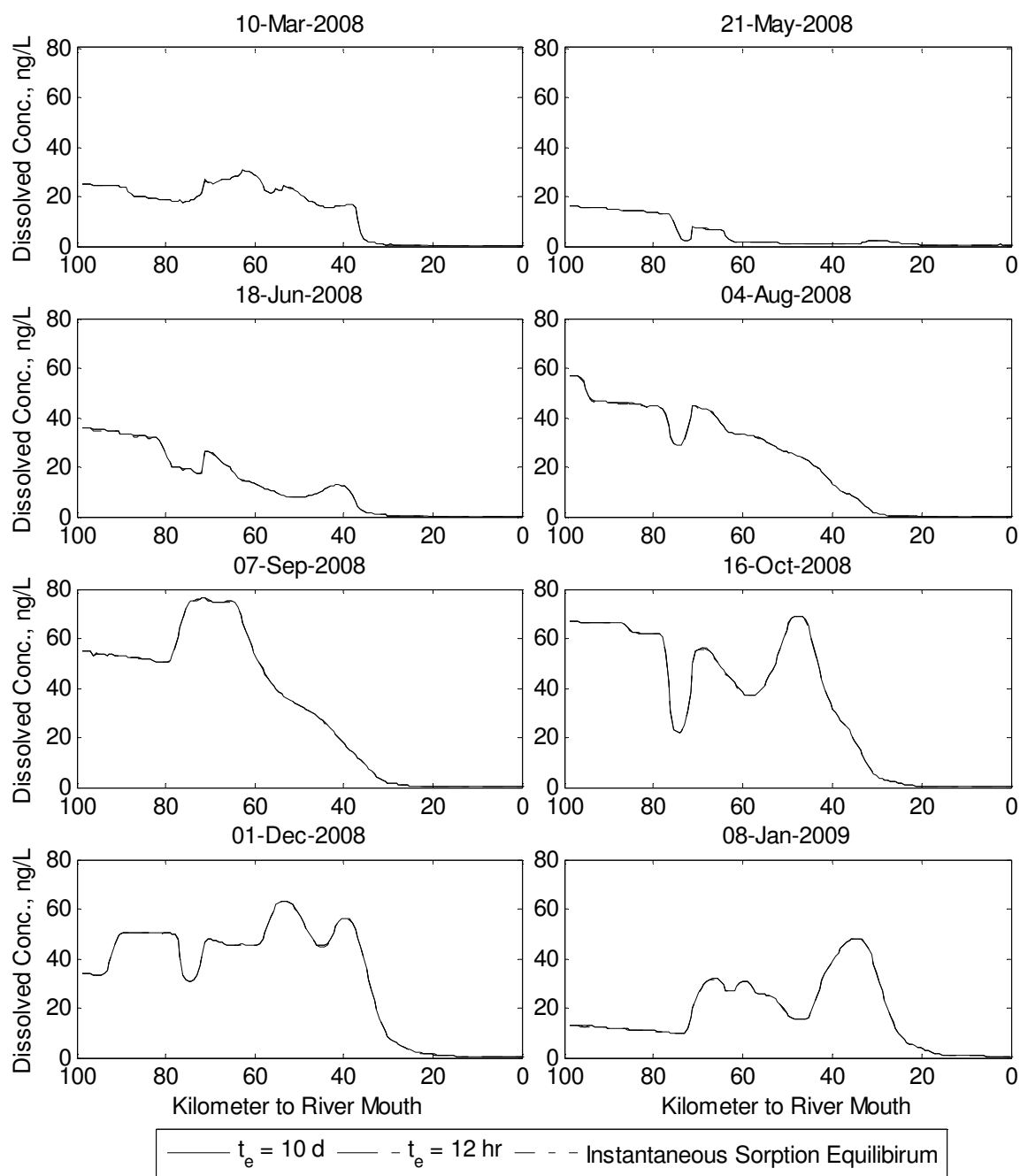


**Figure 3-12 Spatial distribution of dissolved-phase concentrations for the hypothetical pharmaceuticals exhibiting low sorption coefficient ( $K_d = 80$  L/kg)**

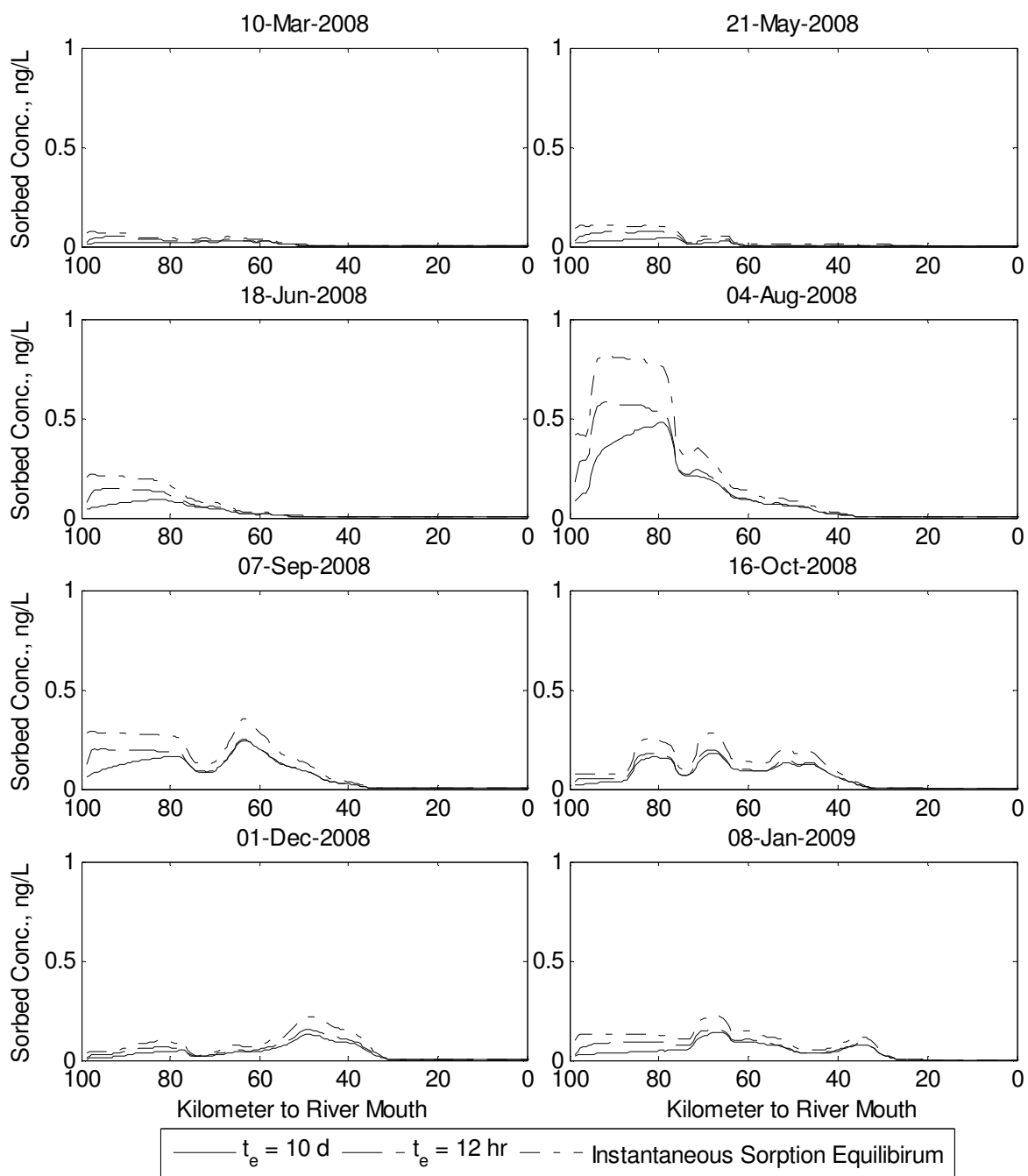


**Figure 3-13 Spatial distribution of sorbed-phase concentrations for the hypothetical pharmaceuticals exhibiting low sorption coefficient ( $K_d = 80 \text{ L/kg}$ )**

### 3.5 Summary and Conclusions

The kinetics model developed in this study, which combines the theory of diffusion in porous media and the multiple domain features of sediment particles, well describes the features of sorption process observed from experiments, which include the rapid linear sorption at the initial stage, the dramatic decrease of sorption rate over time and the decrease of linearity over time. It also captures that the time to reach sorption equilibrium would increase when sorbent concentrations decrease and verifies that this is due to nonlinear sorption behavior of some chemicals.

In natural water/sediment systems, failure to incorporate sorption kinetics into water quality modeling for pharmaceutical fate and transport could result in significant underestimation of dissolved-phase concentrations; up to 80-150% at upstream locations for compounds exhibiting fast sorption and slow sorption in this study. For this reason, sorption kinetics (fast or slow) should always be considered for chemicals whose environmental fate and transport are affected by sorption processes (i.e., those exhibiting high  $K_d$ ). At upstream locations, the difference between instantaneous equilibrium and sorption kinetics approaches is strongly impacted by TSS concentrations. Sorption kinetics also affects the accumulation of pharmaceutical compounds onto the riverbed. Thus the removal of contaminants from the water column is not as rapid as expected in traditional instantaneous-equilibrium based water quality models, which tend to under-predict pollutant levels along the entire estuary. Scouring of bottom sediments, and the mass transport and deposition of re-suspended solids further amplify the differences between predictions from two approaches. This means that pharmaceutical compounds

can be transported downstream more efficiently than has been previously assumed, potentially impacting a larger area of ecosystem or water supply. The findings from this generic study can be applied to a wide range of pollutants, which do not reach sorption equilibrium instantaneously.

This study also pointed out that interactions between sorption kinetics and estuarine mass transport play a key role in quantifying the fate and transport of pharmaceuticals in the water column. Sorption alone may not necessarily explain the behavior of the pharmaceuticals in natural water systems. Coupling sorption kinetics with mass transport processes, including sediment transport in the water column, is utmost important in fate and transport analyses of many emerging chemicals like the pharmaceuticals.

## **Chapter 4: Measurement of Sorption Parameters for Selected Pharmaceuticals**

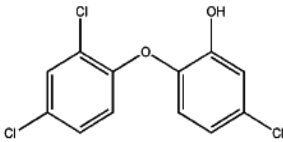
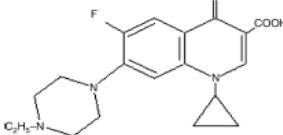
### **4.1 Introduction**

Recently, pharmaceuticals have been widely detected in the natural environment and thus have drawn much research interest. However, a quantitative tool is lacking to evaluate the effect of environmental processes, when acting alone or in conjunction with each other, on their environmental fate and transport, and to improve the understanding of their environmental behaviors. As discussed in previous chapters, sorption kinetics can significantly impact the fate and transport of pollutants in natural environments. It is expected that some pharmaceutical compounds may exhibit slow sorption kinetics, which have intrinsic impacts on their environment behavior. Thus it becomes important to explore the sorption kinetics of pharmaceuticals on natural sediments in order to better understand their environmental fate and transport. Further, the physiochemical properties of pharmaceuticals vary largely, which would likely give rise to different sorption behaviors and different environmental fate and transport behaviors.

The objective of this study was to analyze how physiochemical properties of pharmaceuticals would affect their sorption onto natural sediments. The experimental results would serve as the basis for the further fate and transport analyses. For this study, the sorption behaviors of two pharmaceutical compounds, triclosan (TCS) and enrofloxacin (ENR), were examined and compared. Both chemicals are widely detected in the natural environment (Focazio et al., 2008; Kolpin et al., 2002) but possess unique physicochemical properties compared to each other. The structures of these chemicals are

depicted in Table 4-1. The impacts of physicochemical properties on the sorption behaviors of pharmaceuticals were analyzed in this study.

**Table 4-1 Molecular Structures and Properties of Triclosan and Enrofloxacin**

<i>Sorbate</i>	<i>Structure</i>	<i>log K<sub>ow</sub></i>	<i>pK<sub>a</sub></i>	<i>Water Solubility (mg/L)</i>
<b>Triclosan</b>		<sup>a</sup> 4.76 <sup>b</sup>	7.9 <sup>b</sup>	10 <sup>b</sup>
<b>Enrofloxacin</b>		<sup>c</sup> 0.7 <sup>c</sup> - 1.1 <sup>d</sup>	$pK_{a1} = 5.94^e$ $pK_{a2} = 8.70^e$	3400 <sup>b</sup> 545 (pH = 5.8) <sup>e</sup> 380 (pH = 6.0) <sup>e</sup> 280 (pH = 7.3) <sup>e</sup> 1430 (pH = 8.8) <sup>e</sup>

<sup>a</sup>. Tixier et al., 2002; <sup>b</sup>. The National Library of Medicine Toxnet (2009) (<http://toxnet.nlm.nih.gov>); <sup>c</sup>. Boxall et al., 2006; <sup>d</sup>. Tolls, 2001. <sup>e</sup>. Lizondo et al., 1997;

#### 4.1.2 Background on TCS

TCS has been used as an antimicrobial substance in many medical, consumer care, and everyday household products. It is added as a preservative or as an antiseptic in a wide range of products such as hand soaps, medical skin creams, toothpastes, mouthwash, household cleaners, and even textiles (e.g., bed linens and shoes) (Singer et al., 2002). TCS eventually reaches surface water through WWTP effluents (Ricart et al., 2010; Singer et al., 2002). Chalew and Halden (2009) reported that the concentration of TCS in WWTP effluents ranged from 0.027 to 2.7 µg/L, with a maximum concentration of 2.3 µg/L being detected in natural aquatic ecosystems. Individual personal contributions of

TCS to natural waters can be significant. Singer et al. (2002) estimated that the daily per capita loading of TCS to a lake in Switzerland was 100 mg/day per 1000 persons. In the U.S., the frequency of TCS detection in untreated drinking water resources is 8.1% (Focazio et al., 2008).

There are two major environmental impacts that make TCS a source of concern in natural systems. First, as a broad-spectrum antibacterial agent, TCS possesses documented toxicity to certain algal and bacterial species in natural waters (Singer, et al., 2002; Ricart et al., 2010; Wilson et al., 2003). The presence of TCS in streams has significant impacts on the algal genera *Chlamydomonas* and *Scenedesmus* and may lead to a significant increase in the relative biomass of *Melosira* (Wilson et al., 2003). Thus, TCS has the potential to change both the structure and function of algal communities in natural waters. It is particularly alarming that the “no effect concentrations” (NEC) for algae photosynthesis (0.45 µg/L) and bacterial reproduction (0.21 µg/L) are comparable to previously detected TCS concentrations in natural water (Ricart et al., 2010) The second major environmental impact pertains to TCS’s capacity to be phototransformed into highly toxic polychlorinated dioxins in sunlit surface waters (Buth et al., 2010). These chemicals pose severe adverse health risks to biota and humans.

#### **4.1.2 Background on ENR**

ENR is a fluoroquinolone antibiotic used in veterinary medicine (Lizondo et al., 1997; Boxall et al., 2003) most notably in swine and cattle farming (Sturini et al., 2009). In Europe, it was detected in municipal WWTP influents (122– 447ng/L) and effluents (53.7

- 212 ng/L), and its seasonal variation was significant (Seifrtová et al. 2008). In the U.S., measured effluent ENR concentrations have been <34 ng/L (Nakata et al, 2005) to 270 ng/L (Karthikeyan and Meyer, 2006). ENR has also been measured in untreated and treated drinking water sources: 6.8% of untreated drinking water sources in the U.S. (Focazio et al., 2008); and 3% of treated drinking water sources in Ontario, Canada (Kleywegt et al. 2011) It has been reported that the apparent affinity of ENR for sediments reduces its detection frequency in water (Kolpin et al., 2002); therefore, it is suspected that ENR could be significantly accumulated in bottom sediments. ENR is toxic to certain organisms in aquatic environments. For example, it shows a 5-day effective concentration (EC<sub>50</sub>) of 49 µg/L for *M. aeruginosa* (Robinson et al., 2009). Park and Choi (2008) illustrated that ENR exhibited acute toxicity to *M. macrocopa* with a 48-hour EC<sub>50</sub> of 56.7 mg/L, and chronic toxicity to *D. magna* with an EC<sub>50</sub> of 11.5 mg/L.

#### **4.1.3 Experimental Overview – TCS and ENR**

For this study, sorption kinetics experiments were conducted using relatively low concentration levels (µg/L) for both selected pharmaceuticals to verify the assumption that pharmaceuticals may not reach equilibrium instantaneously. These experiments were then conducted under different conditions (e.g., pH) to examine the impact of environmental conditions on sorption behavior of each chemical. This latter set of experiments was done to verify the assumption that different molecular properties of pharmaceutical compounds would give rise to different sorption behaviors



## 4.2 Materials and Methods

### 4.2.1 Materials

A stream sediment sample obtained from K. J. Ottmar of the Department of Civil and Environmental Engineering at the University of Virginia was used as natural sorbent for this study. It was collected from Meadow Creek in Charlottesville, VA, then dried at 105°C for 24 hours and passed through a #20 sieve. The organic-carbon content ( $f_{oc}$ ) of the sediment was 1% and the specific-surface area was  $3.38 \pm 0.34 \text{ m}^2/\text{g}$ . The sediment sample was prepared and characterized by Ottmar et al. (2010a; 2010b).

Triclosan (purity  $\geq 98\%$ , HPLC grade) and enrofloxacin (purity  $> 98\%$ , LC grade) were obtained from Sigma-Aldrich and Tokyo Chemical Industry Co., Ltd., respectively. The molecular structures and properties of the two sorbates are listed in Table 4-1. ENR has multiple  $pK_a$ 's and exists in multiple species as a function of pH (Figure 4-1). Thus its water solubility is dependent on pH. The lowest water solubility, which is around 300 mg/L, is found at the neutral pH condition. TCS shows higher hydrophobicity than ENR, thus exhibiting smaller solubility. Under alkaline conditions, TCS molecules lose one proton and become negatively charged (Figure 4-2).

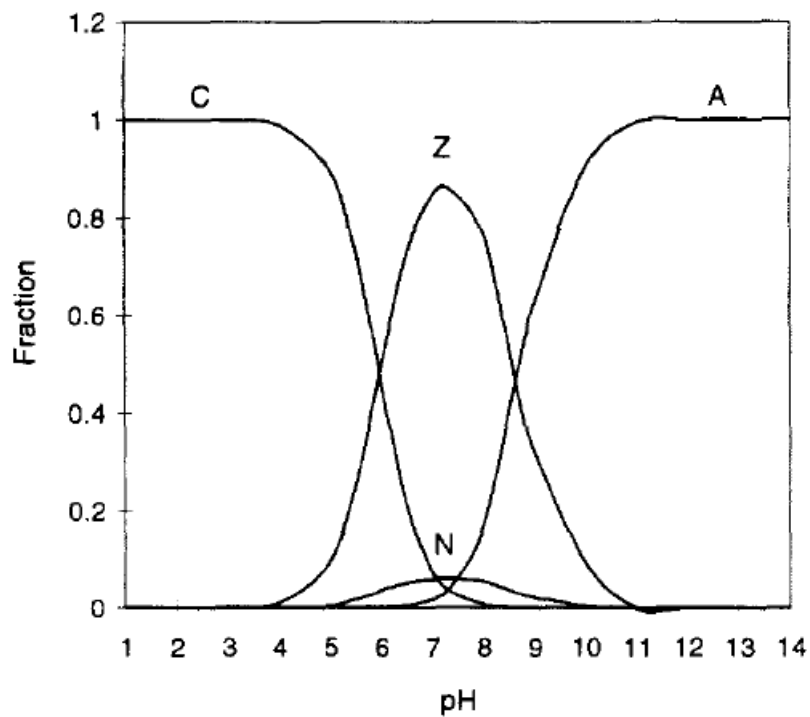


**Figure 4-1 The Distribution of the fraction of four enrofloxacin Species: the cation (C), the neutral (N), the Zwitterion (Z) and the anion (A) (Figure adapted from Lizondo et al., 1997)**

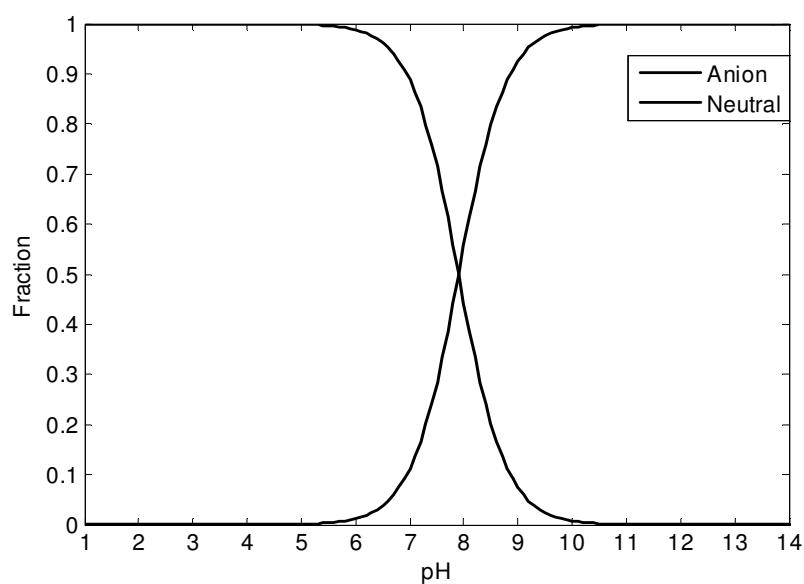


**Figure 4-2 The Distribution of the Fraction of Two Triclosan Species (Calculated using a  $pK_a$  value of 7.9)**

#### **4.2.2 Methods**

##### ***Sorption Kinetic Batch Experiment Setup***

Sorption kinetic experiments were conducted using an initial sorbate concentration of 200  $\mu\text{g/L}$  for both chemicals. Stock solutions were prepared by first adding solid pharmaceuticals to methanol to prepare 1-g/L methanol solutions and then further diluting the 1-g/L methanol solutions to 2mg/L using de-ionized water (DI water). 15-mL centrifuge tubes were used as reactors for each kinetic batch experiment. Each reactor was prepared by adding a known mass of sorbent, which was determined in preliminary experiments to ensure that the fraction of dissolved-phase sorbates ranged from 20% to 80% of the total sorbate mass. Each reactor was then filled with analyte-free DI water to half of its total volume, after which a constant volume of the 2-mg/L stock solutions was added to each. Each reactor was then filled to the top to minimize the amount of headspace in the reactor. All reactors were then sealed using Teflon-lined caps. Two types of controls (one negative control, and one positive control or blank) were prepared following this procedure. The positive control (blank) was free of sorbent, and the negative control was lacking sorbate. All of the centrifuge tubes were completely mixed and placed in a rotating horizontal reaction apparatus at a constant temperature (20 °C). At different times, sets of three reactors were centrifuged for 30 minutes at 3000 rpm. Aqueous-phase sorbate concentrations in the reactor supernatants were determined by high performance liquid chromatography (HPLC) analysis. Then reactors were put back into the incubated, shaking apparatus for use in subsequent desorption kinetic studies.

After sorption equilibrium had been reached in all reactors, test tubes were centrifuged and all supernatants were replaced by sorbate-free DI water to start the desorption process. All reactors were then placed in the incubated mixing apparatus again at a constant temperature of 20 °C. The time-dependent concentrations of desorption process were determined following the same procedure as that developed in sorption kinetics experiments.

The whole protocol for the kinetic experiments was repeated under different pH conditions. The sorbed-phase concentration was determined by:

$$q(t) = \frac{C_{Total} - C(t)}{C_{SOLID}} \quad (4.1)$$

Where  $q(t)$  is the sorbed-phase concentration at time  $t$ ,  $C_{Total}$  is the total concentration of sorbate in both phases,  $C(t)$  is the dissolved-phase concentration of sorbate at time  $t$ , and  $C_{SOLID}$  is the concentration of sorbent. The sorption kinetics model discussed in *Section 3.3.1* of Chapter 3 was used to fit kinetic experimental results. The goodness-of-fit was evaluated by the root-mean-squared-error (RMSE) metric, which was calculated by:

$$RMSE = \sqrt{\frac{\sum_{i=1}^n (obs_i - model_i)^2}{n - p}} \quad (4.2)$$

Where  $n$  is the number of observations,  $obs_i$  is the experimental result from the  $i^{th}$  observation and  $model_i$  is the corresponding model result, and  $p$  is the number of parameters adjusted to fit the experimental data ( $p = 2$  since two coefficients were adjusted).

### ***Sorption Isotherm Batch Experiment Setup***

A similar protocol to that used in the sorption kinetic batch experiments was applied to the isotherm batch experiments. For TCS, 15-mL centrifuge tubes were used as reactors and the same amount of sorbent (0.05 g) was added to each. For ENR, 50-mL centrifuge tubes were used as reactors, thus the amount of sorbent added to each was also changed (Table 4-2). The 20-mg/L ENR stock solutions were prepared by directly diluting ENR into DI water. Varying volumes of the stock solutions were added to each reactor to adjust initial concentrations. All reactors were placed in the incubated mixing apparatus at 20 °C. After reaching sorption equilibrium (based on equilibrium times from previous sorption kinetic batch experiments), all samples were centrifuged and aqueous-phase concentrations were determined by HPLC analysis. The isotherm batch experiments for ENR were conducted under different pHs. The equilibrium sorbed-phase concentration was calculated by:

$$q_e = \frac{C_{Total} - C_e}{C_{SOLID}} \quad (4.3)$$

And the sorption coefficient was determined by

$$K_d = \frac{q_e}{C_e} \quad (4.4)$$

Where  $K_d$  is the sorption coefficient,  $q_e$  is the equilibrium sorbed-phase concentration, and  $C_e$  is the equilibrium dissolved-phase concentration. Several models were used in attempt to fit the resulting experimental data, including: the Freundlich nonlinear isotherm (Eq. 3.21); the single Langmuir isotherm (Eq. 4.5); and the two-compartment Langmuir isotherm, assuming linear sorption in certain compartment of sediment particles (e.g. amorphous organic matter) (Eq. 4.6).

$$q_e = \frac{Q_{\max} b C_e}{1 + b C_e} \quad (4.5)$$

$$q_e = K_{d, Linear} C_e + \frac{Q_{\max} b C_e}{1 + b C_e} \quad (4.6)$$

Where  $q_e$  is the chemical concentration in the sorbed phase at equilibrium;  $C_e$  is the aqueous-phase concentration at equilibrium;  $K_{d, Linear}$  represents the sorption coefficient to a certain component of sediment particles exhibiting linear sorption; and  $Q_{\max}$  and  $b$  are maximum sorption capacity and affinity of chemicals to sediments or to the compartment exhibiting nonlinear sorption, respectively.

### ***pH Control***

The selection of pH conditions to use for experiments was based on typical conditions in ambient waters, ranging from 6.5 to 8.5. Kinetics and isotherm experiments were thus conducted at pH = 6.0, 7.2, and 8.3. Because all three pHs are in the circumneutral range, wherein pH is especially sensitive to dissolution of carbon dioxide from the atmosphere and impacts caused by sediment particles, it was difficult to maintain constant pH in preliminary experiments. Therefore, all subsequent experiments were performed in phosphate buffers, which were prepared by adding monopotassium phosphate ( $\text{KH}_2\text{PO}_4$ ) and dipotassium phosphate ( $\text{K}_2\text{HPO}_4$ ) to DI water. For TCS, 0.1 M phosphate buffer was used to set pH to 6.0 or 8.3. At pH 7.2, no phosphate buffer was used since the pH of reaction systems (the mixtures of DI water, sediments and TCS) was around 7.2. For ENR, the concentration of phosphate buffer was adjusted down to avoid confounding effects caused by higher than normal ionic strength. In kinetic batch experiments of ENR, all three pH levels were controlled using 1 mM phosphate buffer. In contrast, 0.2 mM

phosphorus buffer was applied in ENR isotherm batch experiments. In order to address the impact of ionic strength on the sorption of ENR, kinetic experiments at pH 7.2 were repeated but pH was controlled by 0.1 M phosphorus buffer. The setup of kinetic and isotherm batch experiments for both chemicals are summarized in Table 4-2.

**Table 4-2 The Concentration of Sorbents and pH Control for Each Experiment**

<i>Sorbate</i>	<i>Experiment</i>	<i>Conc. of Sorbent</i>	<i>Concentrations of Phosphorus Buffer</i>
<i>Triclosan</i>	<i>Kinetic Batch Experiments</i>	3.05 g/L	0.1 M for pH 6 and 8.3
	<i>Isotherm Batch Experiments</i>	3.05 g/L	-
<i>Enrofloxacin</i>	<i>Kinetic Batch Experiments</i>	0.428 g/L	1 mM for pH 6, 7.2 and 8.3
	<i>Kinetic Batch Experiments (Higher Ionic Strength)</i>	0.672 g/L	0.1 M for pH 7.2;
	<i>Isotherm Batch Experiments</i>	0.328 g/L for pH 7.2 and 8.3; 0.164 g/L for pH 6.0;	0.2 mM for all three pHs

### ***Analytical Procedures***

Both chemicals were analyzed using either a SHIMADZU LC-20AB HPLC equipped with an SPD-20A UV-VIS detector or an Agilent 1100-series HPLC equipped with a diode array detector (DAD). A C-18 column was used to obtain satisfactory chromatographic resolution in both instruments. Mobile phases were composed of Acetonitrile (ACN) and DI water, which were in some cases acidified using 2% acetic acid (vol/vol) for TCS or 0.5 M phosphorus acid for ENR to better resolve the TCS from background peaks caused by the buffer solution, or to mitigate formation of multiple ENR peaks. For the measurement of ENR, samples for HPLC analysis were prepared by adding 0.2 M phosphate buffer (pH 7.2) to experiment solutions (1:1 by volume). Detailed procedures are summarized in Table 4-3.

Table 4-3 HPLC Method for Triclosan and Enrofloxacin

<i>Sorbate</i>	<i>Instrument</i>	<i>Detection Wavelength</i>	<i>pH</i>		
			<i>6.0</i>	<i>7.2</i>	<i>8.3</i>
<b>Triclosan</b>	SHIMADZU	198 nm	-	80% ACN + 20% DI water; Flow Rate: 0.7 mL/min; Injection Volume: 100 $\mu$ L	-
	AGILENT	198 nm / 230 nm	30% acidified DI water (2% acetic acid by volume) + 70% ACN Flow Rate: 0.35 mL/min; Injection Volume: 60 $\mu$ L	-	Acidified DI water (2% acetic acid by volume) + ACN; Flow rate: 0.35 mL/min; Injection Volume: 60 $\mu$ L Gradient Method (Linear change): 0.00 min: 85% DI water + 15% ACN; 1.50 min: 65% DI water + 35% ACN; 2.00 min: 25% DI water + %75 ACN; 13.00 min: 25% DI water + %75 ACN;
<b>Enrofloxacin</b>	SHIMADZU	270 nm / 277 nm	23% acidified ACN (0.5 M phosphorus acid) + 77% acidified DI water (0.5 M phosphorus acid); Flow rate: 1 mL/min; Injection Volume: 100 $\mu$ L 0.2 M phosphate buffer (pH 7.2) was added to samples (50% V/V) for HPLC analysis		
	AGILENT	-	-		



## 4.3 Results and Discussion

### 4.3.1 Sorption Kinetics of Triclosan and Enrofloxacin onto Natural Sediments

The sorption kinetics of TCS and ENR were examined at three pH levels. Both chemicals exhibited slow sorption kinetics (Figure 4-3 and Figure 4-4). At ambient pH (7.2), times to reach equilibrium were roughly 9 and 6 days for TCS and ENR, respectively. This strongly suggests that instantaneous sorption equilibrium is an invalid assumption for these two pharmaceuticals. Low partition rates of the two chemicals may result from slow mass transfer rates of the chemicals into sediment particles. The mass transfer of sorbates in sediment particles was controlled by diffusion of sorbates in the porous particles, and was retarded by properties of sediment particles and local sorption of sorbates on pore walls, the latter leading to less sorbate molecules available for diffusion. In other words, sorbate molecules cannot reach sorption sites of sorbents immediately. They need time to *travel* into sediment particles. The long equilibrium times derived from this study are reasonable since initial concentrations of both chemicals, which were at sub-micrograms per liter levels, were much lower than their water solubility, and the sorbents were natural sediments. Yu et al. (2004) pointed out that lower concentrations of sorbates led to longer time to reach sorption equilibrium. Further, Ottmar et al. (2010a) illustrated that chemicals exhibit lower partition rates to natural sorbents (e.g. sediments) than to biosolids. Results from this study are important to understand the fate and transport of pharmaceuticals in natural environments, since these chemicals are generally detected in sub-micrograms per liter levels in surface water and are frequently attached to natural sediments.

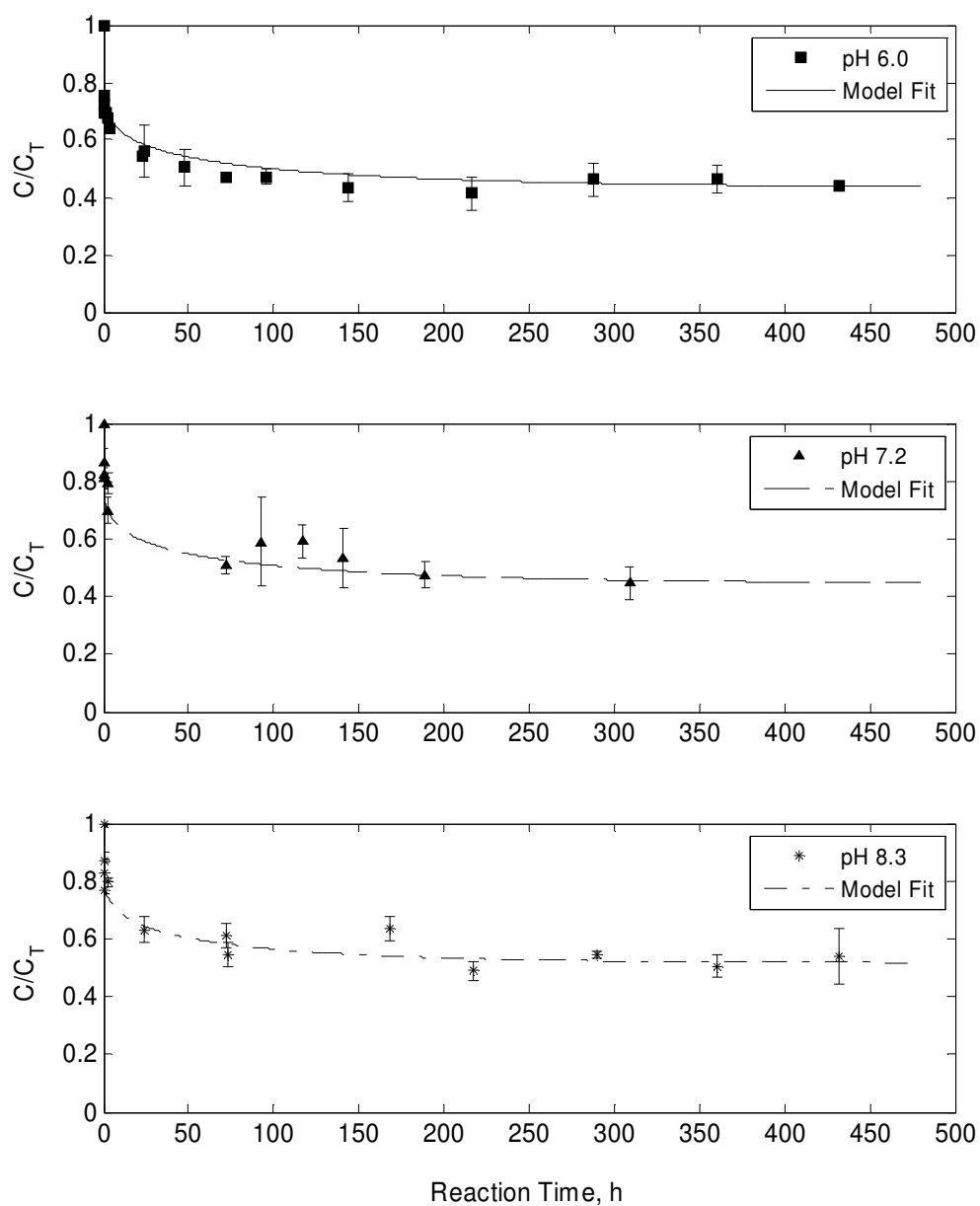


**Figure 4-3 Sorption Kinetics of Triclosan at three pHs with Model Fit (Error bars represent 90% confidence interval of experimental results)**

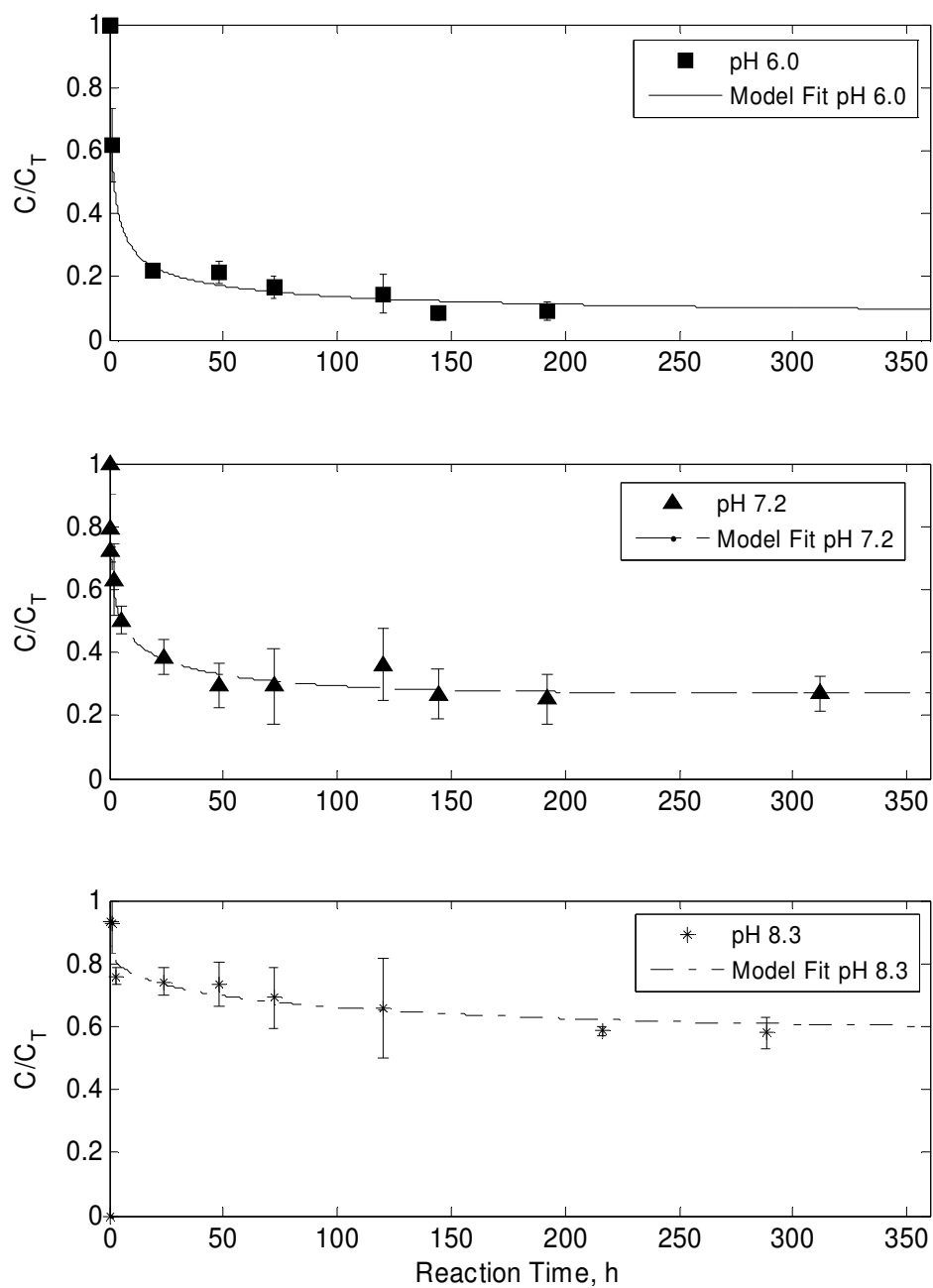


**Figure 4-4 Sorption Kinetics of Enrofloxacin at three pHs with Model Fit (Error bars represent 90% confidence interval of experimental results)**

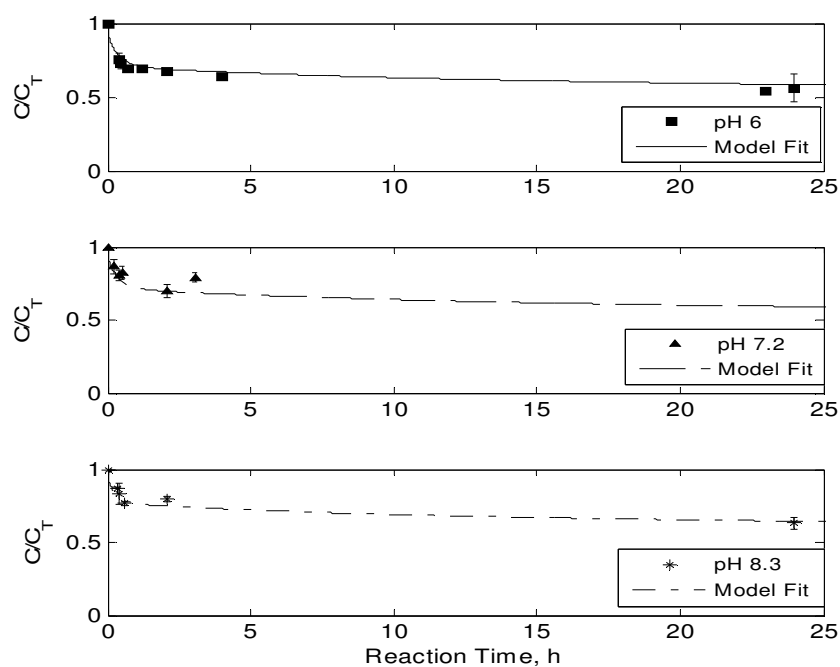


**Figure 4-5 Sorption Kinetics of Triclosan during the First Day of the Reaction**  
(Error bars represent 90% confidence interval of experimental results)

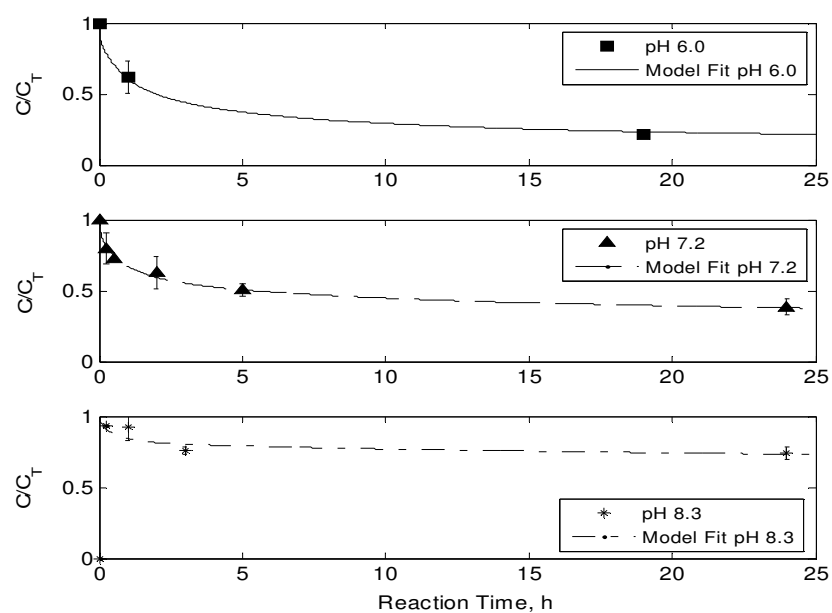


**Figure 4-6 Sorption Kinetics of Enrofloxacin during the First Day of the Reaction**  
(Error bars represent 90% confidence interval of experimental results)

Concentration versus time measurements exhibit interesting behavior, whereby both chemicals initially showed high sorption rates (Figure 4-5 and Figure 4-6), which then decreased dramatically over time. This is indicative of multiple domain features for the sediment particles used for this study. The high and low sorption rates corresponded to high and low mass transfer (diffusion) rates into two distinct sorption domains of sediment particles: labile organic matter and condensed organic matter, respectively. Condensed organic matter is covered by labile organic matter, such that chemicals can only reach the condensed phase after having penetrated the labile organic matter. Thus the initial, relatively high sorption rates result from the rapid transfer of sorbates into labile organic matter. Further, ENR may attach to exposed mineral surface of the sediment, which manifests itself as fast sorption rates. As sorbates reach the condensed organic matter, sorption rate begins to drop because mass transfer slows down considerably. Quantitatively, the amount of both TCS and ENR attached to sediment particles during the first 30-min reaction was approximately 35% of the final amount of sorbed-phase chemicals at equilibrium.

Even though TCS is more hydrophobic than ENR, experimental results indicate that ENR exhibits stronger sorption than TCS. This suggests that the sorption mechanisms of these two chemicals are different from one another. At pH 7.2, 85% and 4% of ENR molecules exist as zwitterions and cations, respectively (Figure 4-1). For these two species, the basic 7-piperazinyl group is protonated and thus exists in a positively charged state (Lizondo et al., 1997). This promotes ionic interactions between the protonated 7-piperazinyl group and the negatively charged surfaces of sediment particles, significantly increasing the

sorption of ENR onto sediment particles. Although zwitterionic species also possess a negatively charged 3-carboxylic acid group, the contribution of the protonated 7-piperazinyl group appears to dominate the behavior of this species; as made evident by such a large fraction of ENR (73%) existing in the sorbed phase at pH 7.2. The sorption of ENR increases dramatically at lower pH, as the ENR becomes increasingly cationic. At pH 6, about 35% of ENR molecules exist as cations, such that more than 90% of the ENR exists in the sorbed-phase. Although ENR shows higher solubility at this pH than at neutral condition (Table 4-1), which likely decreases sorption capacity, this effect is compensated for by the increased electrostatic attraction of positively charged species towards negatively charged sediment particles. At slightly alkaline conditions (pH 8.3), 65% and 30% of ENR molecules exist as zwitterions and anions, respectively, and the sorption of ENR decreases significantly. Upon reaching equilibrium, only 40% of the ENR exists in the sorbed-phase. This is probably due to decreased affinity of anionic ENR (most specifically, the negatively charged 3-carboxylic group) towards sediment particles. The small fraction of ENR, which exists in the sorbed-phase under alkaline conditions, could represent zwitterions, which would have some positively charged functionality. Or, it may be possible that cation bridging, whereby polyvalent cations ( $\text{Ca}^{2+}$ ,  $\text{Fe}^{3+}$  and  $\text{Al}^{3+}$ ) or even monovalent cations act as *bridges* to connect anionic species to negatively charged sediment surfaces, mediates some portion of the ENR sorption exhibited under slightly alkaline conditions (Nowara et al., 1997).

The sorption kinetic experiments for ENR at pH 7.2, which were originally performed using ionic strength of roughly 2mM, were repeated at an ionic strength of roughly 0.2M,

to explore the effect of ionic strength on ENR sorption. From Figure 4-7, increased ionic strength dramatically reduces sorption of ENR onto sediment particles. Although higher sorbent concentration was used at higher ionic strength (Table 4-2), the equilibrium fraction of ENR existing in the sorbed-phase was 28%, much lower than the 73%, which was observed at the same pH at lower ionic strength. The sorption coefficient ( $K_d$ ) decreases by a factor of 10 when ionic strength is increased by a factor of 100. This could be because, as ionic strength increases, metal cations increasingly compete with ENR cations for attachment at negative sediment surfaces (Brownawell et al., 1990; ter Laak et al., 2006), leading to lower affinity of ENR to sediment surfaces.

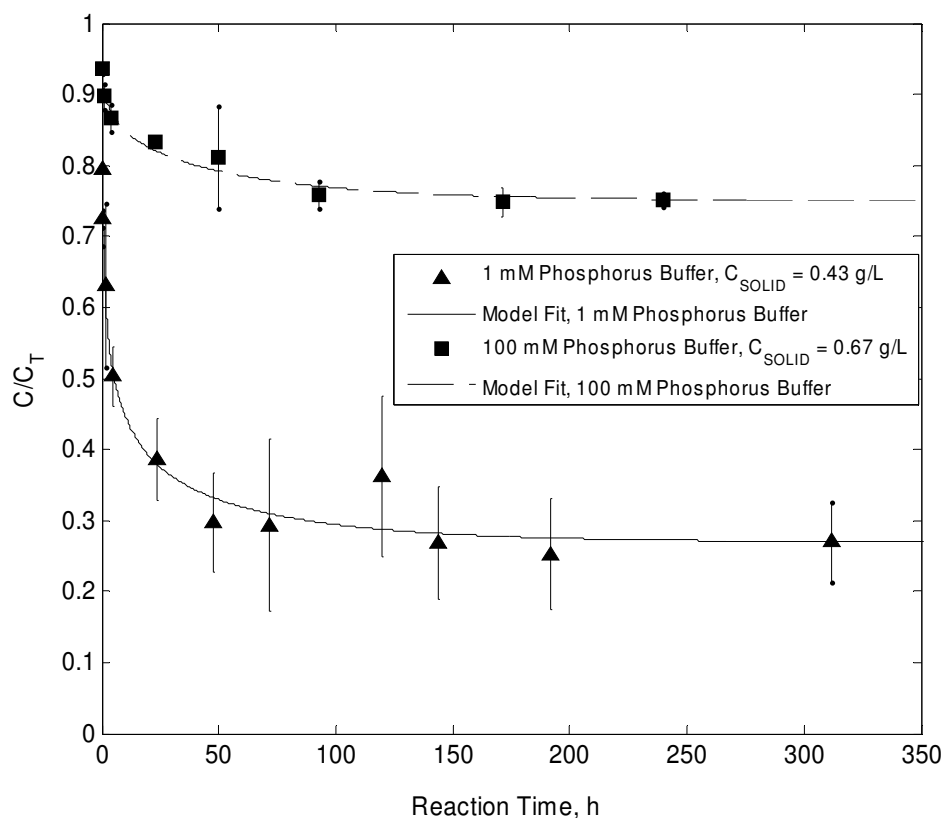


**Figure 4-7 Sorption Kinetics of Enrofloxacin at pH 7.2 under Different Ionic Strength (Error bars represent 90% confidence interval of experimental results; Solid line represents results of model fit)**

In contrast to ENR, TCS exhibits much lower sorption capacity to the sediments. The sorption behavior is also less dependent on either pH or ionic strength. For the measured pH levels used in this study, TCS exists as either a neutral or anionic species. For  $pK_a = 7.9$ , the fractions of TCS existing in anionic form are 1.2%, 16.6% and 71.5% at pH 6.0, 7.2 and 8.3, respectively (Figure 4-2). Despite this wide variation fraction, only minor differences were observed between equilibrium sorbed fractions for different pH values. There was almost no differences for pH = 6.0 (57% sorbed) versus pH = 7.2 (55% sorbed), and neither of these was dramatically different than the result for pH = 8.3 (45% sorbed) (Figure 4-3). Because the dramatic increase in anionic fraction, which should be expected to mediate dramatically increase electrostatic repulsion, does not significantly impact the equilibrium sorbed-phase ENR fraction, it can be inferred that hydrophobic interactions between TCS and the sediment organic phase must compensate for the effect of increased electrostatic repulsion to some extent. Additionally, it should be noted that the pH = 6.0 and pH = 8.3 experiments were performed using a much higher ionic strength buffer than pH = 7.2; therefore, it would seem that neither pH nor ionic strength have an appreciable impact on equilibrium ENR sorption.

The sorption kinetics model developed in *Section 3.3.1* of Chapter 3 was fitted to experimental data, and diffusion coefficients ( $D_a$ ) were adjusted to acquire best fits (lowest RMSE). The model generated reasonable fits for both TCS and ENR (see Figure 4-3 through Figure 4-7 and Table 4-4). For TCS, the same diffusion coefficient was applied to all three pH values, since there was found to be a negligible effect of pHs



on TCS sorption. Results indicate that one single diffusion coefficient (Table 4-4) can adequately fit experimental data of TCS measured from all pH values.

Although both TCS and ENR exhibited slow sorption (Figure 4-3 and Figure 4-4), kinetic modeling revealed much higher diffusion coefficients for ENR (Table 4-4). Thus, the slow sorption of ENR may largely result from the high local sorption, which decreased the mobility of ENR molecules thus retarding mass transfer. The diffusion of ENR showed apparent dependence on pH. At alkaline conditions (pH 8.3), ENR exhibited lower diffusion rate than at other two pHs, suggesting that the diffusion was retarded by some mechanisms such as electrostatic repulsion. However, this slow diffusion may also result from inefficient pH control at this pH. Alkaline condition tends to be more easily affected by sediment particles and/or carbon dioxide from the atmosphere, the latter resulting in slight pH reductions. Since the sorption of ENR was largely dependent on pH, this slight reduction pH would apparently increase sorption coefficients. Thus, the sorption coefficient derived at the end of the experiments, which was used for model fitting, could be higher than the actual sorption coefficient at the initial stage of the reaction (e.g., first two points at pH 8.3 in Figure 4-6). To account for the effect of higher sorption coefficient being used, diffusion coefficients had to be reduced to generate good fit. Further evidence could be found in Figure 4-4 that the kinetics model generated relatively poor fit to the last two observed data at pH 8.3, at which experimental results indicated an actual sorption equilibrium. However, model results showed that sorption equilibrium had not been achieved yet. This proves that the ENR diffusion coefficient was likely underestimated at pH 8.3. Diffusion coefficients derived for pH 6.0 and 7.2

were quite similar, and both were much higher than the diffusion coefficient of TCS. Finally, the diffusion coefficient of ENR showed negative dependence on ionic strength. This seems reasonable, since it has been reported that increased ionic strength would reduce the diffusion rate of charged macromolecules (Anderson, et al., 1978; Tivant, et al., 1983).

**Table 4-4 Kinetics Model Results of Triclosan and Enrofloxacin**

	<i>pH</i>	<i>Diffusion Coefficient (cm<sup>2</sup>/s)</i>	<i>RMSE</i>
<i>Triclosan</i>	6.0, 7.2, 8.3	$3.0 \times 10^{-8}$	0.0458
<i>Enrofloxacin</i>	6.0	$7.5 \times 10^{-7}$	0.0297
	7.2	$9.0 \times 10^{-7}$	0.0331
	8.3	$9.7 \times 10^{-8}$	0.0436
	7.2 (0.1M Buffer)	$9.0 \times 10^{-8}$	0.0121

#### **4.3.2 Desorption Kinetics of Triclosan and Enrofloxacin**

Desorption kinetics batch experiments were started after sorption processes approached equilibrium. Solutions in the reactors were replaced by analyte-free solvents. The concentrations of sorbates in the original solutions were measured to determine the amount of sorbates removed. The total amounts of sorbates used in the desorption kinetics experiments were calculated by subtracting the amounts in removed solutions from initial amounts used for sorption experiments. For TCS, desorption experiments were conducted for all three pHs. However, the desorption kinetics of ENR were only explored at pH 7.2 and an ionic strength of 0.1 M since, as discussed above, the sorption of ENR was strongly dependent on pH. Inefficient pH control using 0.1mM phosphate buffer caused slight variations of pH in the reactors but relatively large errors on sorption results. Desorption experiments generated even larger errors, again due to inefficient pH

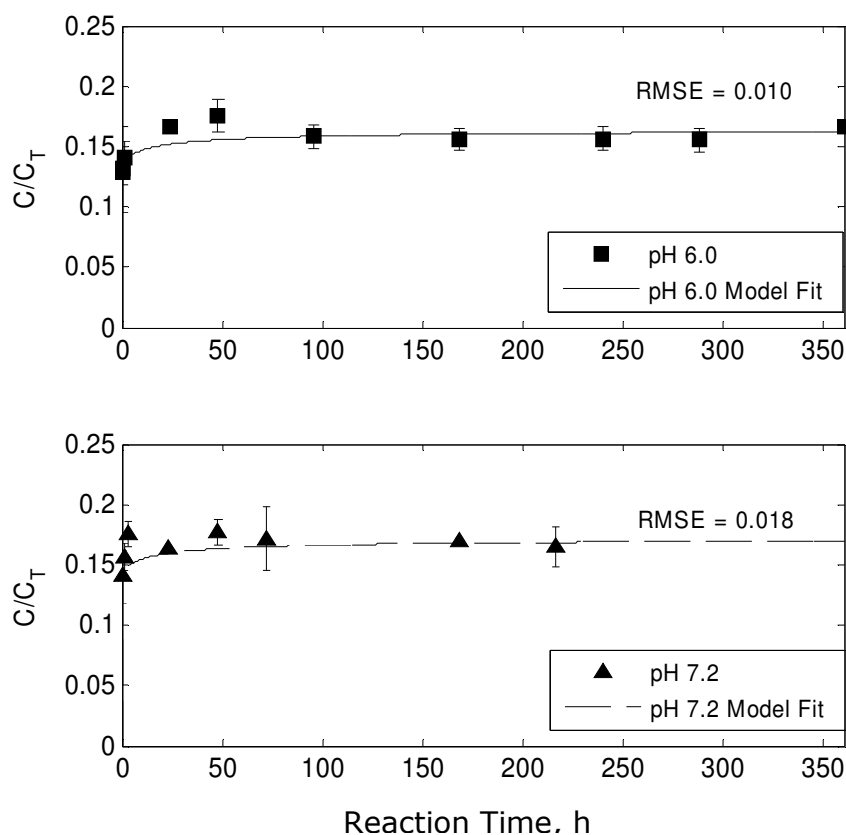
control, likely compounding the errors from sorption experiments and thus causing large variations within the final desorption measurements.

The experimental results are displayed in Figure 4-8 and Figure 4-9. Both chemicals exhibited slow desorption kinetics due to mass transfer. For the desorption process, chemicals diffused from porous media into the aqueous phase due to concentrations gradients. As the amount of chemicals in the pore water decreased, sorbed chemicals detached from sorption sites and entered pore water to compensate for the decrease. Thereby, slow mass transfer retarded the decrease of concentrations in pore water thus preventing the detachment of sorbates. Similar to the sorption process, relatively high desorption rates were observed initially, corresponding to the relatively high mass transfer rates from labile organic matter into the aqueous phase. These high rates reflect direct interaction between the labile organic matter and the aqueous phase. Over time, desorption rates began to decrease, as molecules within the condensed organic matter began to participate in the desorption process.

For triclosan, the fractions existing in the dissolved-phase were quite similar at pH 6.0 and 7.2. This is consistent with the findings from the sorption experiments. Nevertheless, the value of the sorption coefficient at each pH derived from desorption kinetics experiments was higher than the value of the sorption coefficient derived from sorption kinetics experiments (Table 4-5). This is indicative of sorption-desorption hysteresis.

**Table 4-5 Sorption Coefficient Derived from Kinetics Experiments**

	<i>Triclosan</i>			<i>Enrofloxacin</i>
<i>pH</i>	<i>6.0</i>	<i>7.2</i>	<i>8.3</i>	<i>7.2 (0.2M buffer)</i>
<i>K<sub>d</sub> from Sorption Experiments (L/kg)</i>	<i>418±80 (n=33)</i>	<i>405±76 (n=20)</i>	<i>310±119 (n=9)</i>	<i>559±42 (n=5)</i>
<i>K<sub>d</sub> from Desorption Experiments (L/kg)</i>	<i>534±79 (n=12)</i>	<i>503±100 (n=15)</i>	-	<i>1213±208 (n=6)</i>

**Figure 4-8 Desorption Kinetics of Triclosan at pH 6.0 and 7.2**

Hysteresis may be caused by extremely slow desorption rates (Miller and Pedit); irreversible sorption due to heterogeneity of SOM, since two SOM domain exhibited distinct sorption behaviors (Weber et al., 1998); and/or sorbate-induced pore deformation (Sander and Pignatello, 2005). Miller and Pedit (1992) illustrated that equilibrium

distribution between the aqueous (dissolved) and sorbed phase was not actually achieved after a desorption step due to sufficiently slow desorption rates. This likely suggests that the sorption-desorption hysteresis would be less apparent if the reaction time is sufficiently long. Pignatello and Xing (1996) pointed out that slow desorption rates may be caused by high activation energy of sorptive bonds, since the activation energy of desorption is generally greater than that of sorption. As adsorption could be unactivated or slightly activated thus achieving equilibrium instantaneously when chemicals reach specific sorption sites, desorption of large molecules should be activated. Thereby, desorption is rate-limited by both mass transfer (diffusion) and the release of chemicals from sorption sites, which further slows down desorption processes.

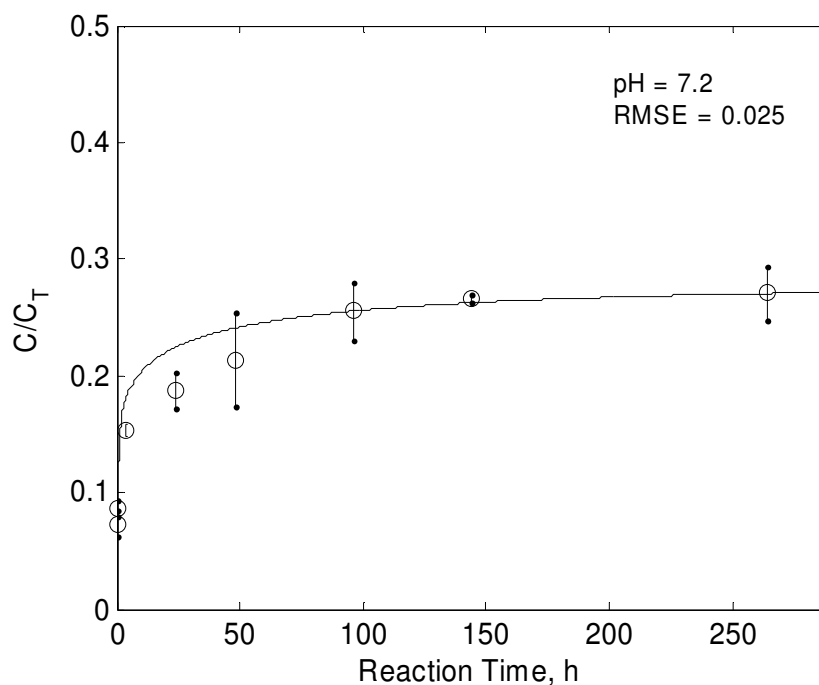


**Figure 4-9 Desorption Kinetics of Enrofloxacin at pH 7.2**

Hysteresis may also result from irreversible processes, such as chemical bonding; entrapment of sorbed molecules in meso- and micro-pores within inorganic components of natural sorbents; and entrapment of sorbed molecules in the SOM matrix (Weber et al., 1998). Some studies have verified that sorbate molecules can be entrapped by the condensed organic phase of soils/sediments sorbents, whereby more pronounced desorption hysteresis is observed in sediment samples containing higher condensed-phase SOM content (Huang et al, 1997b; Weber et al, 1998; Ran et al, 2004). Gu et al. (2007) attributed the hysteretic behavior of tetracycline sorption to a significant fraction of sorbed molecules being irreversibly retained in humic acid through physical entrapment and sorbent deformation. Sander and Pignatello (2005) ascribed the sorption-desorption hysteresis of naphthalene, when being sorbed onto lignite, to structural deformation of the sorbents (i.e., swelling). Pore-deformation may occur by via dilation of existing holes, due to thermal motions of the sorbate, or via creation of new holes by incoming sorbates. The sorbate-induced irreversible pore-deformation generally gives rise to hysteresis because sorption and desorption processes are required to proceed via different pathways.

TCS sorption coefficients computed based on desorption measurements were 27.8% larger at pH 6.0 and 24.2% larger at pH 7.2 than their corresponding sorption coefficients computed using sorption measurements (Table 4-5). This suggests that pH may not significantly affect the fraction of sorbates entrapped by SOM. However, for ENR, the sorption coefficient derived from desorption measurements was 117% larger than the sorption coefficient computed based on sorption measurements (Table 4-5). This more

pronounced increase could result from *true* hysteresis and nonlinear sorption of ENR, as discussed in *Section 4.3.3*.

The kinetics model was used to fit desorption data. Moving forward, it was necessary to decide which values of TCS sorption coefficients were most appropriated for *desorption kinetics* modeling since sorption kinetics experiments and desorption kinetics experiments generated different sorption coefficients (Table 4-5). By using sorption coefficients derived from desorption kinetics experiments, which are 503 L/kg at pH 7.2 and 534 L/kg at pH 6.0, the kinetics model generated good fit to experimental data at last several points. However, it significantly *underestimated* dissolved-phase concentrations at first two points, corresponding to the desorption in the labile organic matter domain of sediment particles. In other words, more sorbed-phase molecules were released from the labile organic matter domain than model predicted values. This likely suggests that the sorption-desorption hysteresis did not occur in this domain. For this reason, sorption coefficient of this domain were adjusted back to the values derived from sorption kinetics experiments: 405 L/kg at pH 7.2 and 418 L/kg at pH 6.0. Correspondingly, the sorption coefficients in the condensed organic matter domain were raised so that the sorption coefficients on the *whole* sediment particle were still 503 L/kg and 534 L/kg at pH 7.2 and pH 6.0, respectively. By this way, the kinetics model yielded better fit, likely verifying that the hysteresis largely occurred in the condensed organic matter. Generally, the kinetics model reasonably reproduced desorption experimental results (Figure 4-8 and Figure 4-9), indicating that the effect of irreversible entrapment of sorbates could be implied in higher sorption coefficients of desorption process.

### **4.3.3 Sorption Isotherm Batch Experiments for Triclosan and Enrofloxacin**

Sorption isotherm batch experiments were conducted to further study the differences in sorption behavior between the two selected chemicals. For TCS, a sorption isotherm was derived only at pH 7.2, because initial sorption kinetics experiments (*Section 4.3.1*) indicated that TCS sorption is less affected by pH over the range 6.0-8.3 (Table 4-5). For ENR, sorption isotherms were derived for pH 6.0, 7.2, and 8.3. For the isotherm experiments, 2mM phosphate buffers, rather than 1 mM, were used to control pH more efficiently. At pH 6.2, ENR concentrations in blank samples (i.e. positive controls) were found to keep decreasing over time, indicating degradation at this pH. Thus, sorbed-phase concentrations of ENR were determined by extracting sorbed molecules into ACN. Freundlich and Langmuir models were used to fit experimental data. Results are presented in Figure 4-10, Figure 4-11, and Table 4-6.

TCS exhibits generally linear sorption behavior within the tested range, from 20 µg/L to 400 µg/L. A Freundlich exponent ( $1/n$ ) of 0.9484 in Figure 4-10 indicates slightly nonlinear sorption. Thus, the sorption of TCS is not significantly dependent on sorbate concentrations. TCS exhibits relatively high hydrophobicity, based on its low water solubility (10 mg/L), its somewhat high molecular weight (300 g/mol), and its somewhat high octanol-water partitioning coefficient ( $\log K_{ow} = 4.76$ ); therefore, the measurements in Figure 4-10 are consistent with previous measurements in which “hydrophobic” compounds have shown linear sorption isotherms for equilibrium dissolved-phase concentrations less than  $10^{-5}$  mol/L or less than one-half of their water solubility (de



Maagd, et al, 1998; Walters et al., 1989). Moreover, the TCS isotherm results also exhibit sorption coefficients that are consistent with those that were computed using kinetics experiments (*Section 4.3.1* and Table 4-5).

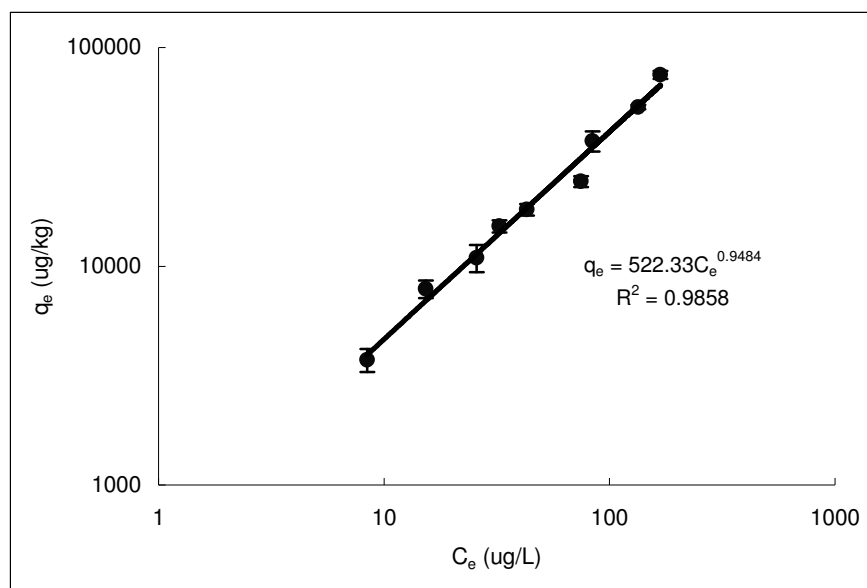


**Figure 4-10 Sorption Isotherm of Triclosan Fitted by the Freundlich Equation**

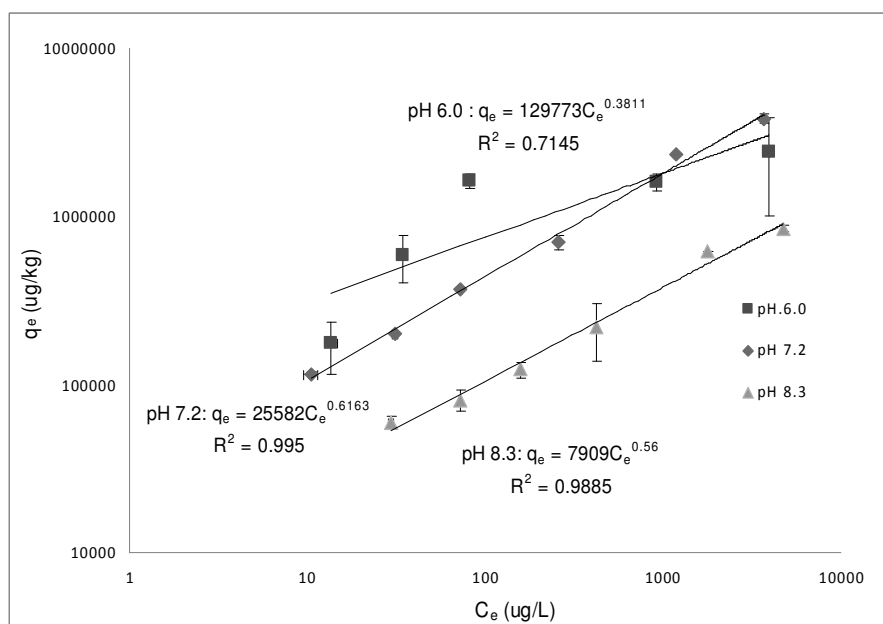


**Figure 4-11 Sorption Isotherms of Enrofloxacin Fitted by the Freundlich Equation at Three pHs**

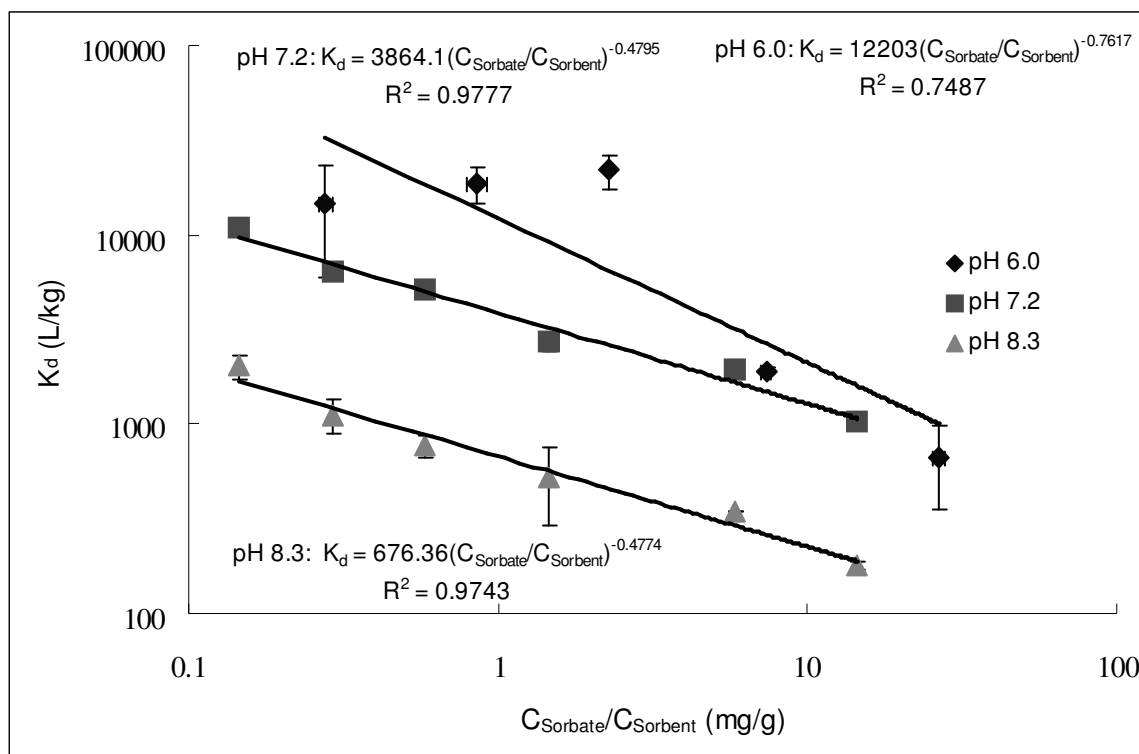


**Figure 4-12 The Dependence of Sorption Coefficient ( $K_d$ ) on Sorbate-Sorbent Ratio**

In contrast to TCS, ENR exhibited strongly nonlinear sorption. Within the tested concentration range (50 to 5000  $\mu\text{g/L}$ ), the nonlinearity ( $1/n$ ) was 0.3811 at pH 6.0, 0.6163 at pH 7.2, and 0.56 for pH 8.3. This nonlinearity may result from a limited number of sorption sites in the SOM. For the nonlinear sorption, the sorption coefficient could be a function of sorbate-sorbent ratio ( $C_{\text{Sorbate}}/C_{\text{Sorbent}}$ ) (Figure 4-12). Higher sorbate-sorbent ratio leads to smaller fractions of sorbates being sorbed, and therefore results in lower sorption coefficients. Quantitatively, based on the regression equations in Figure 4-12, every 100% increase in sorbate-sorbent ratio would result in a 39% drop in sorption coefficient at pH 7.2. As mentioned in *Section 4.3.2* and summarized in Table 4-5, a 117% increase was observed for ENR sorption coefficient computed using desorption versus sorption kinetics experiments. This may be largely due to a much lower

sorbate-sorbent ratio used in the desorption experiments since it is unlikely that sorption-desorption hysteresis alone could cause such a dramatic change. Assuming that this is true and that ionic strength did not appreciably impact the dependence of  $K_d$  on sorbate-sorbent ratio, the lower concentrations of sorbates used in the desorption experiments relative to the sorption experiments are likely responsible for the large majority (76.5%) of the observed increase in sorption coefficient. The remainder of the increase in  $K_d$  (22.9%) is likely due to sorption-desorption hysteresis.

Although the overall sorption of ENR was nonlinear, its sorption onto certain domains of the sediment particles could be linear (e.g., the labile organic matter). A model combining a linear sorption and a Langmuir nonlinear sorption (Eq. 4.6) was thus used to fit the experimental data. The nonlinear compartment of this two-compartment Langmuir model combines the contribution of two sediment domains on sorption processes: an exposed mineral surface domain and a condensed organic matter domain. Model results are shown in Table 4-6. By assuming there is some linear sorption contribution, the two-compartment Langmuir model yielded a much better fit to experimental results than the single Langmuir model. This likely suggests that the assumption of linear sorption in specific compartments of sediment particles is valid. The Freundlich equation still generates better fits than the two-compartment Langmuir model, even though the latter uses more parameters. However, one possible advantage of the two-compartment Langmuir model is that it can describe some features of sorption processes. For example, Weber et al. (1996) illustrated that the nonlinearity of sorption processes grew over reaction time. As presented in Figure 3-6, combining the sorption kinetics model

developed for current study and the two-compartment Langmuir model may adequately predict this time-dependent increase of nonlinearity.

**Table 4-6 Parameters derived from the Langmuir Isotherm for enrofloxacin**

<i>pH</i>	<i>Single-Compartment Langmuir Isotherm</i>			<i>Two-Compartment Langmuir Isotherm</i>			
	$Q_{max} (\mu\text{g/g})$	$b (\text{L}/\mu\text{g})$	$R^2$	$K_d (\text{L/kg})^a$	$Q_{max} (\mu\text{g/g})^b$	$b (\text{L}/\mu\text{g})$	$R^2$
<b>6.0</b>	7176	0.00193	0.7227	438	1832	0.0081	0.7860
<b>7.2</b>	1003	0.0116	0.7161	485	802	0.014	0.9727
<b>8.3</b>	315	0.007	0.7702	79	252	0.0088	0.9578

<sup>a</sup>. The physical meaning of  $K_d$  here is the amount of chemical being sorbed by the sediment component exhibiting *linear* sorption, as normalized by the *total mass* of sediments.

<sup>b</sup>. The physical meaning of  $Q_{max}$  here is the maximum sorption capacity of the sediment component showing *nonlinear* sorption, as normalized by the *total mass* of sediments.

#### 4.4 Conclusions and Environmental Significance

The sorption kinetics of TCS and ENR were examined in the laboratory and fitted to a kinetics model. Results reveal that both chemicals exhibit slow sorption behavior for both sorption and desorption processes; that is, both chemicals require long times to achieve sorption equilibrium. This indicates that the traditional assumption of instantaneous equilibrium is invalid. Both chemicals showed initial high sorption rates, verifying the relative high mass transfer rates in labile organic matter of sediment particles. Nevertheless, mechanisms behind the sorption of the two compounds were different. The sorption of TCS results largely from its hydrophobicity, thus showing less dependence on pH or ionic strength. In contrast, ionic interactions participated in the sorption of ENR. For this reason, ENR, though it is less hydrophobic than TCS, exhibits stronger sorption capacity onto sediment particles, because the energy associated with ionic interactions is

much higher than that of hydrophobic bonding. Increases in pH and/or ionic strength dramatically reduce the sorption of ENR because of increased electrostatic repulsion and/or reduced surface negative charge of sediment particles. Desorption kinetics experiments revealed an approximate 23-28% increase of sorption coefficients compared to the values computed from sorption experiments. This suggests that there is some amount of sorption-desorption hysteresis for each chemical. This hysteresis was likely caused by irreversible entrapment in SOM.

The two-compartment sorption *kinetics* model developed for this study, which was based on the theory of pore diffusion, adequately reproduces experimental data for both sorption process and desorption process. Although both chemicals show slow sorption, the kinetics model derived much higher diffusion coefficients for ENR. This indicates that the high local sorption of ENR onto pore walls reduces the mobility of ENR molecules, thus retarding the whole sorption process. Further, the diffusivity of ENR may adversely depend on ionic strength. By fitting desorption kinetics data, kinetics modeling may offer evidence that irreversible bonding of sorbates does not occur in the labile organic matter of sediments.

Sorption isotherm batch experiments revealed linear (or slightly nonlinear) sorption for TCS and apparently nonlinear sorption for ENR; the latter exhibiting a linearity of 0.62 at pH 7.2. Results from sorption batch experiments were consistent with the results from kinetic batch experiment, especially as pertaining to the inverse dependence of sorption coefficient on pH. The sorption coefficients of ENR showed strong dependence on

sorbate-sorbent ratio. Thereby, sorbate-sorbent ratio may be used to adequately predict sorption coefficient under various chemical or sediment concentrations. A higher ratio, indicative of fewer sorption sites, leads to a lower sorption coefficient. Quantitatively, at pH 7.2, a 100% increase of sorbate-sorbent ratio causes a 39% drop in sorption coefficient for ENR. Two Langmuir models were adapted to fit the isotherm data: a single compartment Langmuir model; and a two-compartment Langmuir model assuming one compartment exhibits linear sorption. The two-compartment model yielded better fit, suggesting that the assumption of linear sorption in specific components of sediment particles is valid. Although the Freundlich equation still generated better fit than the two-compartment Langmuir model, the Langmuir model may be better suited explaining or predicting sorption behaviors such as the apparent decrease in sorption linearity over time.

The sorption of pharmaceuticals affects their mobility, reactivity and bioavailability in natural environments, such as rivers and soils, thus significantly influencing their environmental behaviors and exposure levels. Nonlinear sorption and sorption-desorption hysteresis would prohibit their release from the sorbed phase, likely causing them to be more persistent in the natural environment. Environmental conditions such as pH also influence their sorption and give rise to different environmental behaviors. Better assessment of sorption behaviors of pharmaceutical compounds could assist in better, more quantitative evaluation and prediction of their fate and transport in natural environments.

The experiments in this study were conducted under conditions close to natural environments; i.e., low chemical concentrations, circumneutral pH, and natural sorbents. Therefore, it is appropriate to apply the experimental results garnered from this work to fate and transport analyses for natural environments. In particular, the sorption kinetics model developed for this study was tested by the fitted experimental data arising from lab experiments, and the measured parameters were found adequate for use in large-scale fate and transport models for natural environments.

## **Chapter 5: Fate and Transport Modeling of Selected Pharmaceuticals in Estuaries**

### **5.1 Introduction**

As the occurrence of pharmaceuticals (e.g. antibiotics) in natural waterbodies has been frequently reported during the past decade (Ficazio et al., 2008; Kolpin et al., 2002) and they may cause adverse impacts on human health and aquatic organisms, it is crucial to understand their fate and behavior in aquatic ecosystems. Natural attenuation processes of pharmaceuticals in natural aquatic ecosystems include dilution, sorption, photodegradation and biodegradation/biotransformation. Hydrolysis and volatilization generally are not efficient pathways for the removal of pharmaceuticals from waterbodies (Gurr et al., 2006; Nicolaou et al., 2007). Biodegradability is generally poor for most antibiotics tested up to date (Kümmerer 2009; Tamtam et al., 2008). The photodegradability and sorption varies significantly among pharmaceuticals. Thus it is expected that different pharmaceuticals are affected by different attenuation processes due to their intrinsic physiochemical properties, which eventually render them different fate and behaviors in natural environments. A quantitative tool is necessary to evaluate the contribution of individual process and identify fate-control processes.

Two pharmaceuticals compounds, triclosan (TCS) and enrofloxacin (ENR), were selected as target compounds. Their fate and transport in natural water/sediment systems were examined by modeling analyses. Both compounds have been widely detected in natural waterbodies, even in finished drinking water (Ficazio et al., 2008; Kleywegt et al., 2011; Kolpin et al., 2002). As discussed in Chapter 4, TCS is an antibacterial agent added to



many household products (e.g. toothpaste and hand soap), and eventually reaches natural environments through urban wastewater (Ricart et al., 2010; Singer et al., 2002). It is toxic to certain algae species, such as *Chlamydomonas* and *Scenedesums* (Wilson et al., 2003), and bacteria (Ricart et al., 2010). The no effect concentration (NEC) of triclosan, which was determined by Ricart et al. (2010), could be comparable to its measured concentrations in natural waters. ENR is a fluoroquinolone (FQ) antibiotic agent for veterinary medicine, most notably used in poultry, swine and cattle farms (Boxall et al., 2003; Lizondo et al., 1997; Sturini et al., 2009). Thus its occurrence in surface waters might be due to rural runoff. Another source of ENR to rivers is urban wastewater since it has been measured in effluents of municipal wastewater (Karthikeyan and Meyer, 2006; Nakata et al, 2005). The detection in municipal wastewater is likely due to pet medicine.

As discussed in Chapter 4, TCS and ENR exhibit quite different sorption behaviors from each other such as sorption kinetics, sorption capacity and linearity. From literatures, both TCS and ENR are resistant to hydrolysis but exhibit high photodegradability (Knapp et al., 2005; Singer et al., 2002). Photolysis was a major removal pathway for TCS in the water column of a Swiss Lake and daily averaged half-lives varied from 2 to 2000 days, dependent on latitude and time of year (Tixer et al., 2002). Further, the photodegradation of TCS is highly dependent on pH since neutral species are much more resistant to photolysis than anionic species. Aranami et al. (2007) reported that half-life of TCS in the freshwater and seawater was 8 and 4 days, respectively. The photodegradation rate of ENR was 0.034 / hr under full sunlight exposure during fall, corresponding to a half-life of 0.85 days (Knapp et al., 2005).

In this study, sorption and photolysis of the two chemicals were modeled, and incorporated into a large-scale fate and transport model for estuaries, the Patuxent Model. The significance of these two processes on the attenuation of TCS and ENR, when in conjunction with estuarine mass transport, were evaluated. The goal of this study, therefore, was to quantitatively evaluate the fate of the two chemicals in natural aquatic environments and address how their properties would affect their environmental behaviors and distributions.

## **5.2 Method**

### ***5.2.1 Study Area and Water Quality Model***

The study area was the 100-km reach of the Patuxent Estuary (Figure 3-2), bounded upstream by Route 50 at Bowie, MD, and downstream by the river mouth entering the Chesapeake Bay. The entire study area could be affected by tidal currents. It receives wastewater from ten major WWTPs (Figure 3-1), which serve as the sources of focused pharmaceuticals. The effluent volume and served population of each WWTP is summarized in Table 3-1.

An existing water quality model, the Patuxent Model, was used at the starting point of this study since its hydrodynamic component was previously well calibrated. It was previously developed to simulate the fate and transport for constituents including chlorophyll *a*, dissolved oxygen, nitrate, ammonia, phosphate, arsenic, copper and cadmium (Lung and Bai, 2003; Lung and Nice, 2007; Nice and Lung, 2008). The model consists of 163 longitudinal and 39 maximum vertical grids (Figure 3-3). In this study, it

was linked to several modules, such as *sorption kinetics*, *sediment transport*, *sorption adjustment* and *photolysis module*. Processes simulated include hydrodynamics, mass transport, sorption kinetics, settling/resuspension at water/sediment interface, pH-dependent sorption, nonlinear sorption and photodegradation. This improved model also can account for the longitudinal variations of some parameters such as pH, sorption coefficient, critical velocity, settling rate, resuspension rate, and particle size. Table 5-1 summarizes parameters and coefficients used in the modeling analysis.

**Table 5-1 Parameters for Modeling Analysis**

	<b>Loading (g/day)</b>		<b>Sorption</b>		<b>Photolysis</b>	
	<i>Upper Patuxent</i>	<i>Western Branch</i>	$K_d$ (L/kg)	<i>Diffusion Coef.</i> ( $\text{cm}^2/\text{s}$ )	$k_0 I_0$ ( $\text{hr}^{-1}$ )	$I_0$ ( $\text{W}/\text{m}^2$ )
<b><i>Triclosan</i></b>	32.3	19.49	1,820	$3.0 \times 10^{-8}$	$0.3^{a, c}$	$208^{a, b}$
<b><i>Enrofloxacin</i></b>	13.4	7.3	<i>Dependent on sorbate -sorbent ratio (maximum: 17,000)</i>	$9.0 \times 10^{-7}$	$0.063^a$	$360^{a, b}$

<sup>a</sup>. Daily averaged; <sup>b</sup>. Values estimated for the latitude 40° N based on day of year (Allen et al., 1998); <sup>c</sup>. Photodegradation rate of anionic species.

### 5.2.2 Loading Estimation

As TCS has been mainly added to household products, the contribution of household effluents is quite significant. Thus the major sources of TCS to river are effluents from municipal WWTPs. Singer et al. (2002) reported a loading rate of 100 mg per 1000 capita per day, which was used as the basis for the estimation of TCS loading. Based on the population served by the major WWTPs of the Patuxent River (Table 3-1), the loading of TCS to the study area was 32.3 g/day from the upper Patuxent River at Bowie and 19.49 g/day from the Western Branch (Table 5-1). According to these two values, the

concentrations in the effluents of WWTPs ranged from 241 ng/L to 266 ng/L, which were in the range of reported values (Chalew and Halden, et al., 2009).

The sources of ENR could be land run-off (non-point sources) due to application to farm animals and municipal WWTPs due to pet treatment. However, the strong sorption capacities of ENR to soils likely reduce its mobility in soil matrix. Thus, effluents from municipal WWTPs are important source of ENR to rivers since a significant amount of ENR was found in the effluents, which ranged from < 34 ng/L ((Nakata et al, 2005) to 270 ng/L (Karthikeyan and Meyer, 2006). A median value, 100 ng/L, was used to estimate the loadings of ENR to the study area. Based on the effluent volume of each WWTP, the loading was 13.4 g/day from the upper Patuxent River at Bowie and 7.3 g/day from the Western Branch.

### ***5.2.3 Sorption Process Modeling***

Sorption processes were simulated by considering both sorption kinetics and sorption capacity of the selected pharmaceuticals onto sediment particles. The sorption kinetics of selected pharmaceuticals was explored in Chapter 4 and diffusion coefficients derived from the experiments were directly used in the fate and transport modeling.

Sorption coefficients ( $K_d$ ) determined from experiments were adjusted based on pH and sorbate-sorbent ratio. TCS exhibited linear sorption with a  $K_d$  of 405 L/kg at pH 7.2. Since it is hydrophobic, its variation in  $K_d$  onto different sediment particles could be largely explained by organic content of sorbents ( $f_{OC}$ ). The organic carbon normalized

sorption coefficient ( $K_{OC}$ ) was 40500 L/kg, corresponding to a  $f_{OC}$  of 1% for the sediments used in the sorption experiments. According to the data from USGS monitoring station 01594440, suspended sediments of the focused area exhibited an average  $f_{OC}$  of 4.5%. Thus a  $K_d$  of 1820 L/kg was used for the fate and transport modeling for TCS.

ENR exhibited nonlinear sorption and its sorption largely resulted from ionic interactions. The Langmuir isotherm and the nonlinear Freundlich isotherm were used to predict  $K_d$  of ENR, which were based on sorbate-sorbent ratio. However, since the concentrations of pharmaceuticals in natural waters were generally at the level of nanogram per liter, the Freundlich isotherm predicted *unrealistic* high  $K_d$  at this low sorbate-sorbent ratio. For example, at a pharmaceutical concentration of 50 ng/L and a suspended sediment concentration of 50 mg/L (typical), the Freundlich isotherm predicted a  $K_d$  of 106,059 L/kg at pH 7.2. In contrast, the Langmuir isotherm predicted much lower but constant  $K_d$  at low sorbate-sorbent ratios, suggesting a linear sorption at low sorbate concentrations. This is consistent with have been expected that chemicals may exhibit linear sorption when their concentrations are quite low compared to sorbent concentrations, since sorption sites are not limited. For this reason, both the Langmuir isotherm and the Freundlich isotherm were used to predict  $K_d$ , but the lower  $K_d$  was adopted.

Sorption coefficients of both TCS and ENR were further adjusted according to pH based on pH-dependent  $K_d$  developed in Chapter 4. Also sorption-desorption hysteresis was considered for both chemicals by increasing  $K_d$  for desorption processes. The strategy of

simulating the hysteresis was that the amount in the sorbed phase at equilibrium was firstly calculated based on the  $K_d$  of sorption processes. If this value had been lower than the actual amount in the sorbed phase, a desorption would occur thus the value of  $K_d$  being increased.

#### **5.2.4 Photolysis Modeling**

Both TCS and ENR show high photodegradability. A photolysis module was used to simulate direct photodegradation. Although indirect photodegradation was a possible elimination pathway for some chemicals, Tixier et al. (2002) elucidated that indirect photolysis seemed to be negligible for TCS. The photodegradation rates of chemicals in natural water are a function of solar radiation intensities. Sunlight reaching water surface would be attenuated by water. As it penetrates water, its intensity decreases exponentially over depth, which can be expressed as (Lung, 2001):

$$I(z) = I_0 e^{-k_e z} \quad (5.1)$$

Where  $I(z)$  is the light intensity at depth  $z$ ,  $I_0$  is the light intensity at water surface ( $z=0$ ), and  $k_e$  is the light extinction coefficient ( $\text{m}^{-1}$ ). The average value of light intensity for a water layer can be determined by:

$$I_a = \frac{I_0}{k_e (z_2 - z_1)} [e^{-k_e z_1} - e^{-k_e z_2}] \quad (5.2)$$

Where  $I_a$  is the average light intensity in the layer, and  $Z_1$  and  $Z_2$  are the depth at the top and the bottom of the layer, respectively. Thus the photodegradation rate can be derived as:

$$k = \frac{k_0 I_0}{k_e (z_2 - z_1)} [e^{-k_e z_1} - e^{-k_e z_2}] \quad (5.3)$$

In which  $k$  is the average photodegradation rate ( $s^{-1}$ ) in the layer and  $k_0$  is the photodegradation rate at water surface ( $z=0$ ).

The photodegradation rate of TCS was derived based on the data reported by Tixier et al. (2002), which evaluated the seasonal variations of photodegradation rates of TCS in a Swiss Lake located at the latitude around 40° N. Since the neutral form of TCS shows resistance to photodegradation, the photodegradation rate should be further adjusted by following equation

$$k = k_{anion} \cdot \frac{1}{1 + 10^{pK_a - pH}} \quad (5.4)$$

Where  $k_{anion}$  is the photodegradation rate of anion species and  $pK_a$  is the acidity constant of TCS. The photodegradation of ENR was derived from Knapp et al. (2005), which conducted experiments under natural sunlight during the fall of 2003 in an area near Lawrence, KS, U.S. (latitude: 39° N). Photodegradation rates of both compounds for modeling analyses are summarized in Table 5-1.

The intensity of sunlight reaching water surface ( $I_0$ ) depends on the angle between the direction of sunlight and the normal to the surface of atmosphere, which is a function of time of day, day of year and latitudes. Then it is attenuated by atmosphere due to particles and cloud cover (Allen et al., 1998; Deas and Lowney, 2000). When reaching the water surface, a small fraction of incident radiation is reflected back by the water surface. Thus,

the solar radiation reaching the water surface can be calculated based on the time, day of year, locations, and atmosphere conditions (e.g. cloud cover). The light intensity is zero during nighttime, thus no photolysis occurring during nighttime. The water quality model used for this study, the Patuxent Model, involves a function to automatically perform such calculations. The calculated light intensities were then incorporated into the photolysis module.

The light extinction coefficient ( $k_e$ ) was determined according to data from the Chesapeake Bay Program (CBP) monitoring stations. The study area showed an average  $k_e$  of 2.5 /m from the monitoring stations. A relatively small value of  $k_e$ , 2.2 /m, was adopted for the modeling analysis. Then two additional values, 1.5 /m and 5.0 /m were used to examine the response of the selected pharmaceuticals to different photolysis conditions.

#### ***5.2.5 Data to Support the Modeling Analysis***

Inflow rates and total suspended solid concentrations (TSS) from the mainstream (the upper Patuxent River at Bowie) and the Western Branch to the study area were obtained from USGS gauging stations 01594440 and 01594526, respectively. Tributary inflows, which were closely related to watershed areas, were estimated from mainstream inflow according to Weller et al. (2003). The pH data were obtained from CBP data hub. There are 11 CBP monitoring stations (TF 1.1, TF 1.3 - TF 1.7, RET 1.1, and LE 1.1 – LE 1.4) along the study area, which are shown in Figure 3-2. The pH data recorded by the stations were interpolated to derive pH for each longitudinal model segment. The light extinction



coefficients ( $k_e$ ) were recorded by TF 1.5, TF 1.7 and LE 1.1. Secchi depth was recorded by TF 1.3, which could be converted to  $k_e$  based on the relationship established by Harding (1994).

## 5.3 Results and Discussion

### 5.3.1 The Fate and Transport of TCS and ENR in the Patuxent Estuary

#### *Water Column*

*Dissolved Phase.* The model-calculated longitudinal profiles of TCS and ENR in the dissolved are displayed in Figure 5-1 and Figure 5-2. Each figure displays results for four specific days representing four different combinations of flow rate and TSS levels: low flow + high TSS, low flow + low TSS, high flow + high TSS, and high flow + median TSS (Table 5-2). As dilution and sorption/settling could be two important natural attenuation mechanisms, higher flow rate may result in higher dilution and higher TSS may cause more efficient removal by sorption. For each day, concentration profiles at two different times are shown: one before sunrise (around 4:30 am) and one at afternoon (around 4:30 pm). The spatial distribution of TSS for these days is displayed in Figure 5-3.

**Table 5-2 Flow Rates, Levels of Total Suspended Solid and Light Intensities for the Four Specific Days**

	<i>Aug-01-2008</i>	<i>Mar-11-2009</i>	<i>Jun-19-2009</i>	<i>Oct-30-2009</i>
<i>Flow Rate (m<sup>3</sup>/s)</i>	<i>6.5 (Low)</i>	<i>4.7 (Low)</i>	<i>32.7 (High)</i>	<i>21.3 (High)</i>
<i>Total Suspended Solid Level</i>	<i>High</i>	<i>Low</i>	<i>High</i>	<i>Median</i>
<i>Light Intensity (W/m<sup>2</sup>)</i>	<i>870</i>	<i>486</i>	<i>826</i>	<i>533</i>

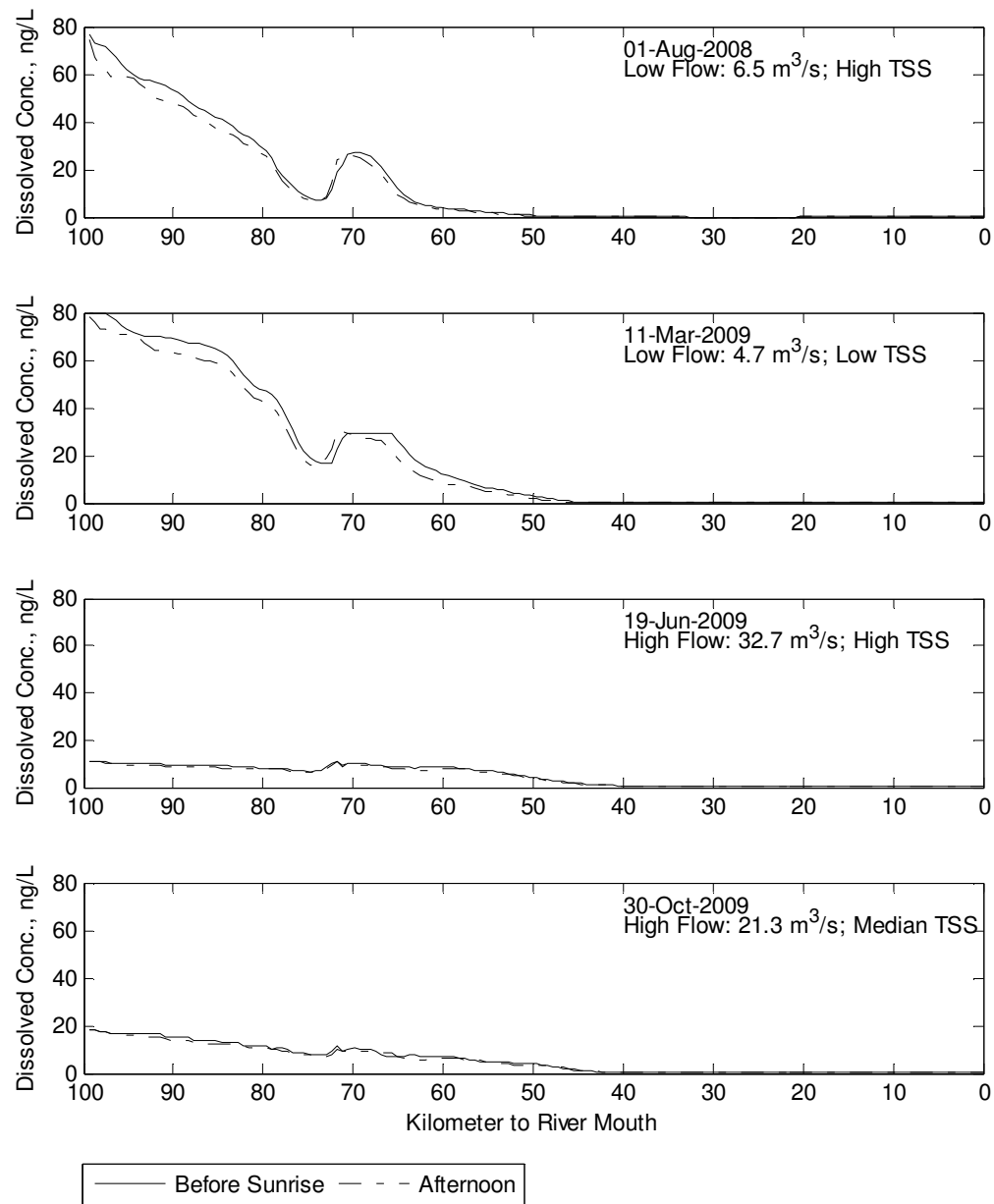


**Figure 5-1 Longitudinal Distribution of Dissolved-Phase Concentrations of Triclosan**

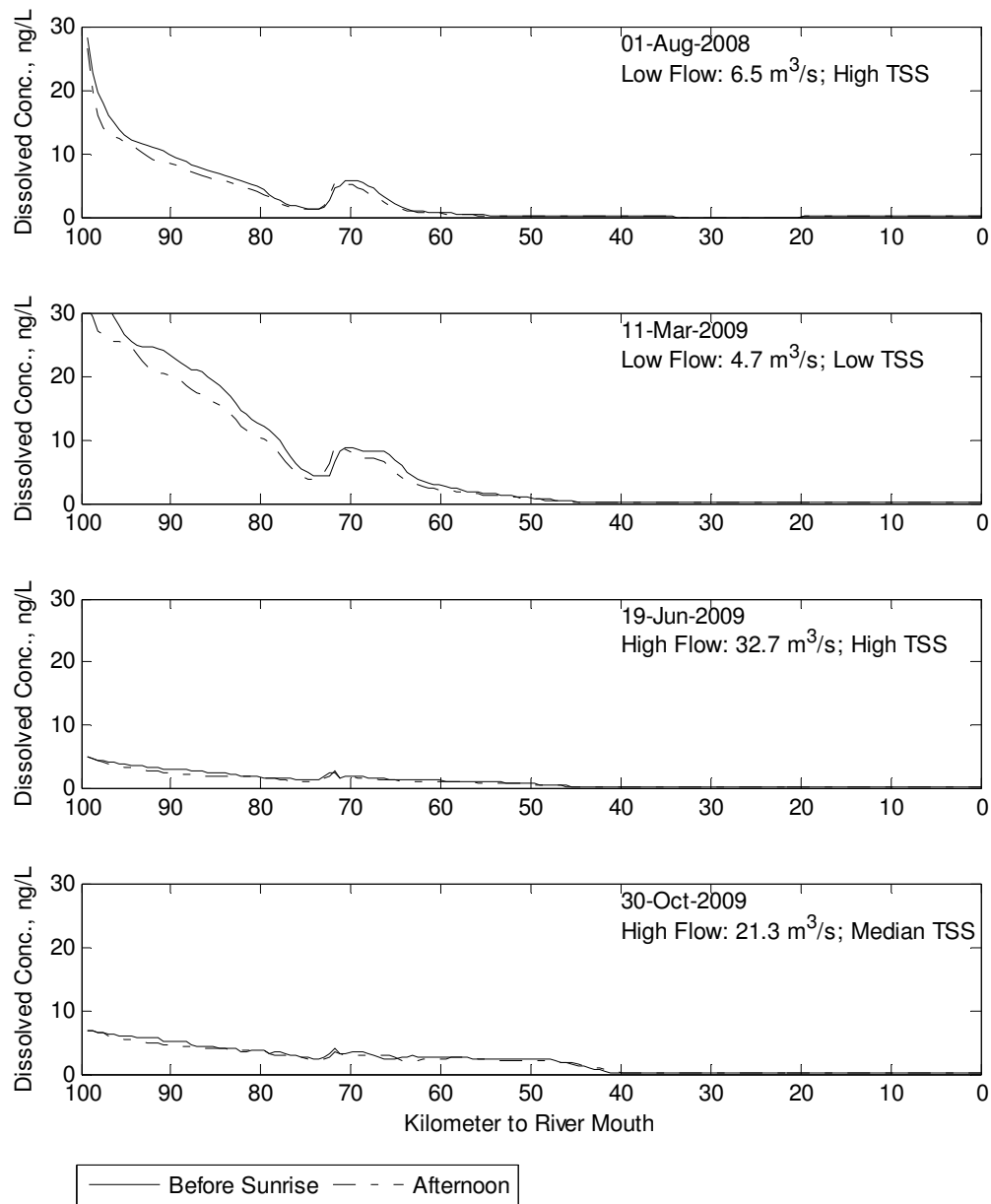


**Figure 5-2 Longitudinal Distribution of Dissolved-Phase Concentrations of Enrofloxacin**

Generally, ENR shows lower concentrations than TCS due to lower estimated loadings for ENR. Both chemicals show apparent diurnal variations in dissolved-phase concentrations due to photolysis. They exhibit higher concentrations before sunrise than

during afternoon. Thus, potentially a larger area could be affected by pharmaceuticals during night. The dissolved-phase concentrations of both chemicals drop significantly when moving from upstream to downstream due to natural attenuation by dilution, sorption and photolysis. The apparent effect of dilution can be observed approximately 75-80 km from the mouth, where a sudden drop in dissolved-phase concentrations occurs for both chemicals due to the rapid increase of the river channel width. The fate and transport of both chemicals are largely affected by flow conditions. Under lower flow rate, both chemicals show higher dissolved-phase concentrations near the upper boundary, which decrease dramatically over travel distance. In contrast, higher flow results in much lower concentrations near the upper boundary due to dilution but milder decrease over distance. This milder decrease then causes that the dissolved-phase concentrations at high flow conditions eventually exceeded those at low flow conditions at the middle of the estuary (approximately 50 km from the river mouth). In other words, high flow could transport pharmaceuticals downstream more efficiently. This is because both photolysis and sorption, when considering sorption kinetics, need time to remove pharmaceuticals from the dissolved phase. The rapid mass transport caused by high flows would not afford sufficient reaction time for both processes, thus fewer pharmaceuticals being removed. This could be further proved by less apparent diurnal variations of dissolved-phase concentrations at high flow conditions for both chemicals (Figure 5-1 and Figure 5-2).

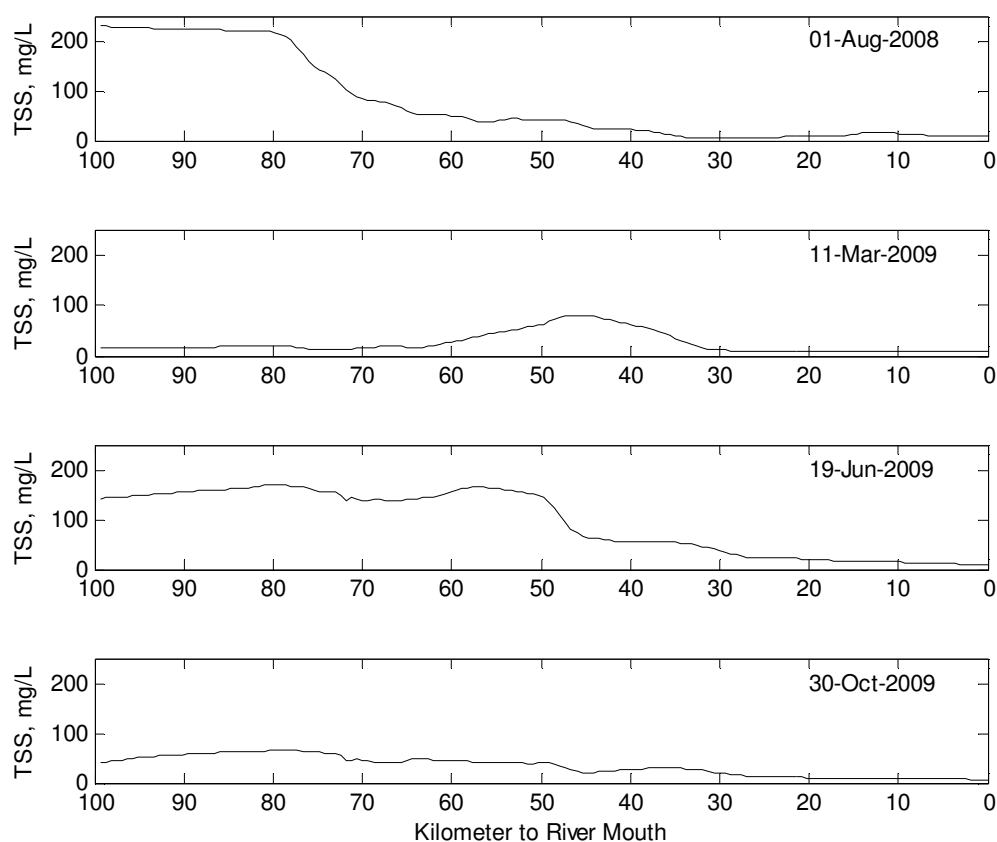


**Figure 5-3 Longitudinal Distribution of Total Suspended Solids**

The attenuation of dissolved-phase TCS and ENR at the location 20 km downstream of the upper boundary is presented in Figure 5-4. This location is chosen because the effect of dilution can be determined. Upon the determination of the effect of dilution, the contribution of sorption and photolysis on the elimination of chemicals can be quantified. It is noticeable that the intensities of solar radiation were different at the four specific days (higher during August and June), which would result in different photodegradation rates.

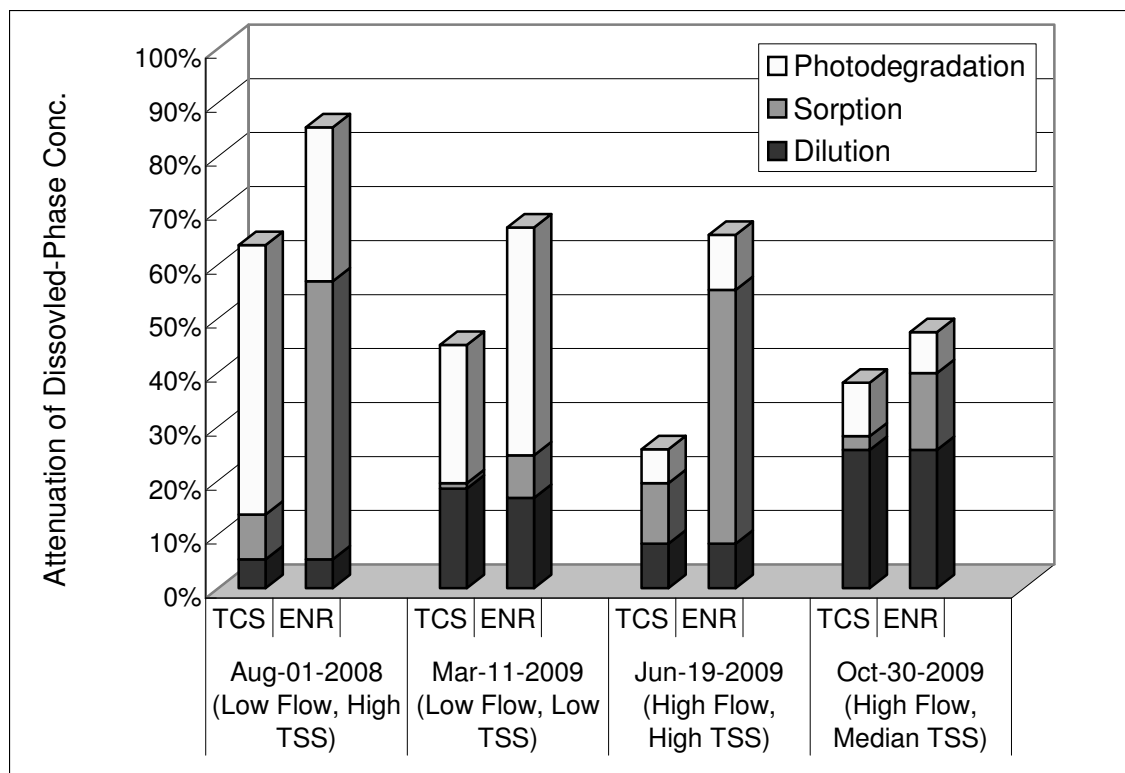


**Figure 5-4 Attenuation of Dissolved-Phase Triclosan (TCS) and Enrofloxacin (ENR) within 20 km of Travel Distance**

Apparently, photolysis and sorption could significantly reduce dissolved-phase concentrations. Sorption causes a 7.9% - 51.5% decreases in dissolved-phase concentrations for ENR and a 1.0% - 11.2% decrease for dissolved-phase TCS. Photolysis results in further decrease in dissolved-phase concentrations: 7.6% - 42.4% for ENR and 6.3% - 49.9% for TCS. Dilution would reduce dissolved concentrations for both chemicals up to 25.6% within the 20-km study area. Low flow rates result in higher removal for both TCS and ENR. The effect of high flow rate could be highlighted at the situation that both TSS concentration and light intensity were quite high. For example, compared to Mar-11-2009, Jun-19-2009 showed both higher light intensity and higher TSS concentrations, which would enhance removal efficiency. However, lower removal rates are still observed on Jun-19-2009 for both compounds, indicating the importance of

rapid mass transport. Especially, photodegradation shows minimum effect on removing dissolved TCS on this day, likely indicating the strong dependence of TCS photolysis on flow conditions. The photodegradation of ENR depends on both flow conditions and TSS concentrations. Higher TSS concentration would drive a larger portion of ENR into the sorbed phase, thus reducing the effect of photolysis. The role of sorption is quite significant for the elimination of dissolved ENR, accounting for more than 60% of total attenuation under high TSS concentrations or 30% of total attenuation under low TSS concentrations. In contrast, photolysis is a leading elimination pathway for TCS since it shows much lower  $K_d$ . However, sorption could still be more important than photolysis for the removal of TCS under certain circumstances such as accounting for 43.6% of the total attenuation on Jun-19-2009, even though light intensity was high on this day. It is noticeable that the sorption of both chemicals less depends on flow conditions than photodegradation. Thus sorption could be a quite efficient attenuation mechanism at high flow conditions even for chemicals showing low  $K_d$  such as TCS. For all four situations, ENR shows greater attenuation than TCS due to sorption. For this reason, ENR has both lower detection frequency and lower measured concentrations in rivers than TCS.

*Sorbed Phase.* The model-calculated longitudinal profiles of sorbed TCS and ENR for the four specific days are displayed in Figure 5-5 and Figure 5-6. For each day, two concentration profiles are shown: one before sunrise and one at afternoon. Both ENR and TCS exhibit an initial increase in sorbed-phase concentrations near the upper boundary. At low flow conditions, in contrast to the rapid decrease in dissolve-phase concentrations over travel distance, both chemicals show gradual decrease or even no decrease in

sorbed-phase concentrations within the first 20-km study area. This is because sorbed chemicals do not undergo photodegradation. For this reason, sorbed chemicals exhibit less diurnal variations. Another reason for the mild drop of sorbed-phase concentrations is that as chemicals move from upstream to downstream, more chemicals would be sorbed by suspended solids due to considering sorption kinetics. This increasing amount of sorbed chemicals would compensate for the effect of dilution to some extent. For example, on Aug-01-2008 (low flow), the fraction of sorbed chemicals increased from 5.8% and 18.2% at the upper boundary to 18.5% and 77.8% at the location 20-km downstream for TCS and ENR, respectively.

A sudden drop in sorbed-phase concentrations could be observed around 75-80 to the river mouth (Figure 5-5 and Figure 5-6) due to maximum settling at this location, where significant increase in the volume of the water column leads to low water velocities. However, this sudden drop cannot be found at high flow conditions because of high water velocities. This further enhances the efficiency of mass transport under high flow conditions, not only for dissolved chemicals but also for chemicals in the sorbed phase.

As presented in Figure 5-4, sorption could be a more important removal process for ENR. This can be seen by Figure 5-6, which shows sorbed-phase concentrations for ENR. The sorbed-phase concentrations of ENR can be comparable to those in the dissolved-phase or even higher, thus causing dramatically reduce in dissolved-phase concentrations. Especially at low flow but high TSS conditions, rapid increase of sorbed-phase concentrations can be observed immediately downstream of upper boundary (97-100 km to the river mouth) (the first row in Figure 5-6). Correspondingly, a quick drop of



dissolved-phase concentrations is observed (the first row in Figure 5-2). This likely suggests that high mass transfer rate in the labile organic matter domain will speed up the removal of ENR from the dissolved phase.

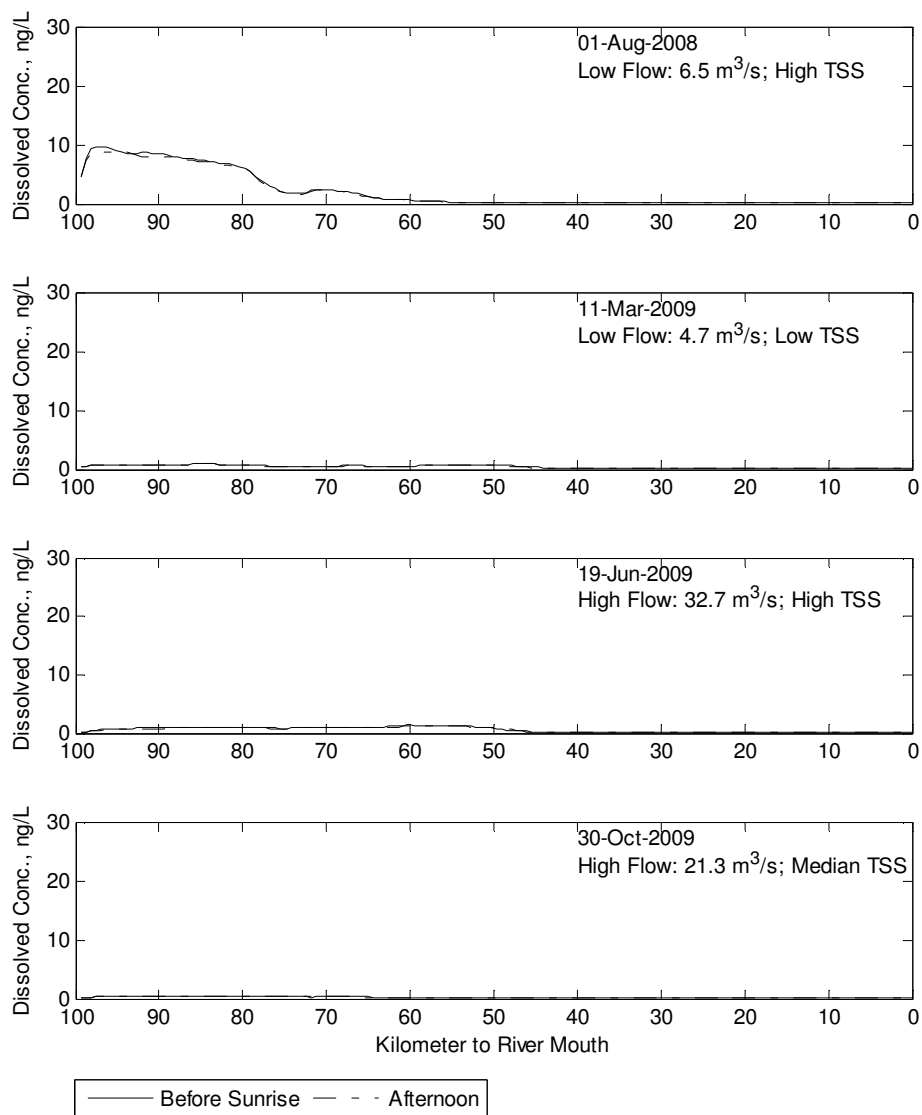


**Figure 5-5 Longitudinal Distribution of Sorbed-phase Concentrations of Triclosan**

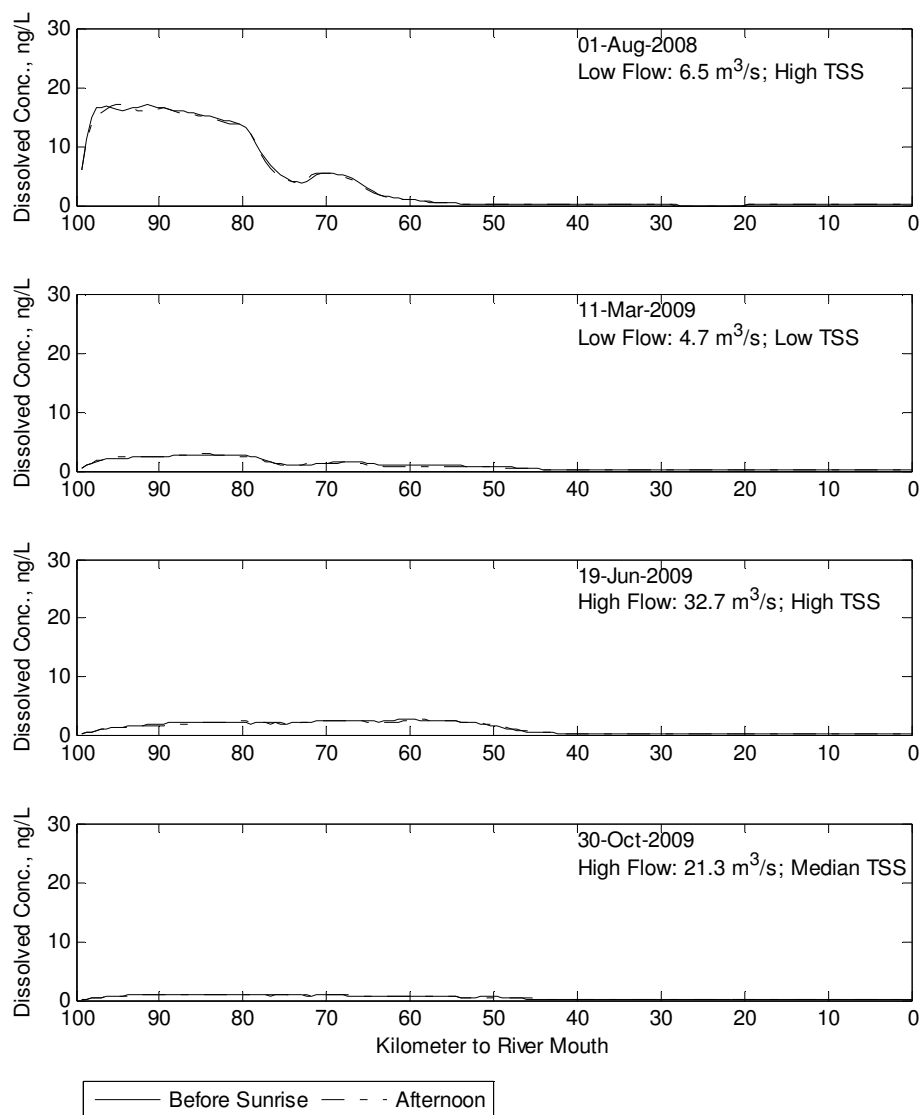


**Figure 5-6 Longitudinal Distribution of Sorbed-phase Concentration of Enrofloxacin**

### ***River Bed***

Figure 5-7 shows the spatial distribution of pharmaceutical concentrations in riverbeds at the end of a 2.5-year simulation period. Both chemicals exhibit significant accumulation into riverbeds. The maximum accumulations are observed at the location around 75-80 km from the river mouth for both TCS and ENR, where suspended solids exhibit

maximum deposition. The sudden drops of chemical concentrations in the water column are also observed at this location since as suspended solids settle they take sorbed chemicals to riverbeds. The concentrations at this location are 1.92  $\mu\text{g/L}$  (3.84  $\mu\text{g/kg}$ ) and 5.38  $\mu\text{g/L}$  (10.76  $\mu\text{g/kg}$ ) for TCS and ENR, respectively, which are much greater than concentrations in the water column.

Quantitatively, during the first year of the simulation, about 592 g of TCS and 1378 g of ENR are accumulated into riverbeds, accounting for 3.1% and 18.2% of the total annual loading of TCS and ENR, respectively. This suggests that bottom sediment could be an important sink for pharmaceuticals. During the second year, these values (net accumulation) reduce to 185 g and 401 g for TCS and ENR, respectively, indicating that a significant amount of chemicals were brought back to the water column by resuspension. Thus bottom sediments could be a source of pharmaceuticals under certain circumstances.

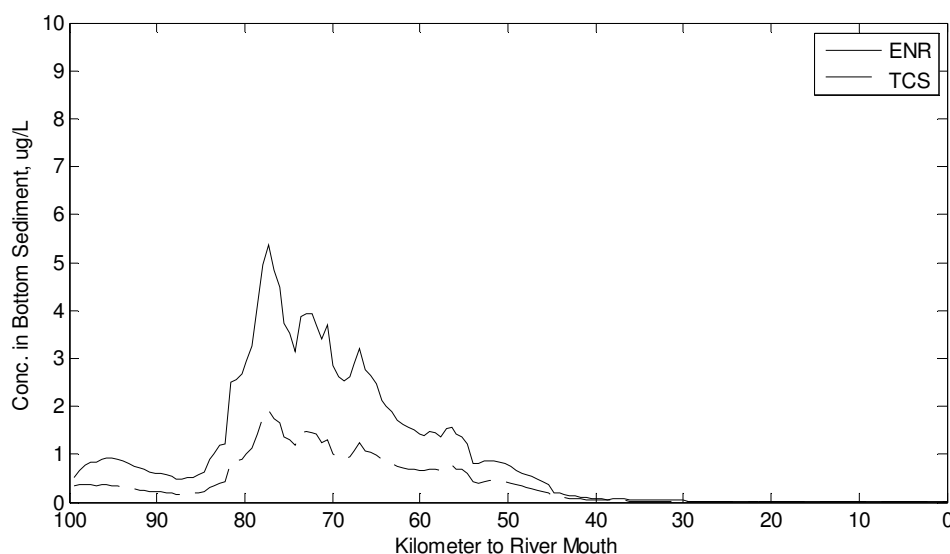


**Figure 5-7 Concentration of Triclosan (TCS) and Enrofloxacin (ENR) in the Active Layer of Bottom Sediment**

### **5.3.2 The Effect of pH**

The study area exhibits alkaline conditions to some extent. The upstream area shows relatively low pH, 7.3 on average. This value increases to 7.5 at the middle and 7.9 at the downstream of the study area likely due to tidal currents from the Chesapeake Bay. Since pH affects the sorption of chemicals and eventually cause different fate and behavior for pollutants, its effect was evaluated by running the model under two scenarios: pH-dependent sorption and pH-independent sorption. The  $K_d$  at pH 7.2 was used for the scenario of pH-independent sorption. For the pH-dependent sorption scenario,  $K_d$  was adjusted based on pH. Since during most simulation period the study area showed alkaline conditions, the values of  $K_d$  used for the scenario of pH-dependent sorption were generally lower than that for pH-independent scenario. All the results presented in *Section 5.3.1* were predicted by considering pH-dependent sorption.

For TCS, the differences in predicted dissolved-phase concentrations between the two scenarios range from -0.5 ng/L (under-prediction) to 1.0 ng/L (over-prediction). For sorbed TCS, the differences ranges from -0.16 to 0.43 ng/L. The maximum over-prediction and under-prediction are found at the locations near the upper boundary of the study area. Considering that TCS generally shows relatively high upstream concentrations, these values seem to be not significant. For this reason, TCS concentrations in water columns are not shown. No apparent effect of pH on the distribution of TCS is because TCS exhibited both low  $K_d$  and less pH-dependent sorption.

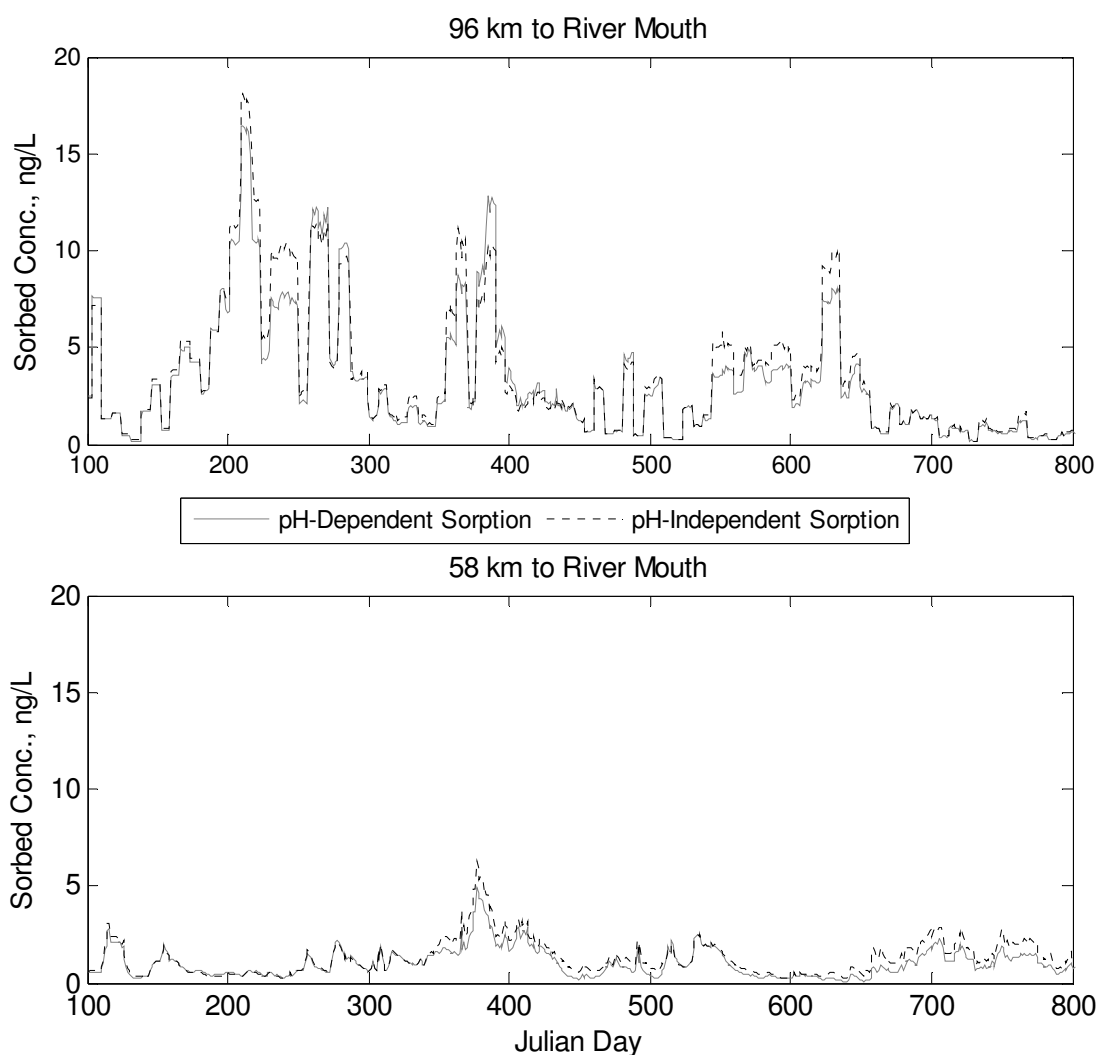


**Figure 5-8 Temporal Distribution of Sorbed-Phase Enrofloxacin from pH-Dependent Sorption Scenario and pH-Independent Sorption Scenario**

The distribution of ENR shows significant dependence on pH. Figure 5-8 displays the temporal distribution of ENR in the sorbed phase for two locations: one upstream (96 km to the mouth) and one middle (58 km to the mouth). During the period shown in the figure, neglecting pH-dependent sorption could either overestimate sorbed-phase concentrations up to 34% corresponding to a pH of 7.8, or underestimate them up to 29% at a pH of 6.8. The chance for the overestimation is 77% over the simulation period. At

the middle location, the difference would be more significant: up to 73% of overestimation or 30% of underestimation. And sorbed-phase concentrations would be overestimated more frequently (81%) since middle locations more possibly show alkaline conditions.

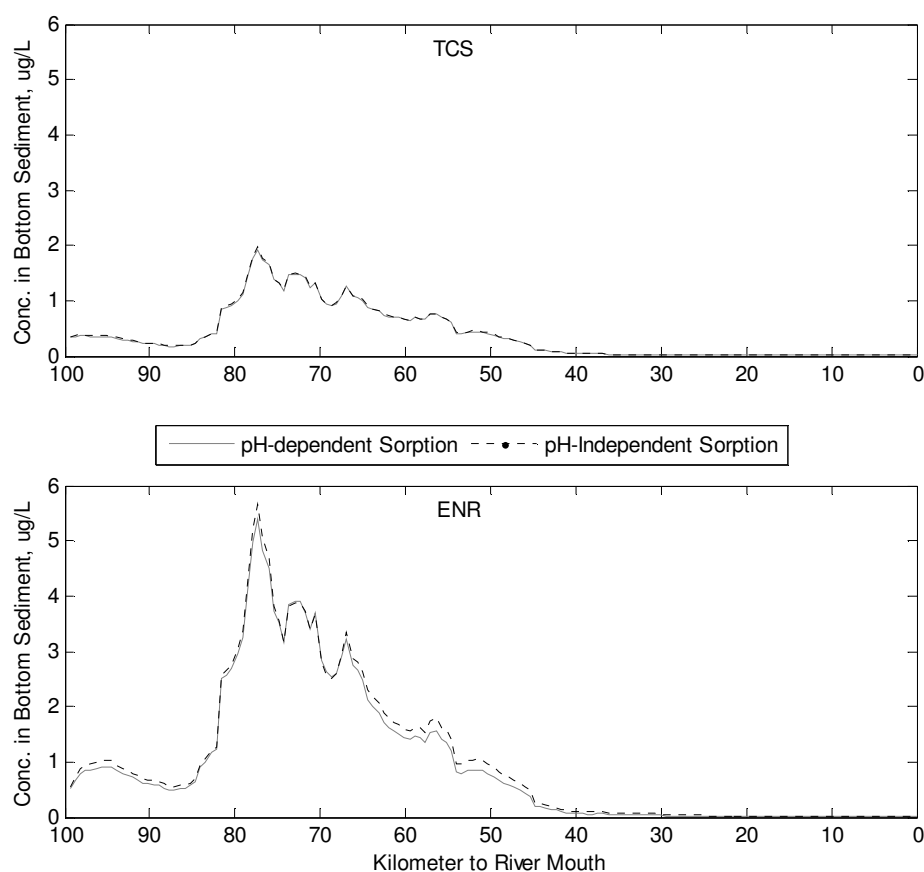


**Figure 5-9 Predicted Temporal Distribution of Triclosan (TCS) and Enrofloxacin (ENR) in the Active Layer of Bottom Sediments from Two Scenarios**

Although overlooking pH-dependent sorption may result in both underprediction and overprediction, the net effect is overestimating sorbed-phase concentrations. This can be proved by the concentrations of ENR on the bottom sediments (Figure 5-9). The

accumulation of ENR into riverbeds is apparently overestimated by the pH-independent sorption scenario: up to 14.5% for the whole study area. Compared to upstream locations, differences in predicted concentrations in bottom sediments between the two scenarios are more apparent at the middle of the study area due to increased pH. For TCS, still no apparent effect could be observed in bottom sediments (see the first row of Figure 5-9).

### **5.3.3 Photolysis**

The photodegradation of chemicals is strongly dependent on light conditions, which would be attenuated by water. Thus the light extinction coefficient ( $k_e$ ) of waterbodies, which determines the amount of solar radiation attenuated over depth, is an important environmental parameter affecting the photodegradation of pollutants, thus eventually causing different fate and distribution. According to the data from CBP monitoring stations, the study area shows a minimum  $k_e$  of  $0.63 \text{ m}^{-1}$  and a maximum value of  $7.0 \text{ m}^{-1}$ , with an average of  $2.95 \text{ m}^{-1}$ . A relatively small  $k_e$ ,  $2.2 \text{ m}^{-1}$ , was used for the modeling analyses presented in previous sections. Two additional  $k_e$  values,  $1.5 \text{ m}^{-1}$  and  $5.0 \text{ m}^{-1}$ , were used to evaluate the response of pollutants to the change of photolysis.

Results for the same four specific days, representing four combinations of flow rates and TSS concentrations, are shown in Figure 5-10 and Figure 5-11. The fate of both chemicals appeared to be sensitive to  $k_e$ . At low flow conditions, lower  $k_e$  leads to apparently higher dissolved-phase concentrations for both chemicals. However, the responses of the two chemicals to the change of  $k_e$  could be different.

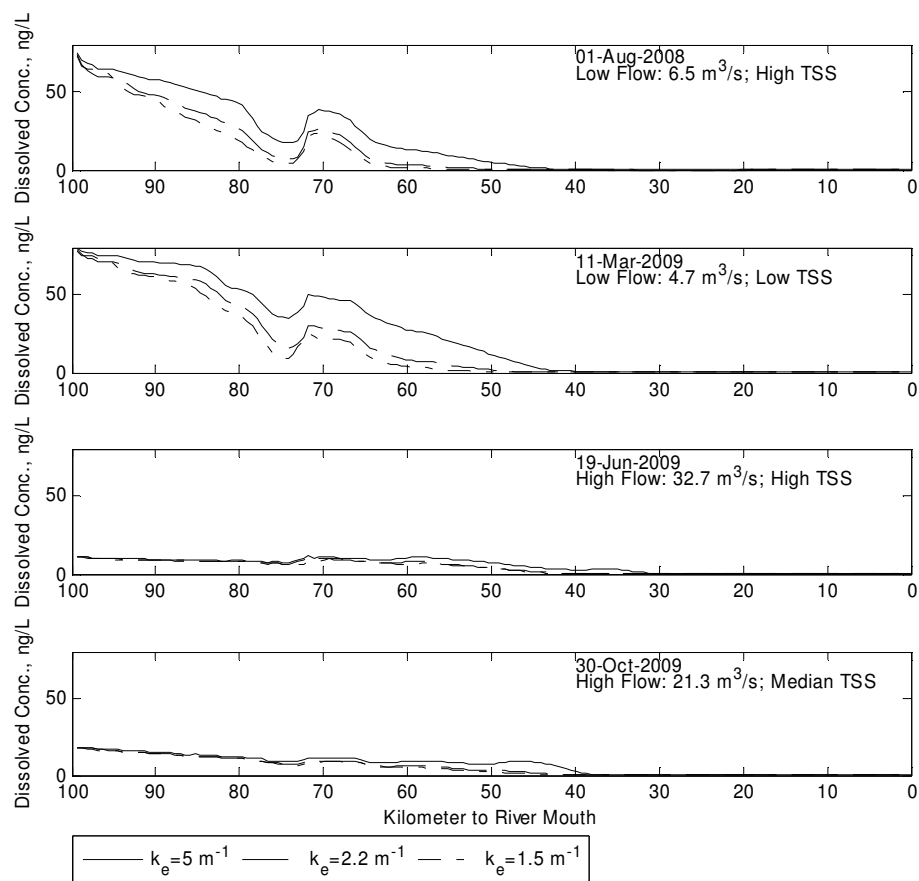


**Figure 5-10 Longitudinal Distribution of Dissolved Triclosan at Different Extinction Coefficients**

The relative significances of sorption and photolysis on the attenuation of dissolved-phase chemicals at different  $k_e$  are evaluated, and are presented in Figure 5-12. Generally lower  $k_e$  leads to higher fractions of dissolved chemicals eliminated by photolysis but lower fractions removed by sorption for both chemicals. Nonetheless, the relative significance of photolysis on the fate of chemicals varies depending on flow conditions, TSS levels and the properties of chemicals. High flow conditions would cause fewer variations in the *total* attenuation of dissolved-phase chemicals. For example, on Oct-30-2009, the total decrease in dissolved-phase concentrations of TCS only slight changed from 20.9% to 22.8% when modifying  $k_e$  from  $5 \text{ m}^{-1}$  to  $1.5 \text{ m}^{-1}$ . The effect of  $k_e$  is even



less pronounced for ENR at high flow conditions. At low flow conditions, dissolved-phase concentrations showed higher sensitivity to  $k_e$  because photolysis could be an important removal mechanism under these circumstances. Yet the effect of  $k_e$  still depends on TSS concentrations and chemical properties. For example, at a low flow and low TSS condition (Mar-11-2009), changing  $k_e$  from  $5 \text{ m}^{-1}$  to  $1.5 \text{ m}^{-1}$  would significantly enhance the elimination of dissolved-phase concentrations for both TCS (from 42.8% to 73.3%) and ENR (from 49.8% to 75.4%). However at a low flow but high TSS condition (Aug-11-2008), the effect of  $k_e$  on the attenuation of dissolved-phase ENR seems to be less significant since a larger portion of ENR could be in the sorbed phase.

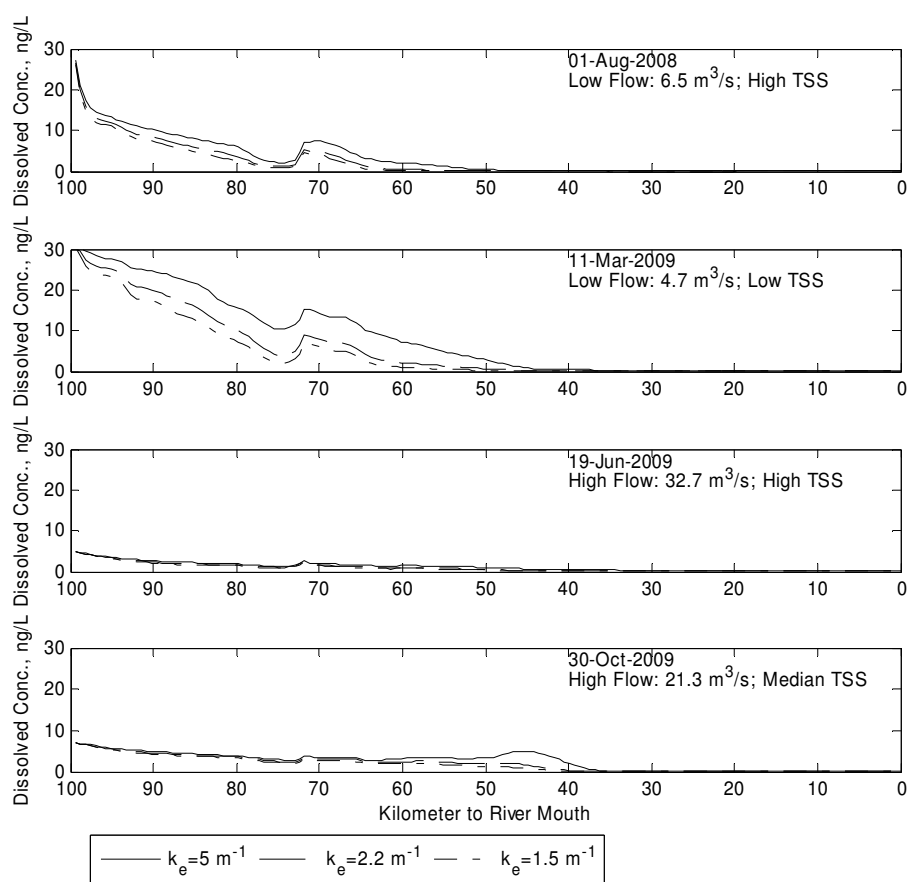


**Figure 5-11 Longitudinal Distribution of Dissolved Enrofloxacin at Different Extinction Coefficients**

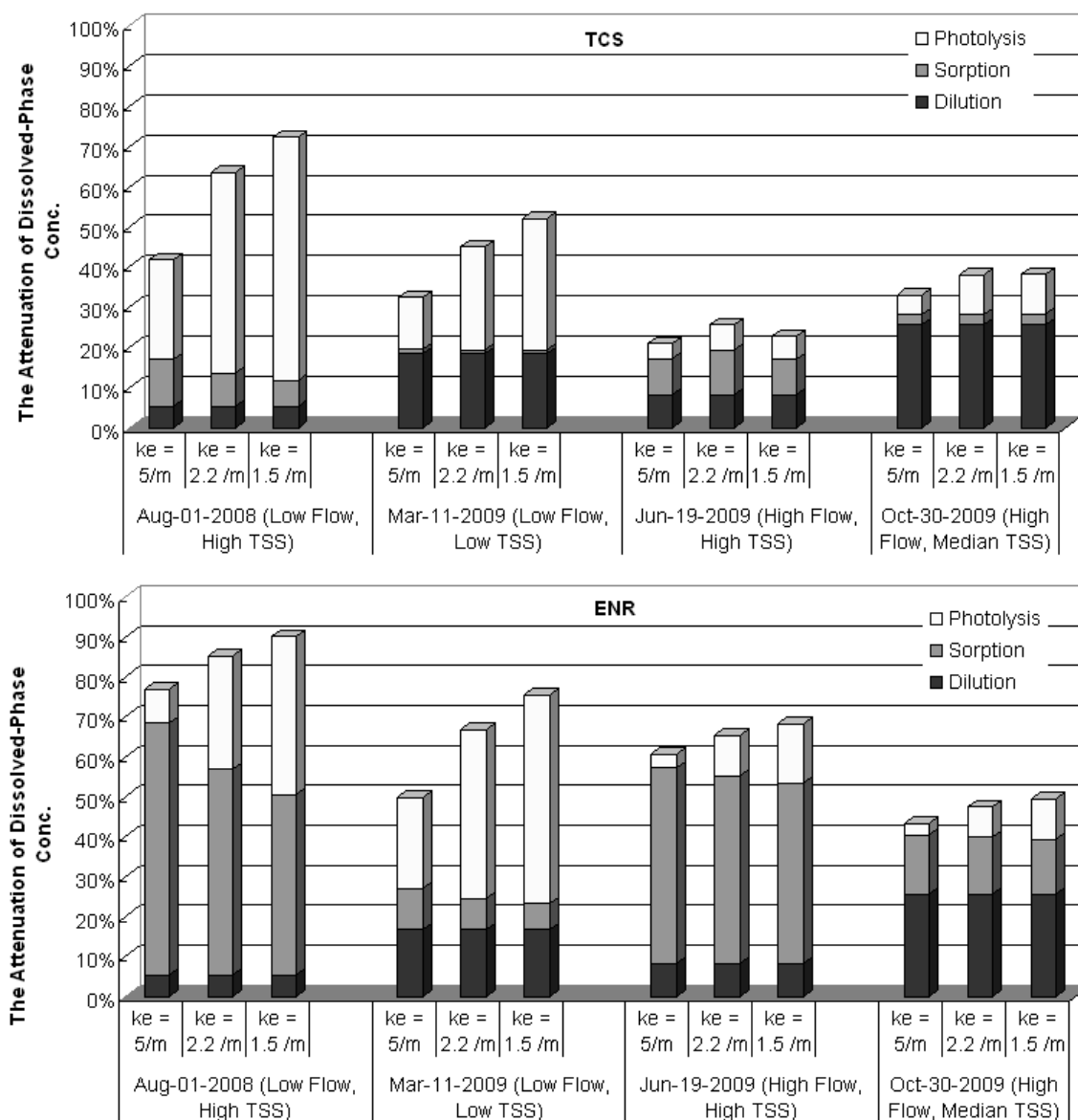


**Figure 5-12 The Effect of Light Extinction Coefficients on the Attenuation of Dissolved-Phase Triclosan (TCS) and Enrofloxacin (ENR)**

The removal of dissolved-phase chemicals reflects a competition between photolysis and sorption. Generally, a higher  $k_e$  would reduce the effect of photodegradation but lead to a higher portion of chemicals in the sorbed-phase, which may compensate the effect of photolysis on the elimination of dissolved chemicals to some extent. Since TCS shows low sorption capacity, its sorption would not efficiently compensate for the decreased

effect of photolysis, thus showing significantly less removal in dissolved-phase concentrations under higher  $k_e$ . That's why generally dissolved TCS is more sensitive to  $k_e$  than dissolved ENR. In contrast, *sorbed* ENR is more significantly affected by  $k_e$  than sorbed TCS. This could be proved by that increasing  $k_e$  from  $1.5 \text{ m}^{-1}$  to  $5 \text{ m}^{-1}$  would raise the accumulation in bottom sediment by 39.6% and 65.0% for TCS and ENR, respectively (Figure 5-13).

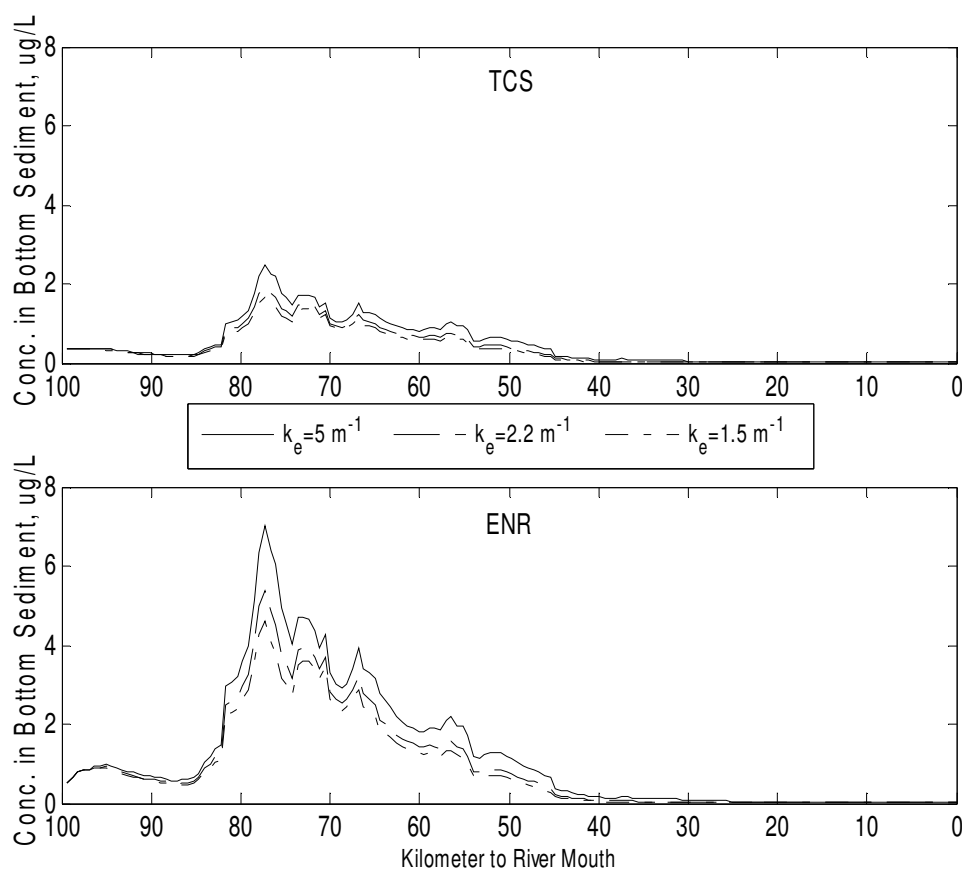


**Figure 5-13 The Effect of Extinction Coefficient on the Accumulation of Triclosan (TCS) and Enrofloxacin (ENR) in the Active Layer of Riverbeds**

#### **5.3.4 Long-Term Simulation**

The accumulation of chemicals onto bottom sediments seems to be an important but very slow process. As pollutant concentrations in bottom sediments increase, more pollutants can be brought into the water column by resuspension. To evaluate the maximum amount of chemicals that could be present in bottom sediments, long-term simulations of the model were conducted for both TCS and ENR. The long-term simulations were performed by repeating a series of two-year simulations. The results at the end of each simulation were output and used as the initial conditions for the next two-year simulation. Model results suggest that without sediment removal mechanisms equilibrium concentrations would not be reached within 24.5 years of simulations for both TCS and ENR (Figure 5-14 and Figure 5-15). During this period, the amount in the bottom sediment keeps increasing for both chemicals. However, the last two two-year simulations yields only slightly different results, suggesting equilibrium would be achieved shortly after that. At the end of the simulation, TCS and ENR reach a maximum of concentrations at the location 78-80 km to the river mouth: 7.4 µg/L and 21 µg/L, respectively. These values are quite significant since benthic biota could be affected by such high concentrations, especially by TCS, which shows a NEC of 0.21 µg/L for bacteria mortality and 0.45 µg/L for algae communities (Ricart et al., 2010).

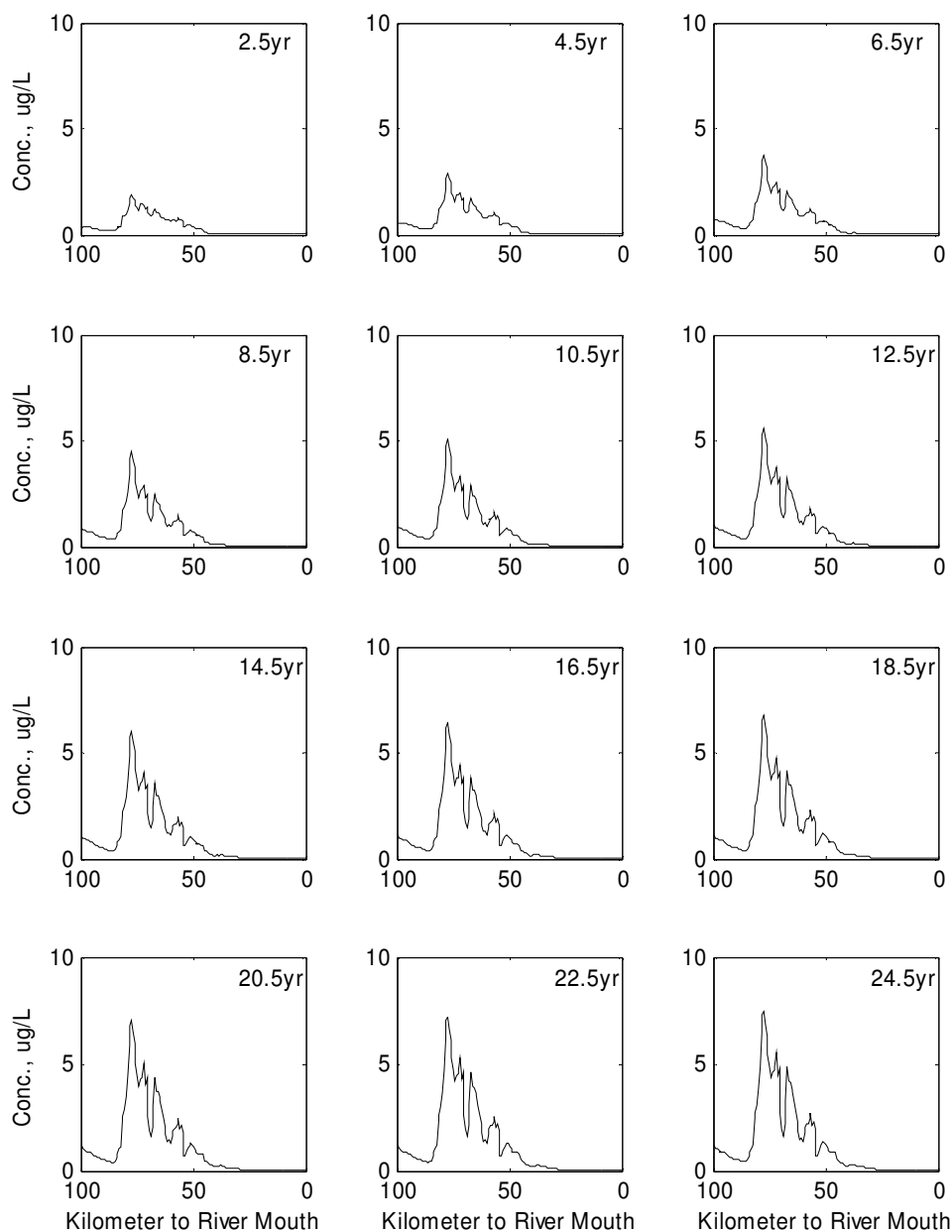


**Figure 5-14 Spatial Profile of Triclosan Concentrations in the Active Layer of Bottom Sediments**

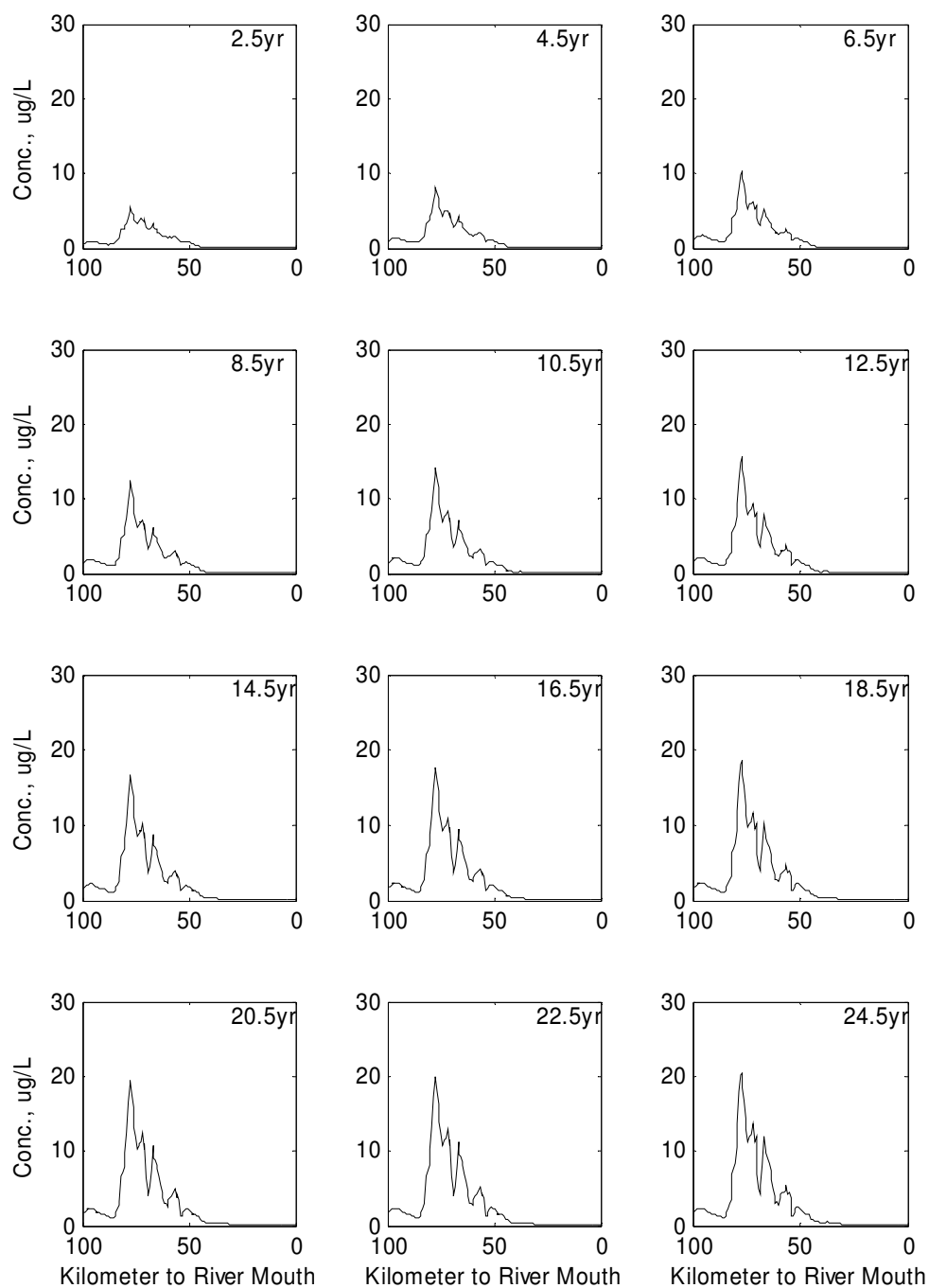


**Figure 5-15 Spatial Profile of Enrofloxacin Concentrations in the Active Layer of Bottom Sediments**

## 5.4 Conclusions

The fate and transport of the two selected pharmaceuticals, TCS and ENR, were evaluated in the Patuxent Estuary. Although both chemicals show high photodegradability, they exhibit significantly different environmental fate and response to the change of environmental parameters. Compared to TCS, sorption could be a more effective elimination pathway for ENR. The decrease in dissolved-phase concentrations caused by sorption is 7.9% - 51.5% for ENR and 1.0% - 11.2% for TCS. Photolysis results in further decrease in dissolved-phase concentrations: 7.6% - 42.4% for ENR and 6.3% - 49.9% for TCS. The relative significance of sorption and photodegradation on the elimination of chemicals in this area varies dependent on actual conditions. Under low flow conditions both chemicals show significant photodegradation. However, TSS may cause different effect of photolysis on the attenuation of ENR. High TSS concentrations would drive a larger fraction of ENR in the sorbed phase thus reducing the effect of photolysis. For TCS, photolysis would be a dominant elimination pathway at low flow conditions.

Higher flow rates would cause much lower concentrations of chemicals near the upper boundary of the study area due to dilution. However, it may transport chemicals downstream more efficiently and eventually result in higher chemical concentrations in both the dissolved phase and the sorbed phase at the middle of the estuary. This is due to two reasons: short reaction time and less settling. First, both photolysis and sorption, when considering sorption kinetics, need time to remove dissolved-phase chemicals. The rapid mass transfer resulted from high flow rate would not afford such long times, thus

leading to less elimination. Second, high flow rates would cause high water velocities, at which suspended solids are less probably to deposit onto riverbeds. Although both sorption and photolysis are influenced by high flow conditions, sorption could be a leading removal mechanisms for ENR since high flow conditions may take more suspended solids to the study area and the high mass transfer rates (diffusion) in the labile organic carbon domain of sediment particles could absorb a significant amount of chemicals quickly. Even for TCS, which shows low  $K_d$ , sorption could be an important attenuation process compared to photolysis, especially under high flow conditions since the effect of sorption on the attenuation of dissolved-phase chemicals is less affected by flow conditions. ENR shows low loadings to the study area but is rapidly removed from water columns due to sorption. This may be the reason that ENR exhibits both low detection frequency and low measured concentrations in natural waters. A significant amount of ENR is accumulated in the riverbed with a maximum annual deposition of 1,378 g. Although less TCS is accumulated into the bottom sediments, its levels in sediments are still significant with a maximum value of 1.92  $\mu\text{L}$  being obtained after a 2.5-year simulation period.

The sorption of TCS and ENR exhibit different response to the change of pH. For TCS, the variations of pH would not apparently affect both dissolved and sorbed concentrations in the water column, and its accumulations bottom sediments. In contrast, the fate of ENR could be strongly affected by pH. Neglecting the pH-dependent sorption of ENR would result in either significant overestimation (up to 73%) or underestimation (up to



30%) of sorbed-phase concentrations in the water column, and 14.5% overestimation of the amount in bottom sediments.

Another environmental parameter,  $k_e$ , was adjusted to evaluate the response of both chemicals under different photolysis scenarios. Results indicate that the fate and behavior of both compounds are sensitive to  $k_e$ . But the actual sensitivity depends on flow conditions and chemical properties. Chemicals in the dissolved phase tend to be less sensitive to  $k_e$  under high flow or high TSS level conditions since photolysis may not be an effective removal mechanism under these situations. The removal of dissolved-phase chemicals appears to be a competition between photolysis and sorption. Generally, lower  $k_e$  would lead to higher removal by photolysis but less removal by sorption. Compared to TCS, the attenuation of ENR is less sensitive to  $k_e$  since the reduced effect of photolysis can be largely compensated by sorption. However, sorbed ENR is probably more sensitive to  $k_e$  than sorbed TCS, which is proved by that raising  $k_e$  from  $1.5 \text{ m}^{-1}$  to  $5 \text{ m}^{-1}$  would increase the accumulation in bottom sediments by 65.0% for ENR and 39.6% for TCS.

Further, long-term simulations reveal that the system takes long time to reach equilibrium accumulation in bottom sediments, likely around 24.5 yr. The maximum concentration that could be achieved in bottom sediments is  $7.4 \text{ }\mu\text{g/L}$  for TCS and  $21 \text{ }\mu\text{g/L}$  for ENR. These high values may cause quite significant impacts on benthic organisms, especially TCS.

## **Chapter 6: Summary, Conclusions and Recommendations for Future Work**

### **6.1 Summary**

The research presented herein provides insight into the relative significances of processes that control the fate and transport of pharmaceuticals in estuaries, and the effect of properties of pharmaceuticals on their environmental behaviors. Special emphasis is placed on sorption and sorption kinetics. The work for this research was performed in three separate, but related, stages: 1) modeling sorption kinetics, incorporating it to a large-scale fate and transport model for estuaries and evaluating the effect of sorption kinetics on the fate and behavior of pollutants; 2) conducting laboratory experiments to study the sorption behavior of two selected pharmaceuticals, including sorption kinetics; 3) Simulating the environmental fate and transport of these two selected pharmaceuticals in the Patuxent River using the improved water quality model and analyzing the similarity and differences of their environmental behaviors.

One major contribution of this research to the field of water quality modeling is that the effect of sorption kinetics, which has been neglected by most current water quality models, has now been evaluated. Chapter 3 examines the environmental behavior of four hypothetical pharmaceuticals, representing four combinations of sorption coefficient and time to reach sorption equilibrium, in a natural water/sediment system. Results reveal that two modeling approaches, instantaneous sorption equilibrium and sorption kinetics, generate significantly different predictions from each other. Sorption kinetics alone may not necessarily explain the different behaviors of chemicals predicted by the two approaches. Interactions between sorption kinetics and mass transport processes,

including sediment transport in the water column, play a key role in quantifying the fate and transport of pharmaceuticals in natural water/sediment systems.

The research presented in Chapter 4 explores the sorption behavior of two selected pharmaceuticals, TCS and ENR, onto suspended sediments to 1) further verify the hypothesis that pharmaceuticals may exhibit slow sorption kinetics; 2) compare the similarities and differences of the sorption of these two chemicals; and 3) measure necessary parameters for the fate and transport analyses. The examined processes include sorption and desorption kinetics, pH-dependent sorption and sorption linearity. The experiments were conducted under environmentally relevant conditions; i.e., microgram per liter chemical levels, circumneutral pH, and natural sorbents. The mathematical models for this study, including sorption kinetics models and sorption isotherm models, were tested by the fitted experimental data; and the measured parameters were found adequate for use in fate and transport models for natural environments.

The research presented in Chapter 5 focuses on fate and transport modeling for these two pharmaceuticals to analyze how their sorption properties, coupled with environment parameters (e.g. pH and  $k_e$ ), control their fate and behavior in water/sediment systems, and evaluate the relative significances of processes on the attenuation of pharmaceuticals. The simulated processes include hydrodynamics, mass transport, sorption/sorption kinetics, photolysis, and settling and resuspension of sediment particles. The two chemicals exhibit different environmental fate and distribution due to their properties. The results also point out that mass transport significantly affects the attenuation of pharmaceuticals.

## 6.2 Conclusions

As presented in Chapter 3, failure to consider sorption kinetics would result in significant underestimation of dissolved-phase concentrations; up to 80-150% at upstream locations for compounds exhibiting fast sorption ( $t_e = 12$  h;  $K_d = 10,000$  L/kg) and slow sorption ( $t_e = 10$  d;  $K_d = 10,000$  L/kg). For this reason, sorption kinetics should always be considered for chemicals whose environmental fate and transport are affected by sorption processes (i.e., those exhibiting high  $K_d$ ). At upstream locations, the difference between instantaneous equilibrium and sorption kinetics approaches is strongly impacted by TSS concentrations. Sorption kinetics also affects the accumulation of pharmaceutical compounds onto the riverbed. Thus the removal of contaminants from the water column is not as rapid as expected in traditional instantaneous-equilibrium based water quality models, which tend to under-predict pollutant levels along the entire estuary. Scouring of bottom sediments, and the transport and deposition of re-suspended solids further amplify the differences between predictions from two approaches.

As presented in Chapter 4, pharmaceuticals may exhibit slow sorption kinetics. The examined pharmaceuticals, TCS and ENR, need 9 and 6 days to achieve sorption equilibrium, respectively. Although ENR exhibits higher diffusion coefficients than TCS, high local sorption of ENR retards the mass transport in pore media, thus leading to long times to reach equilibrium. The different mechanisms behind the sorption process render TCS and ENR different sorption behaviors. Ionic interaction renders ENR much higher sorption coefficients than TCS but stronger dependence on ionic strength and/or pH. Desorption kinetics experiments reveal an approximate 23-28% increase of sorption coefficients compared to the values computed from sorption experiments, suggesting

some amount of sorption-desorption hysteresis occurs for each chemical. Both sorption and desorption kinetics experimental results could be adequately reproduced by the sorption kinetics model developed in this research. Sorption isotherm batch experiments revealed linear (or slightly nonlinear) sorption for TCS and nonlinear sorption for ENR; the latter exhibiting a Freundlich linearity coefficient of 0.62 at pH 7. A 100% increase of sorbate-sorbent ratio causes a 39% drop in sorption coefficient for ENR. The two-compartment Langmuir model generates better fit than the single compartment Langmuir model, suggesting that the assumption of linear sorption in specific components of sediment particles is valid. The Freundlich generates better fit than the two-compartment Langmuir model, even though the latter involves one more parameter. However, the two-compartment Langmuir model can captures some features of sorption processes (e.g., the decrease of linearity over reaction time).

The results presented in Chapter 5 provide quantitative data about the significance of natural processes on the attenuation of pharmaceutical compounds. For a 20-km area immediately downstream of the upper boundary, the decrease in dissolved-phase concentrations caused by sorption is 7.9% - 51.5% for ENR and 1.0% - 11.2% for TCS. Photolysis results in further decrease in dissolved-phase concentrations: 7.6% - 42.4% for ENR and 6.3% - 49.9% for TCS. The significances of both processes depend on flow conditions and TSS concentrations. Higher flow rate leads to lower concentrations at the upstream boundary but less attenuation, thus higher concentrations at the middle of the estuary than lower flow conditions. Generally, the removal of ENR is more dominated by sorption than that of TCS. Even though, under high flow and high TSS conditions, sorption could be a more important mechanism for the elimination of TCS than

photolysis. Both chemicals show significant accumulation in bottom sediments, with TCS levels exceeding its NEC for algae species. TCS and ENR showed different response to the change of environmental parameters. TCS shows negligible response to the change of pH, but ignoring the pH-dependent sorption of ENR could overestimate the accumulation of ENR into bottom sediments by 14.5%. While both chemicals are sensitive to  $k_e$ , their responses to the change of  $k_e$  are different. High flow or high TSS conditions could lead to less  $k_e$  sensitivity. Generally, lower  $k_e$  would lead to higher removal by photolysis but less removal by sorption. Thus the elimination of ENR in the dissolved phase seems to be less sensitive to  $k_e$  since the effect of photolysis on the elimination of dissolved-phase ENR could be compensated by sorption to some extent. Increasing  $k_e$  from 1.5/m to 5/m would raise the amount accumulated into bottom sediments by 39.6% and 65.0% for TCS and ENR, respectively

### 6.3 Recommendations for Future Work

Overall, although this research provides in-depth analysis of occurrence, and environmental fate and transport of two pharmaceuticals possessing unique properties, additional future work might improve the model results, help gain further insight into the fate controlling processes for pharmaceuticals and expand the application of the model:

- Considering that significant amount of pharmaceuticals could be accumulated onto riverbeds and thus riverbeds could be a source of pharmaceuticals to water columns at some circumstances, incorporation of a true re-suspension mechanism might better quantify the role of the riverbeds as a source of pharmaceuticals. Transport of sediments is an important mechanism to be considered in estuaries.

- As both chemicals tested in this research are quite sensitive to *light extinction coefficients*, addressing how the values of light extinction coefficients depend on TSS concentrations becomes necessary. Higher TSS concentrations could drive a larger portion of pollutants into the sorbed phase but may lead to higher light extinction coefficients, which result in lower photodegradation rates. Incorporating the dependence of light extinction coefficients on TSS may better evaluate the relative significance of sorption and hydrolysis on controlling the fate of pharmaceutical compounds in natural waterbodies.
- Although this study modeled photolysis of chemicals, their photolysis products have not been addressed. Through photodegradation, TCS could serve as a significant source of polychlorinated dioxins in surface water, which may even have higher toxicity to aqueous biota (Buth et al., 2010; Ricart, 2010). Ciprofloxacin, a quinolone antibiotic, whose environmental fate has drawn much research interest, is a major degradation product of ENR (Knapp et al., 2005). Evaluating the photodegradation products, and the environmental fate and transport of the products would enhance the application of model results.
- As TCS is toxic to certain algae species and inhibits diatom photosynthesis with a NEC of 0.45 µg/L (Ricart, 2010), the presence of TCS at high concentration levels probability affects the concentrations of dissolved oxygen and predictions of eutrophication models. If it does, linking the fate and transport model for pharmaceuticals to eutrophication models would provide further insight into the effect of TCS on the whole aquatic ecosystems.

## Cited References

Abraham, M.H. Scales of Solute Hydrogen-bonding: Their Construction and Application to Physicochemical and Biochemical Processes. *Chem. Soc. Rev.* 1993, 22, 73-83.

Allen, R. G., Pereira, L. S., Raes, D., and Smith, M. Crop Evapotranspiration: Guidelines for Computing Crop Water Requirements. *Irr. Drain.* 1998, Paper 56. UN-FAO, Rome.

Amborose, R. B., Wool, T. A., and Martin, J. L. The Water Quality Analysis Simulation Program, WASP5 Part A: Model Documentation. Environmental Research Laboratory, U.S. Environmental Protection Agency, Athens, Georgia. 1993.

Anderson, J. L., Rauh, F., and Morales, A. Particle Diffusion as a Function of Concentration and Ionic Strength. *J. Phys. Chem.* 1978, 82(5), 608.

Bachman L. J., and Krantz D. E. *The Potential for Denitrification of Ground Water by Coastal Plain Sediments in the Patuxent River Basin, Maryland.* US Geological Survey Fact Sheet FS-053-00. 2000; <http://pubs.usgs.gov/fs/fs05300/pdf/fs053-00.pdf>

Bockstael, N. E. Modeling Economics and Ecology: the Importance of a Spatial Perspective. *Am. J. Agric. Econ.* 1996, 78, 1168-1180.

Boxall, A. B. A., Johnson, P., and Smith, E. J. et al. Uptake of Veterinary Medicines from Soils into Plants. *J. Agric. Food Chem.* 2006, 54(6), 2288-2297.

Boxall, A. B., Kolpin, D. W., Halling-Sorensen, B., and Tolls, J. Peer Reviewed: Are Veterinary Medicines Causing Risks? *Environ. Sci. Technol.* 2003, 37(15), 286A-294A



Breitburg, D. L., Adamack, A., Rose, K. A., Kolesar, S. E., Decker, M. B., Purcell, J. E., Keister, J. E., and Cowan, J. H. The Pattern and Influence of Low Dissolved Oxygen in the Patuxent River, a Seasonally Hypoxic Estuary. *Estuaries*, 2003, 26(2A), 280-297

Brouers, F., and Sotolongo-Costa, O. Generalized Fractal Kinetics in Complex Systems (Application to Biophysics and Biotechnology). *Physica A*. 2006, 368, 165-175.

Brownawell, B. J., Chen, H., Collier, J. M., and Westall, J. C. Adsorption of Organic Cations to Natural Materials. *Environ. Sci. Technol.* 1990, 24, 1234-1241.

Buser, H.R., Poiger, T., and Müller, M. D. Occurrence and Fate of the Pharmaceutical Drug Diclofenac in Surface Waters: Rapid Photodegradation in a Lake. *Environ. Sci. Technol.* 1998, 32(22), 3449-2356.

Buth J. M., Steen, P. O., and Sueper, C. et al. Dioxin Photoproducts of Triclosan and Its Chlorinated Derivatives in Sediment Cores. *Environ. Sci. Technol.* 2010, 44, 4545-4551.

Chalew, T. E. A., and Halden, R. U. Environmental Exposure of Aquatic and Terrestrial Biota to Triclosan and Triclocarban. *J. Am. Water Resour. Assoc.* 2009, 45(1), 4-13

Carballa, M., Fink, G., Omil, F., Lema, J. M., and Ternes, T. Determination of the Soil-Water Distribution Coefficient ( $K_d$ ) for Pharmaceuticals, Estrogens and Musk Fragrances in Digested Sludge. *Water Res.* 2008, 42, 287-295.

Cheung, C. W., Porter, J. F., and McKay, G. Sorption Kinetic Analysis for the Removal of Cadmium Ions from Effluents Using Bone Char. *Water Res.* 2001, 35(3), 605-612

Comoretto, L., and Chiron, S. Comparing Pharmaceutical and Pesticide Loads into a Small Mediterranean River. *Sci. Total Environ.* 2005, 349, 201-210.

Conley, J. M., Symes, S. J., and Schorr, M. S. et al. Spatial and Temporal Analysis of Pharmaceutical Concentrations in the Upper Tennessee River Basin. *Chemosphere*. 2008, 73, 1178-1187.

de Maagd, P. G. J., Sinnige, T. L., Schrap, S. M. Opperhuizen, A., and Sum, D. T. H. M. Sorption Coefficients of Polycyclic Aromatic Hydrocarbons for Two Lake Sediments: Influence of the Bactericide Sodium Azide. *Environ. Toxicol. Chem.* 1998, 17, 1899-1907.

Deas, M. L., and Lowney, C. L. Water Temperature Modeling Review: Central Valley. California Water Modeling Forum, CA. 2000. Available at <http://www.cwemf.org/Pubs/BDMFTempReview.pdf>

Endo, S., Grathwohl, P., Haderlein S. B., and Schmidt, T. C. LFERs for Soil Organic Carbon – Water Distribution Coefficient ( $K_{OC}$ ) at Environmentally Relevant Sorbate Concentrations. *Environ. Sci. Technol.* 2009, 43, 3094-3100

Fan, Z.; Casey, F. X. M., Larsen, G. L., and Hakk, H. Fate and Transport of 1278-TCDD, 1378-TCDD, and 1478-TCDD in Soil-water Systems. *Sci. Total Environ.* 2006, 372, 323-333.

Focazio, M. J., Kolpin, D. W., and Barne, K. K. et al. A National Reconnaissance for Pharmaceuticals and Other Organic Wastewater Contaminants in the United States-II) Untreated Drinking Water Sources. *Sci. Total Environ.* 2008, 402, 201-216.

Gong, Y., and Depinto, J. Desorption Rates of Two PCB Congeners from Suspended Sediments – II. Model Simulation. *Wat. Res.*, 1998, 32(8), 2518-2532.

Goss, K-U., and Schwarzenbach, R. P. Linear Free Energy Relationship Used to Evaluate Equilibrium Partitioning of Organic Compounds. *Environ. Sci. Technol.* 2001, 35(1) , 1-9.

Gross, B., Montgomery-Brown, J., Naumann, A., and Martin, R. Occurrence and Fate of Pharmaceuticals and Alkylphenol Ethoxylate Metabolites in An Effluent-Dominated River and Wetland. *Environ. Toxicol. Chem.* 2004, 23(9), 2074-2084.

Gurr, C. J., and Reinhard, M. Harnessing Natural Attenuation of Pharmaceuticals and Hormones in Rivers. *Environ. Sci. Technol.* 2006, 40(9), 2872-2876.

Huang, W., and Weber, W. J., Jr. A Distributed Reactivity Model for Sorption by Soils and Sediments. 9. General Isotherm Nonlinearity and Applicability of the Dual Reactive Domain Model. *Environ. Sci. Technol.* 1997a, 31, 1703-1710.

Huang, W., and Weber, W. J., Jr. A Distributed Reactivity Model for Sorption by Soils and Sediments. 10. Relationships between Desorption, Hysteresis, and the Chemical Characteristics of Organic Domains. *Environ. Sci. Technol.* 1997b, 31, 2562-2569

Huang, W., and Weber, W. J., Jr. A Distributed Reactivity Model for Sorption by Soils and Sediments. 11. Slow Concentration-Dependent Sorption Rates. *Environ. Sci. Technol.* 1998, 32, 3549-3555.

Huang, W., Peng, P., Yu, Z., and Fu, J. Effects of Organic Matter Heterogeneity on Sorption and Desorption of Organic Contaminants by Soils and Sediments. *Appl. Geochem.* 2003, 18, 955-972.

Karthikeyan, K. G., and Meyer, M. T. Occurrence of Antibiotics in Wastewater Treatment Facilities in Wisconsin, USA. *Sci. Total Environ.* 2006, 361, 196-207.

Kleywegt, S., Pileggi, V., and Yang, P. et al. Pharmaceuticals, Hormones and Bisphenol A in Untreated Source and Finished Drinking Water in Ontario, Canada – Occurrence and Treatment Efficiency. *Sci. Total Environ.* 2011, 409, 1481-1488.

Kolpin, D. W., Furlong, E. T., and Meyer, M. T. et al. Pharmaceuticals, Hormones, and Other Organic Wastewater Contaminants in U.S. Streams, 1999-2000: A National Reconnaissance. *Environ. Sci. Technol.* 2002, 36(6), 1202-1211

Kümmerer, K. Antibiotics in the Aquatic Environment – A Review – Part I. *Chemosphere.* 2009, 75, 417-434.

Kwon, J. W., and Armbrust, K. L. Aqueous Solubility, n-Octanol-Water Partition Coefficients and Sorption of Five Selective Serotonin Reuptake Inhibitors to Sediments and Soils. *Bull Environ. Contam. Toxicol.* 2008, 81, 128-135.

Lam, M. W., Young, C. J., Brain, R. A., Johnson, D. J., Hanson, M. A., Wilson, C. J., Richards, S. M., Solomon, K. R., and Mabury, S. A. Aquatic Persistence of Eight Pharmaceuticals in a Microcosm Study. *Environ. Toxicol. and Chem.* 2004, 23(6), 1431-1440.

Li, Z. Sorption Kinetics of Hexadecyltrimethylammonium on Natural Clinoptilolite. *Langmuir*. 1999, 15, 6438-6445

Lin, A. Y., Plumlee, M. H., and Reinhard, M. Natural Attenuation of Pharmaceuticals and Alkylphenol Polyethoxylate Metabolites during River Transport: Photochemical and Biological Transformation. *Environ. Toxicol. and Chem.* 2006, 25(6), 1458-1464.

Lizondo, M., Pons, M., Gallardo, M. and Estelrich, J. Physicochemical Properties of Enrofloxacin. *J. Pharm. Biomed. Anal.* 1997, 15, 1845-1849.

Löffler, D., Römbke, J., Meller, M., and Ternes, T. Environmental Fate of Pharmaceuticals in Water/Sediment Systems. *Environ. Sci. Technol.* 2005, 39(14), 5209-5218.

Lung, W.S., and Bai, S. A Water Quality Model for the Patuxent Estuary: Current Conditions and Predictions Under Changing Land-use Scenarios. *Estuaries*. 2003, 26(2A), 267-279.

Lung, W.S., and Nice, A. J. Eutrophication Model for the Patuxent Estuary: Advances in Predictive Capabilities. *J. Environ. Eng.* 2007, 133(9), 917-930.

Lung, W.S. *Water Quality Modeling for Wasteload Allocations and TMDLs*. John Wiley & Sons, Inc., New York, New York.

Miller C. T., and Pedit, J. A. Use of a Reactive Surface-Diffusion Model To Describe Apparent Sorption-Desorption Hysteresis and Abiotic Degradation of Lindane in a Subsurface Material. *Environ. Sci. Technol.* 1992, 26, 1417-1427

Nakata, H., Kannan, K., Jones, P. D., and Giesy, J. P. Determination of Fluoroquinolone Antibiotics in Wastewater Effluents by Liquid Chromatography-Mass Spectrometry and Fluorescence Detection. *Chemosphere*. 2005, 58, 759-766.

Nice, A.J. Developing a Fate and Transport Model for Arsenic in Estuaries. Ph.D. Dissertation, University of Virginia, Charlottesville, Virginia, 2006.

Nice, A. J., and Lung, W.S. Modeling Arsenic in the Patuxent Estuary. *Environ. Sci. Technol.* 2008, 42(13), 4804-4810.

Nikolaou, A., Meric, S., and Fatta, D. Occurrence Patterns of Pharmaceuticals in Water and Wastewater Environments. *Anal. Bioanal. Chem.* 2007, 387, 1225-1234.

Nilsen, E., Rosenbauer, R., Furlong, E., Burkhardt, M., Werner, S., Greaser, L., and Noriega, M. Pharmaceuticals, Personal Care Products and Anthropogenic Waste Indicators Detected in Streambed Sediments of the Lower Columbia River and Selected Tributaries. *National Ground Water Association*. 2007, Paper 4483, p. 15.

Nowara, A., Burhenne, J., and Spiteller, M. Binding of Fluoroquinolone Carboxylic Acid Derivatives to Clay Minerals. *J. Agric. Food Chem.* 1997, 45, 1459-1463.

Oepen, B. Von, Kördel, W., and Klein, W. Sorption of Nonpolar and Polar Compounds to Soils: Processes, Measurements and Experience with the Applicability of the Modified OECD-Guideline 106. *Chemosphere*. 1992, 22, 285-304.

Ottmar, K. J., Colosi, L. M., and Smith, J. A. Sorption of Statin Pharmaceuticals to Wastewater-Treatment Biosolids, Terrestrial Soils, and Freshwater Sediment. *J. Environ. Eng.* 2010a, 136(3), 256-264.

Ottmar, K. J. An Examination of the Fate, Transport, and Occurrence of Atorvastatin and Simvastatin in Wastewater Treatment Systems. Ph.D. Dissertation, University of Virginia, Charlottesville, Virginia. 2010b

Pan, B., Ning, P., and Xing, B. Part V- Sorption of Pharmaceuticals and Personal Care Products. *Environ. Sci. Pollut. Res.* 2009, 16, 106-116.

Park, S., and Choi, K. Hazard Assessment of Commonly Used Agricultural Antibiotics on Aquatic Ecosystems. *Ecotoxicology*. 2008, 17, 526-538.

Pignatello, J. J., and Xing, B. Mechanisms of Slow Sorption of Organic Chemicals to Natural Particles. *Environ. Sci. & Technol.* 1996, 30(1), 1-11.

Poole, S. K., and Poole, C. F. Chromatographic Models for the Sorption of Neutral Organic Compounds by Soil from Water and Air. *J. Chromatogr., A*. 1999, 845, 381-400.

Ramil, M., Aref, T. E., and Fink, G. et al. Fate of Beta Blockers in Aquatic-Sediment Systems: Sorption and Biotransformation. *Environ. Sci. Technol.* 2010, 44, 962-970

Ran, Y., Xing, B., Rao, P. S. C., and Fu, J. Importance of Adsorption (Hole-Filling) Mechanism for Hydrophobic Organic Contaminants on an Aquifer Kerogen Isolate. *Environ. Sci. Technol.* 2004, 38, 4340-4348.

Renee K., et al. *Maryland Tributary Strategy Patuxent River Basin Summary Report for 1985-2005 Data*. Maryland Department of Natural Resources, Annapolis, MD, 2007; [http://www.co.cal.md.us/assets/Planning\\_Zoning/Comp\\_Plan/PatuxentRiverCommissionReport-Small.pdf](http://www.co.cal.md.us/assets/Planning_Zoning/Comp_Plan/PatuxentRiverCommissionReport-Small.pdf)

Ricart, M., Guasch, H., and Alberch, M. et al. Triclosan Persistence through Wastewater Treatment Plants and Its Potential Toxic Effects on River Biofilms. *Aquat. Toxicol.* 2010, 100, 346-353

Robinson, A. A., Belden, J. B., and Lydy, M. J. Toxicity of Fluoroquinolone Antibiotics to Aquatic Organisms. *Environ. Toxicol. Chem.* 2009, 24 (2) 424-430

Rügner, H., Kleineidam, S., and Grathwohl, P. Long Term Sorption Kinetics of Phenanthrene in Aquifer Materials. *Environ. Sci. Technol.* 1999, 33, 1645-1651.

Sander, M., and Pignatello, J. J. An Isotope Exchange Technique to Assess Mechanisms of Sorption Hysteresis Applied to Naphthalene in Kerogenous Organic Matter. *Environ. Sci. Technol.* 2005, 39, 7476-7484.

Sangsupan, H. A., Radcliffe, D. E., and Hartel, P. G. et al. Sorption and Transport of 17  $\beta$ -Estradiol and Testosterone in Undisturbed Soil Columns. *J. Environ. Qual.* 2006, 35, 2261-2272.

Seifrtová, M., Pena, A., Lino, M., and Solich, L. P. Determination of Fluoroquinolone Antibiotics in Hospital and Municipal Wastewaters in Coimbra by Liquid Chromatography with a Monolithic Column and Fluorescence Detection. *Anal. Bioanal. Chem.* 2008, 391, 799-805.



Singer, H., Müller, S., Tixier, C., and Pillonel, L. Triclosan: Occurrence and Fate of a Widely Used Biocide in the Aquatic Environment: Field Measurements in Wastewater Treatment Plants, Surface Waters, and Lake Sediments. *Environ. Sci. Technol.* 2002, 36, 4998-5004.

Snyder, S. A., Westerhoff, P., Yoon, Y., and Sedlak, D. L. Pharmaceuticals, Personal Care Products, and Endocrine Disruptors in Water: Implications for the Water Industry. *Environ. Eng. Sci.* 2003, 20(5), 449-469.

Spongberg, A. L., and Witter, J. D. Pharmaceutical Compounds in the Wastewater Process Stream in Northwest Ohio. *Sci. Total Environ.* 2008, 397, 48-157.

Stein, K., Ramil, M., Fink, G., Sander, M., and Ternes, T. A. Analysis and Sorption of Psychoactive Drugs onto Sediment. *Environ. Sci. Technol.* 2008, 42(17), 6415-6423.

Strock, T. J., Sassman, S. A. and Lee, L. S. Sorption and Related Properties of the Swine Antibiotic Carbadox and Associated N-Oxide Reduced Metabolites. *Environ. Sci. Technol.* 2005, 39, 3134-3142.

Sturini, M., Speltini, A., Pretali, L., Fasani, E., and Profumo, A. Solid-phase Extraction and HPLC Determination of Fluoroquinolones in Surface Waters. *J. Sep. Sci.* 2009, 32, 3020–3028.

Suntisukaseam, U., Weschayanwiwat, P., and Sabatini, D. Sorption of Amphiphile Pharmaceutical Compounds onto Polar and Nonpolar Adsorbents. *Environ. Eng. Sci.* 2007, 24(10), 1457-1465.

Tao, S., Piao, H., Dawson, R., Lu, X., and Hu, H. Estimation of Organic Carbon Normalized Sorption Coefficient ( $K_{OC}$ ) for Soils Using the Fragment Constant Method. *Environ. Sci. Technol.* 1999, 33, 2719-2725

ter Laak, T. L., Gebbink, W. A., and Tolls, J. Estimation of Soil Sorption Coefficients of Veterinary Pharmaceuticals from Soil Properties. *Environ. Toxicol. Chem.* 2006, 25(4), 933-941.

Tamtam, F., Mercier, F., and Le Bot, B. et al. Occurrence and Fate of Antibiotics in the Seine River in Various Hydrological Conditions. *Sci. Total Environ.* 2008, 393(1), 84-95.

The National Library of Medicine's Toxnet System (2009) United States National Library of Medicine. Available at: <http://toxnet.nlm.nih.gov>.

Thomann, R. V., and Mueller, J. A. 1987. Principles of Surface Water Quality Modeling and Control, Harper & Row, Publishers. pp. 103

Tixier, C., Singer, H. P., Canonica, S., and Müller, S. R. Phototransformation of Triclosan in Surface Waters: A Relevant Elimination Process for This Widely Used-Biocide – Laboratory Studies, Field Measurements and Modeling. *Environ. Sci. Technol.* 2002, 36, 3482-3480.

Tixier, C., Singer, H. P., Oellers, S., and Müller, S. R. Occurrence and Fate of Carbamazepine, Clofibric Acid, Diclofenac, Ibuprofen, Ketoprofen, and Naproxen in Surface Waters. *Environ. Sci. Technol.* 2003, 37(6), 1061-1068.

Tivant, P., Turq, P., Drifford, M., Magdelenat, H. and Menez, R. Effect of Ionic Strength on the Diffusion Coefficient of Chondroitin Sulfate and Heparin Measured by Quasielastic Light Scattering. *Biopolymers*. 1983, 22, 643.

Tolls, J. Sorption of Veterinary Pharmaceuticals in Soils: A Review. *Environ. Sci. Technol.* 2001, 35(17) 3397-3406.

Tsai, W. T., Lai, C. W., and Su, T. Y. Adsorption of bisphenol-A from aqueous solution onto minerals and carbon adsorbents. *J. Hazard. Mater.* 2006, B134, 169-175.

Tülp, H. C., Goss, K., Schwarzenbach, R. P., and Fenner, K. Experimental Determination of LSER Parameters for a Set of 76 Diverse Pesticides and Pharmaceuticals. *Environ. Sci. Technol.* 2008, 42, 2034-2040.

Verma, B., Headley, J. V., and Robarts R. D. Behaviour and Fate of Tetracycline in River and Wetland Waters on the Canadian Northern Great Plains. *J. of Environ. Sci. Health, Part A*. 2007, 42, 109-117.

Vieno, N. M., Tuhkanen, T., and Kronberg, L. Seasonal Variation in the Occurrence of Pharmaceuticals in Effluents from a Sewage Treatment Plant and in the Recipient Water. *Environ. Sci. Technol.* 2005, 39, 8220-8226.

Walters, R. W., Ostazeski, S. A., and Guiseppi-Elie, A. Sorption of 2,3,7,8-Tetrachlorodibenzo-*p*-dioxin from Water by Surface Soils. *Environ. Sci. Technol.* 1989, 23, 480-484.

Wilson, B. A., Smith, V. H., Denoyelles F., and Larive, C. K. Effects of Three Pharmaceutical and Personal Care Products on Natural Freshwater Algal Assemblages. *Environ. Sci. Technol.* 2003, 37, 1713-1719.

Weber, W. J., Jr., and Smith, E. H. Simulation and Design Models for Adsorption Process. *Environ. Sic. Technol.* 1987, 21(11), 1040-1050.

Weber, W. J. Jr., Huang, W., and Yu, H. Hysteresis in the Sorption and Desorption of Hydrophobic Organic Contaminants by Soils and Sediments 2. Effects of Soil Organic Mater Heterogeneity. *J. Cont. Hydrol.* 1998, 31, 149-165.

Weber, W. J., Jr., and Huang, W. A Distributed Reactivity Model for Sorption by Soils and Sediments. 4. Intraparticle Heterogeneity and Phase-Distribution Relationships under Nonequilibrium Conditions. *Environ. Sci. Technol.* 1996, 30, 881-888.

Weber, W. J. Jr., McGinley, P. M., and Katz, L. E. A Distributed Reactivity Model for Sorption by Soils and Sediments. 1. Conceptual Basis and Equilibrium Assessments. *Environ. Sci. Technol.* 1992, 26, 1955-1962.

Weller, D. E., Jordan, T. E., Correll, D. L., and Liu, Z. Effects of Land-use Change on Nutrient Discharges from the Patuxent River Watershed. *Estuaries.* 2003, 26(2A), 244-266.

Williams, C. F., Williams C. F., and Adamsen, F. J. Sorption-Desorption of Carbamazepine from Irrigated Soils. *J. Environ. Qual.* 2006, 35, 1779-1783.

Wu, S.-C., and Gschwend P. M. Sorption Kinetics of Hydrophobic Organic Compounds to Natural Sediments and Soils. *Environ. Sci. Technol.* 1986, 20, 717-725

Wu, S.-C., and Gschwend P. M. Numerical Modeling of Sorption Kinetics of Organic Compounds to Soils and Sedimental Particles. *Wat. Resour. Res.* 1988, 24(8), 1373-1383

Yamamoto, H., Nakamura, Y., and Moriguchi, S. et al. Persistence and Partitioning of Eight Selected Pharmaceuticals in the Aquatic Environment: Laboratory Photolysis, Biodegradation, and Sorption Experiments. *Water Res.* 2009, 43, 351-362.

Yong, Q. Study on Treatment Technologies for Perfluorochemicals in Wastewater. Dissertation, Kyoto Univeristy, 2007. Available online at [repository.kulib.kyoto-u.ac.jp](http://repository.kulib.kyoto-u.ac.jp)

Yu, Z., Peldszus, S., and Huck P.M. Adsorption of Selected Pharmaceuticals and an Endocrine Disrupting Compound by Granular Activated Carbon. 1. Adsorption Capacity and Kinetics. *Environ. Sci. Technol.* 2009, 43, 1467-1473.

Yu, Z., Xiao, B., Huang, W., and Peng, P. Sorption of Steroid Estrogens To Soils and Sediments. *Environ. Toxicol. Chem.* 2004, 23(3), 531-539.

Zeng, G., Zhang, C., Huang, G., and Yu, J. et al. Adsorption Behavior of Bisphenol A on Sediments in Xiangjiang River, Central-south China. *Chemosphere.* 2006, 65, 1490-1499

Zukowska, B., Breivik, K., and Wania, F. Evaluating the Environmental Fate of Pharmaceuticals Using a Level III Model Based on Poly-parameter Linear Free Energy Relationships. *Sci. Total Environ.* 2006, 359, 177-187.